Modulation of the activity of the mitochondrial BK-channel and of the permeability transition pore by hypoxia and apoptotic factors

Dissertation

zur Erlangung des akademischen Grades

Doctor rerum naturalium
(Dr. rer. nat.)

genehmigt durch die Fakultät für Naturwissenschaften
der Otto-von-Guericke-Universität Magdeburg

von M. Eng. Yu Cheng
geb. am 28 November 1976 in Liaoning, VR China

Gutachter: Prof. Dr. Detlef Siemen
Prof. Dr. Ulrich Brandt

eingereicht am: 07 Oktober 2009
verteidigt am: 12 März 2010

AKNOWLEDGMENTS

Table of Contents

1 Introduction

1.1 Mitochondria and mitochondrial ion channels

1.1.1   Fundamentals of mitochondria

Mitochondria are metabolically important cellular organelles, which are producing ATP by phosphorylation of ADP and are additionally involved in cellular signaling. Mitochondria usually appear in oval structure with a length of several micrometers and with a width of 0.5-1 μM [Kleinsmith & Kish, 1995]. A mitochondrion is encompassed by two membranes, an outer mitochondrial membrane (OMM) and an inner mitochondrial membrane (IMM). The characteristics of the OMM are similar to the characteristics of the plasma membrane while the characteristics of the IMM differ from that of the plasma membrane in respect of membrane permeability and protein-to-phospholipid ratio [Kleinsmith & Kish, 1995]. The space between IMM and OMM is termed the intermembrane space. The space enclosed by IMM is called matrix and contains various enzymes for energy production. Moreover, the IMM forms a large number of folds projecting into the matrix enlarging the surface of the IMM. They are known as cristae or tubuli [Kleinsmith & Kish, 1995; Mannella, 2008].

Mitochondria are different from other cellular organelles in several characteristics. Besides the nuclear genome, there is an independent mitochondrial genome, which consists of a circular DNA molecule with a molecular weight of 16 kb and which encodes 37 genes [Chan, 2006]. However, the majority of the mitochondrial proteins is encoded by the nuclear genome (about 900 proteins in rats; 600 proteins in human) [Chan, 2006]. Moreover, the morphological properties and the number of mitochondria differ for different cell types and tissues [Kleinsmith & Kish, 1995]. In this study *e.g.*, the mitochondria of brain astrocytes were considerably larger than the mitochondria from mitochondria of liver cells.

In mitochondria, energy rich molecules such as pyruvate and O_2 are converted into water and CO_2 with high efficiency. By means of the released energy, ATP is synthesized from ADP and phosphate. Therefore, mitochondria are also called the "cellular power plants". Besides, mitochondria play a multifunctional role in physiological and pathophysiological processes, *e.g.*: 1) mitochondrial morphological changes are believed to regulate the cellular metabolism [Scalettar et al., 1991]; 2) the production of reactive oxygen species (ROS) in mitochondria is involved in cellular signaling [Di Lisa et al., 2009]; and 3) the release of cytochrome c from mitochondria into the cytosol plays a central role in intrinsic apoptotic pathway [Paquette et al., 2005].

1.1.2   Ion transport in mitochondria

In the early twentieth century, mitochondria had been considered as cellular organelles providing energy for the cell by synthesis of ATP. The bioenergetic mechanisms in mitochondria have been revealed by a large number of studies. The theories of the Krebs cycle, the oxidative phosphorylation, and the chemiosmotic theory are explaining them well [Nicholls & Ferguson, 2002; O'Rourke, 2006].

According to the theories mentioned above, H^+ and electrons are provided by the Krebs cycle and are transported to the respiratory chain in the IMM. The electrons flow from complex I to complex IV of the respiratory chain enabling the conversion of oxygen and H^+ into water. Energy released by the flow of the electrons is used by complex I, III, and IV for transporting H^+ from the mitochondrial matrix into intermembrane space. Thereby, an H^+ gradient is established and maintained. H^+ is driven back into the matrix by its concentration gradient and by the mitochondrial membrane potential ($\Delta\Psi$). It flows through the ATP synthase (also termed complex V) coupled to production of ATP from ADP and phosphate. In all of the above processes, a selective transport of the ions and metabolites and a low permeability of the IMM for H^+ are required [O'Rourke, 2006].

The IMM possesses a low permeability for ions as compared with the OMM. However, there are various mechanisms of ion transport across the IMM: symports, antiports, and uniports. In symport, two or more ions are transported in the same direction; in antiport, at least two ions are transported across the membrane in the opposite direction; and in uniport, the transport is involved only with one type of ion [Nicholls & Ferguson, 2002]. The ion transport by ion channels such as the Ca^{2+} channels belongs to the type of the uniport. Ion transport by ion channels is driven by the concentration gradient for the particular ion and by the membrane potential. It is of general interest to understand the ion movements across the IMM regulating ATP synthesis and cellular signaling.

1.1.3 Fundamentals of mitochondrial ion channels

The voltage-dependent anion channel (VDAC) is the dominant ion channel in the OMM. It was first identified in 1975 by means of the bilayer technique [Schein et al., 1975]. The VDAC is a large ion channel, in its open state with a full conductance of about 450 pS for anions and anion metabolites including ADP, ATP, and phosphate. The VDAC shows the full conductance at around 0 mV and shows a smaller conductance at both, negative and positive

potentials [Dermietzel et al., 1994; Hille, 2001; Levadny et al., 2002]. The VDAC is not only involved in the transport of ions and metabolites, but also in cellular signaling. In the intrinsic apoptotic pathway, it is suggested to constitute a part of the permeability transition pore (PTP) complex in some hypotheses (apoptotic pathways will be introduced in chapter 1.4) [Tsujimoto et al., 2006]. The release of cytochrome c from mitochondria is regulated by the interaction of the VDAC with the pro- and antiapoptotic factors [Shoshan-Barmatz et al., 2006].

The mitochondrial translocase of the outer membrane (TOM) and translocase of the inner membrane (TIM) are involved in the translocation of those proteins from cytosol into matrix, which are encoded by the nuclear genome and which are synthesized in the cytosol [Grigoriev et al., 2004; Hood et al., 2003; O'Rourke, 2006].

There are various ion channels identified in the IMM. Ca^{2+} channels such as the Ca^{2+} uniporter and the ryanodine receptor; potassium channels including the Ca^{2+} activated large-conductance potassium channel (BK-channel), the ATP sensitive potassium channel (K_{ATP} channel), and a voltage-gated potassium channel (shaker-related subfamily, member 3 ($K_{V1.3}$)); anion channels including the inner membrane anion channel (IMAC), a voltage dependent chloride channel (CLC), and a chloride intracellular channel (CLIC); and the mitochondrial permeability transition pore (PTP) are present in the IMM [O'Rourke, 2006]. In particular, the mitochondrial BK-channel (mtBK-channel) and the PTP are discussed in the following chapters.

The Ca^{2+} uniporter and the ryanodine receptor are supposed to be the main route of mitochondrial Ca^{2+} transport whose driving force is mainly the negative $\Delta\Psi$ [Gunter et al., 2000]. The potassium channels (BK-channel, K_{ATP} channel, and $K_{V1.3}$) in the IMM are involved in the regulation of the mitochondrial volume and can play a cytoprotective role in connection with hypoxia/ischemia injury [Xu et al., 2002; Inoue et al., 1991; Cohen et al., 2000; Garlid et al., 1997; O'Rourke, 2006].

1.2 The BK-channel

1.2.1 Introduction of the BK-channel

The family of potassium channels is strongly diverse and is constituted of several subfamilies, which are distinguished by their membrane topological structures [Hille, 2001]. The potassium channels control the membrane potential so that they can regulate the excitability

of excitable cells. Thus, many physiological processes of excitable cells are regulated by potassium channels, *e.g.* release of neurotransmitter, internal secretion, and smooth muscle contraction [Nelson et al., 1995; Ghatta et al., 2006; Hille, 2001]. Activity of the potassium channels can be regulated by depolarization, Ca^{2+}, ATP, G-protein, and even CO [Hille, 2001; Williams et al., 2004]. One subfamily of potassium channels (K_{Ca}) is activated by free Ca^{2+} from the intracellular side. According to their conductance, three classes of K_{Ca} channels were identified: the large-conductance BK-channel (100-300 pS), the intermediate-conductance IK-channel (25-100 pS), and the small-conductance SK-channel (2-25 pS) [Marty, 1981; Yoshida et al., 1991; Gardos, 1958; Jensen et al., 2001; Ishii et al., 1997; Lingle et al., 1996; Blatz & Magleby, 1986; Ghatta et al., 2006].

BK-channels are present in membranes of a wide variety of cell types. In neuronal cells, BK-channels modulate the release of the neurotransmitters [Robiataille et al., 1993; Wang, 2008]. Furthermore, BK-channels are involved in flow-mediated K^+ secretion in kidney [Pluznick et al., 2006]. BK-channels may also regulate the secretion of insulin from human pancreatic β-cells [Braun et al., 2008]. In smooth muscle, the activation of BK-channels by Ca^{2+} causes vasodilation [Nelson et al., 1995]. And finally, BK-channels are also very important for electrical tuning of cochlear hair cells [Hudspeth et al., 1988]. Agreeing with the diverse functions of BK-channels, its physiological and pathophysiological role was revealed in many basic research and clinical studies. BK-channels were considered as a potential drug target in the cardiovascular system, the urinary system, and the nervous system [Ghatta et al., 2006].

1.2.2 Structure of the BK-channel

Potassium channels including the BK-channel are commonly constituted of α-subunits and β-subunits. 4 α-subunits of the BK-channel form a pore structure and each of them is associated with a β-subunit, which regulates activity of the BK-channel [Toro et al., 1998; Ghatta et al., 2006; Dale et al., 2002] The α-subunit of the BK-channel was first cloned from the mutant slowpoke locus of Drosophila, therefore, the α-subunit of the BK-channel is also called *dSlo* [Hille, 2001]. The counterpart of *dSlo* in Human (*hslo*) and in mouse (*mslo*) was cloned from human brain and from mouse brain and muscle, respectively [Dworetzky et al., 1994; Butler et al., 1993; Ghatta et al., 2006].

The α-subunits are forming the pore of the channel and the β-subunits play a role in regulation of the activity of the channel. The α-subunit is constituted of the N-terminus, 7

transmembrane domains (S0-S6) including the P-loop (between S5 and S6), and the 4 hydrophobic segments (S7-S10) at the C-terminus (Fig.1) [Ghatta et al., 2006]. The N-terminus of the BK-channel is not only connected to the hydrophobic domain (S0), but also acts as the binding domain for the β-subunit [Ghatta et al., 2006]. The S5 domain, the P-loop, and the S6 domain of the α-subunit are forming the inner wall of the pore. In the P-loop, there is a very conserved amino acid sequence, -TXXTXGYGD- (-thr-X-X-thr-X-gly-tyr-gly-glu-), that is termed the potassium channel "signature sequence" [Heginbotham et al., 1992,1994; Hille, 2001].The selectivity filter is a part of the P-loop and is located in the centre of the cavity. The selectivity is the narrowest part of the pore and determines the permeability for potassium as compared with other ions, the relative permeability [Jiang et al., 2002; Ghatta et al., 2006]. The S4 domains of the α-subunits contain the voltage sensor of the BK-channel, which possesses positively charged residues (Arg) at every third position contributing to the voltage sensitivity [Latorre & Brauchi, 2006; Stefani et al., 1997]. Membrane depolarization promotes the movement of the charged residues contained in S4 resulting in a conformational change of the α-subunit, which then causes opening of the pore [Latorre & Brauchi, 2006; Stefani et al., 1997].

The C-terminus region of the α-subunits of the BK-channel is localized at the intracellular side containing four hydrophobic segments (S7-S10) and a Ca^{2+} sensor. The regulator of conductance of the potassium domain (RCK) is constituted of S7 and S8 segments (Fig.1) [Ghatta et al., 2006]. The RCK determines the conductance of the BK-channel and plays a role in the gating mechanism of the BK-channel [Jiang et al., 2001]. The Ca^{2+} sensitivity of the BK-channel is determined by the highly conserved domains S9, S10 and the "Ca^{2+} bowl" between them (Fig.1). The "Ca^{2+} bowl" is the region limited by S9 and S10, where the negatively changed aspartate (Asp) is abundantly expressed providing the Ca^{2+} binding site [Wei et al., 1994, 1996; Schreiber & Salkoff, 1997; Ghatta et al., 2006]. Besides the Ca^{2+} sensor in the C-terminus region, other regulatory sites such as leucine zipper domains, phosphorylation sites for kinases are also identified regulating the activity of the BK-channel [Ghatta et al., 2006].

4 types of the β-subunit of the BK-channel were cloned from different tissues. They all contain 2 transmembrane units (TM_1 and TM_2), the extracellular loop, and the intracellular C-terminus and N-terminus (Fig. 1) [Meera et al., 2000; Hille 2001; Ghatta et al., 2006]. The interaction of α-subunit and β-subunit could modify Ca^{2+} sensitivity, voltage dependence, and

kinetics of the BK-channel. Therefore, the combination of α-subunit and β-subunit could be target of BK-channel openers and inhibitors [Wallner et al., 1995; Ramanathan et al., 1999; Nimigean & Magleby, 1999; Ghatta et al., 2006].
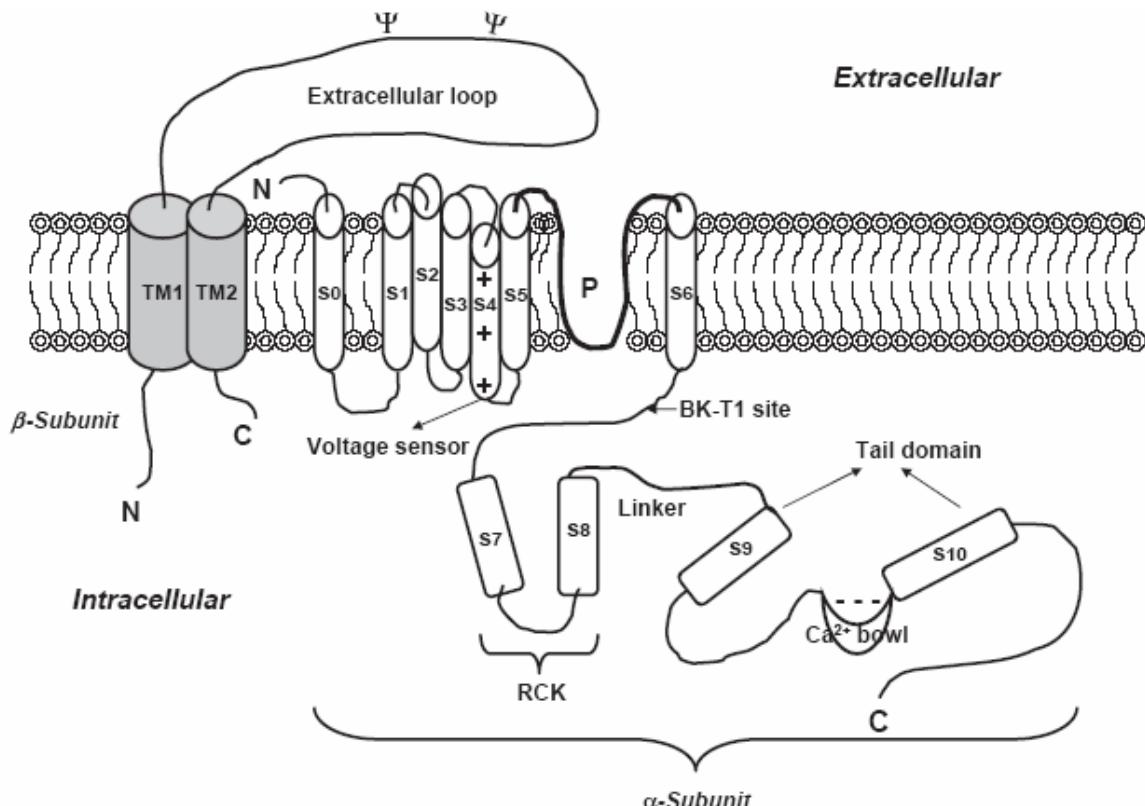
Fig. 1: Schematic representation of the structure of the BK-channel [from Ghatta et al., 2006]. It demonstrates the α-subunit containing N-terminus, S0-S6 domains, pore region, S7-S10 domains, calcium sensor ("calcium bowl"), and C-terminus. The BK-T1 site is localized in the sequence between the core channel domain S6 and the C-terminus domain modulating the tetramerization of the monomers of the α-subunits. The β-subunit is composed of TM_1 and TM_2 domains with the extracellular loop between them [Ghatta et al., 2006].

1.2.3 Inhibitors and openers of the BK-channel

Iberiotoxin (Ibtx), Charybdotoxin (Chtx), and the quaternary ammonium compounds tetraethylammonium (TEA) and tetrabutylammonium (TBA) are the BK-channel inhibitors, which are usually used for the identification of the BK-channel, the investigation of the structure of the BK-channel, and the studying the physiological function of the BK-channel [Ghatta et al., 2006]. Ibtx, which is purified from the Eastern Indian red scorpion (Buthus tamulus), is a selective inhibitor of the BK-channel but of no other type of potassium channel such as IK_{ca} and SK_{ca} [Garcia et al., 1991]. The activity of the BK-channel is reduced when the Ibtx and the Chtx are applied from the extracellular side. Ibtx and Chtx have the similar

structure and the mechanism of inhibition is explained by binding of Ibtx and Chtx to the P-loop causing the occlusion of the pore [Kaczorowski et al., 1996]. TEA and TBA are thought to block the BK-channel from the intracellular side by being trapped in the pore and accelerating the transition of the channel into the closed state [Li & Aldrich, 2004].

The commonly used BK-channel openers NS004 and NS1619 are synthetic benzimidazolone derivatives [Nardi et al., 2003]. Possible mechanisms of activation of the BK-channel are explained in the study of Ghatta et al. as: "1) modulation of the Ca^{2+} affinity in the "Ca^{2+} bowl" in the C-terminus of the α-subunits, 2) enhancement of the interaction of α- and β-subunits, and 3) simulation of the activation of the α-subunits by the β-subunits" [Ghatta et al., 2006]. Activation of the BK-channel by NS1619 and NS004 causes an increased efflux of potassium resulting in a hyperpolarization of the membrane and a decrease of cell excitability [Ghatta et al., 2006]. This mechanism was proved in some studies demonstrating the relaxing effect of the BK-channel opener in vascular smooth muscle cells [Saponara et al., 2006; Holland et al., 1996]. It is suggested that it has a pharmacological potential for some neurological, urological, respiratory and cardiovascular diseases [Nardi et al., 2003; Ghatta et al., 2006].

1.2.4 The mitochondrial BK-channel (mtBK-channel)

The BK-channel is present not only in the plasma membrane, but also in the IMM [Siemen et al., 1999]. In patch-clamp experiments, a single-channel current was recorded in the IMM with a full conductance of about 300 pS well in the range of the conductance of BK-channels in the plasma membrane. Calcium and voltage dependence of this channel in the IMM were described by the authors in detail [Siemen et al., 1999]. Their results are shown here as a Figure which may help with the interpretation of my results (Fig.2). Additionally, it was found that the channel could be blocked by Chtx, a potassium channel inhibitor, and Ibtx, a selective BK-channel inhibitor (EC_{50} value about 100 nM). Taking the results above, this IMM channel was identified as the mtBK-channel [Siemen et al., 1999; Xu et al., 2002; Cheng et al., 2008]. Moreover, the results of immunoblot experiments with mitochondria supported the identification of the BK-channel in the IMM [Xu et al., 2002; Douglas et al., 2006].
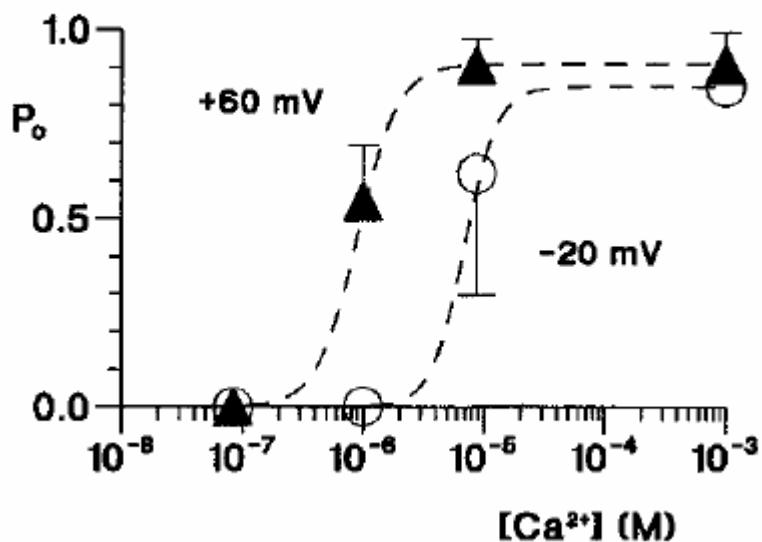
Fig. 2: Calcium dependence and voltage dependence of the mtBK-channel [from Siemen et al., 1999]. P_o (the probability of the ion channel being in the open state) of the mtBK-channel from glioma cells was measured in the cell-attached mode at a holding potential of –20 mV (O) and +60 mV (▲) in solutions with various calcium concentrations (from 10^{-7}-10^{-3} M). A larger P_o was demonstrated at positive potentials (depolarization) and in the solutions with higher Ca^{2+} concentrations [Siemen et al., 1999].

The mtBK-channel is assumed to play a protective role in the cells enhancing the resistance to ischemic injury and apoptosis [Ohya et al., 2005; Xu et al., 2002]. In some physiological or pathophysiological processes, Ca^{2+} can be accumulated in the mitochondrial matrix. The excess Ca^{2+} induces opening of the PTP and the release of cytochrome c leading to apoptosis. Under this condition, the activation of the mtBK-channel increases the potassium current into the matrix that induces a partial depolarization of $\Delta\Psi$ attenuating the driving force for the Ca^{2+} influx [Xu et al., 2002; O'Rourke, 2006]. The activation of the mtBK-channel could be considered as a protective mechanism against excessive mitochondrial Ca^{2+} uptake that would result from an induction of apoptosis [Xu et al., 2002; O'Rourke, 2006]. Moreover, opening of the mtBK-channel has been implicated to lead to both, early and delayed preconditioning against ischemia-reperfusion injury [Wang et al., 2004].

1.3 The mitochondrial permeability transition pore

1.3.1 Fundamentals

Massive swelling of mitochondria induced by Ca^{2+} had been observed for more than 50 years and it was thought to be caused by an increase of the permeability of the mitochondrial membrane [Chance, 1964]. This phenomenon of an increased permeability in response to

stimuli such as an increased Ca^{2+} or phosphate concentration was termed mitochondrial permeability transition (MPT) [Hunter et al., 1976]. In order to understand the mechanism of the MPT, it was suggested that an ion channel in the IMM is involved in the MPT. The opening of this channel would then lead to the MPT. Therefore, this putative channel was named the permeability transition pore (PTP) [Gunter & Pfeiffer, 1990; O'Rourke, 2006]. According to this hypothesis, the flux of water into the mitochondrial matrix after activation of the PTP is driven by the osmotic gradient resulting in mitochondrial swelling.

Accompanied by the increasing interest in apoptosis the PTP became more important because its opening is associated with the release of cytochrome c from the intermembrane space into the cytosol. This is a central step of the intrinsic apoptotic pathway [Tsujimoto et al., 2006]. The molecular basis of the PTP is still unknown. Various putative models were proposed to explain structure and function of the PTP. One of these models hypothesized that the PTP is constituted of the VDAC in the OMM, the ATP nucleotide translocater (ANT) in the IMM, and cyclophilin D in the matrix, which is associated with the ANT [Halestrap et al., 2002]. However, when the genes of ANT in mice were knocked out, the MPT could be reduced by Ca^{2+} leading still to the release of cytochrome c, although the Ca^{2+} requirement was increased [Kokoszka et al., 2004]. From these results, it was suggested that ANT could not be an essential part of the PTP complex, but could be a regulatory part of the PTP complex [Kokoszka et al., 2004; O'Rourke, 2006]. In this dissertation, an independent ion channel, PTP, in the IMM is assumed as the core part of the PTP complex.

1.3.2 Properties of the PTP in patch-clamp experiments

In patch-clamp experiments with mitochondria from rat or human liver cells, a large single-channel current was observed and recorded in symmetrical KCl solutions with a high concentration of Ca^{2+} (100 µM to 1 mM) [Szabo & Zoratti, 1992]. According to its electrophysiological characteristics and responses to inhibitors and activators of the MPT, this large channel matched the putative PTP, in that it was able to induce the mitochondrial permeability transition. Therefore, this channel was identified as the permeability transition pore [Szabo & Zoratti, 1992; Loupatatzis et al., 2002].
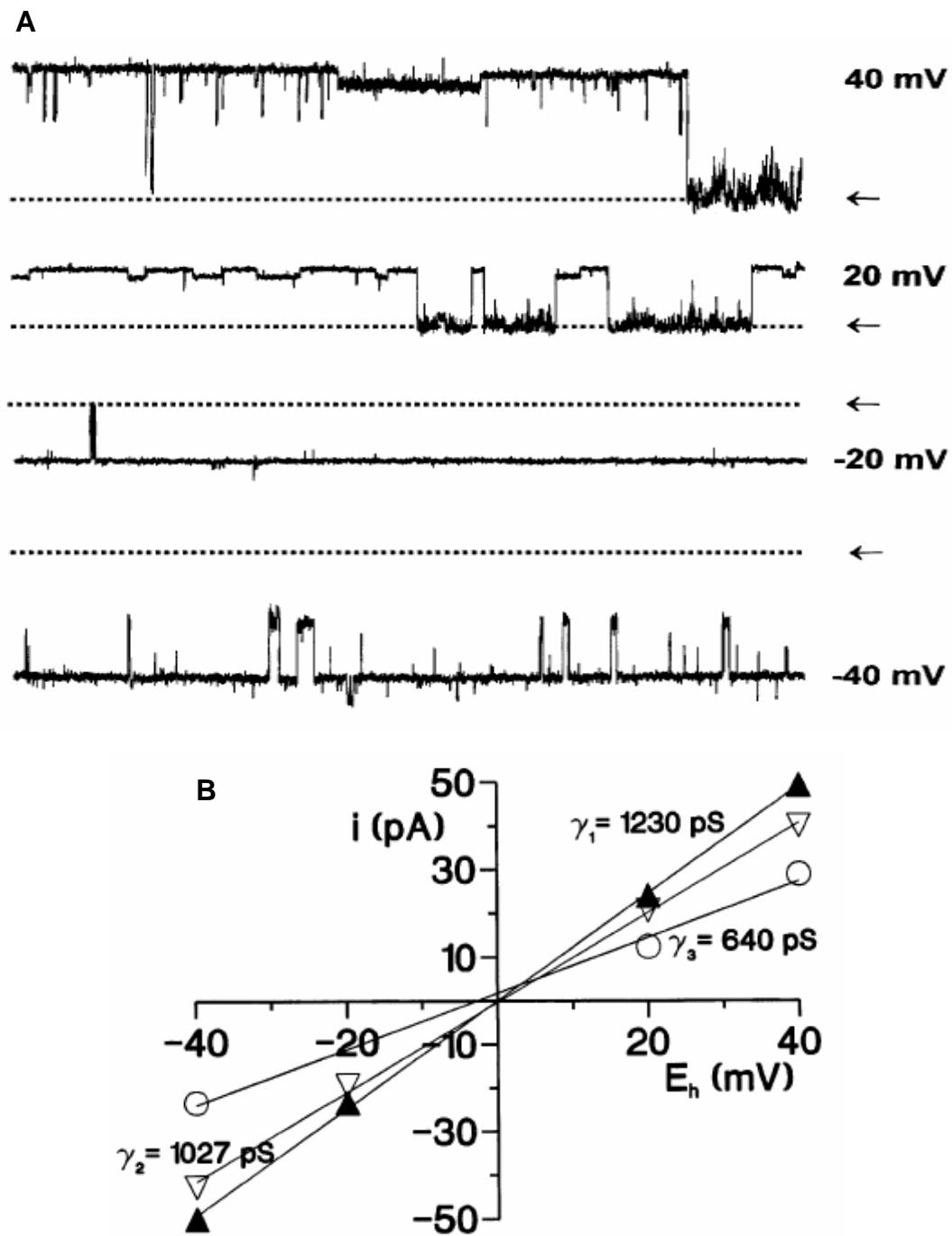
Fig. 3: Single-channel recording and current-voltage relation of the PTP [from Loupatatzis et al., 2002]. A): single-channel currents of the PTP demonstrated in symmetrical KCl medium at -40 mV, -20 mV, +20 mV, and +40 mV by means of the patch-clamp technique. Closed state of the channel is marked by arrows. The PTP shows a relatively slow kinetics with multilevel conductance and larger noise in the closed state than in the open state (*e.g.* at +40 mV) [Loupatatzis et al., 2002]. **B):** Current-voltage relation of the PTP. The conductances γ of the fully open state and of the substates are calculated as the steepness of the current-voltage relations. The maximum conductance is about 1.2 nS, while the conductances of the two most frequent substates are about 1 nS and 0.6 nS, respectively [Loupatatzis et al., 2002].

The PTP is a large channel with a maximum conductance of 1.3 nS. In patch-clamp experiments, the PTP does not stay entirely in the open state or in the closed state, but often switches to one of several substates (Fig. 3) [Loupatatzis et al., 2002; Hille, 2001]. Remarkably, the current noise of the PTP in the closed state may be larger than in the open state, which is opposite to other ion channels such as the mtBK-channel [Loupatatzis et al., 2002]. Moreover, the PTP shows little ion selectivity in patch-clamp experiments. The PTP was recorded not only in KCl medium, but also in Na^+, Cs^+, and I^- medium [Szabo & Zoratti, 1992]. The PTP is permeable to the Na^+, Cs^+, K^+, Cl^- and I^-. This matches the fact that the mitochondrial membrane is permeable to various ions and metabolites during the MPT.

The activity of the PTP depends on the matrix Ca^{2+} concentration. The P_o of the PTP is about 0.5, 0.25, and close to 0 in solutions containing 1 mM Ca^{2+}, 10 µM Ca^{2+}, and 1µM Ca^{2+}, respectively. If the PTP is shifted from the solution with 1 mM Ca^{2+} into the solution with 1 µM Ca^{2+}, the PTP will close within several seconds [Loupatatzis et al., 2002].

Cyclosporine A (CsA), Mg^{2+}, and ADP are inhibitors of the PTP. Mg^{2+} and ADP were first identified to prevent the MPT in intact mitochondria [Haworth & Hunter, 1980; Harris et al., 1979]. Later, the inhibition of the PTP by 100 mM Mg^{2+} or by 10 mM ADP was demonstrated in patch-clamp experiments [Szabo & Zoratti, 1992]. CsA is an immunosuppressive drug and was found to be a selective inhibitor of the MPT that inhibits Ca^{2+}- or Phosphate-induced MPT at a concentration of 60 pM of CsA/mg of mitochondrial proteins [Szabo & Zoratti, 1991; Fournier et al., 1987; Crompton et al., 1988]. The mechanism of inhibition was explained by binding of CsA to cyclophilin D, which is part of the PTP complex [Connern et al., 1992; Woodfield et al., 1997]. When in patch-clamp experiments an open PTP was moved from a control solution into the same solution with 10 µM CsA added, most activity of the PTP disappeared after several seconds. Only a few events remained as very short bursts [Loupatatzis et al., 2002].

1.4 Bax and Bcl-$_{XL}$

1.4.1 Bcl-2 family

The proteins of the B cell lymphoma 2 (Bcl-2) family have been considered as crucial in the cellular pathway of apoptosis and tumorigenesis since the anti-apoptotic activity of the protein Bcl-2 was identified [Vaux et al., 1998; Gill & Perez-Polo, 2008]. Later, a number of proteins which share similar conserved sequences and are involved in cell death were identified as

members of the Bcl-2 family [Adams & Cory, 1998; Tsujimoto, 1998]. The B cell homology (BH 1-4) domains are conserved amino-acid sequences, which are the special structure of the proteins of the Bcl-2 family. At least one BH domain is present in each protein of the Bcl-2 family [Jesenberger & Jentsch, 2002; Gill & Perez-Polo, 2008]. According to their structure and function in apoptosis, the members of the Bcl-2 family were categorized into 3 subfamilies: the Bcl-2 subfamily including Bcl-2, Bcl-$_{XL}$, Bcl-$_{XS}$, and Bcl-$_W$; the Bax subfamily including the proapoptotic members Bax and Bak; and the Bik subfamily including the proapoptotic Bik and Bid [Tsujimoto, 1998].
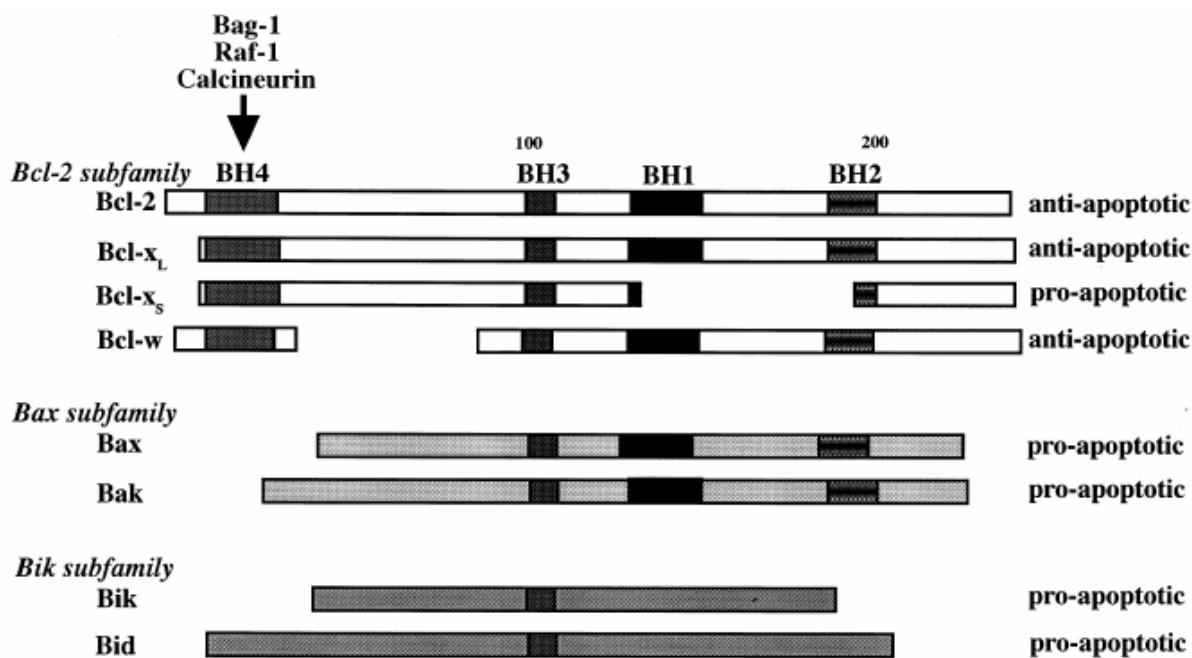
Fig. 4: Homology of the members of the Bcl-2 family [from Tsujimoto, 1998]. Each member of the Bcl-2 subfamily possesses BH 1-4 domains and most of them act anti-apoptotic. The members of the Bax subfamily contain the BH 1-3 domains, whereas the members of the Bik subfamily possess only BH 3 domain [Tsujimoto, 1998].

1.4.2 Bax

Bcl-2 associated protein X (Bax) was identified as a proapoptotic member of Bcl-2 family through its heterodimerization with the protein Bcl-2 and by its ability to promote cell death [Oltvai et al., 1993]. Although there are several splice variants of Bax, the three conserved BH domains (BH 1-3) and the hydrophobic domain in C-terminus are always present in the protein Bax [Apte et al., 1995; Zhou et al., 1998; Thomas et al., 1999; Antonsson, 2001]. The BH 3 domain, which is present in all members of the Bcl-2 family, is considered to be the most important structure of Bax. It was believed that Bax could form homodimers itself or form heterodimers with other proteins of the Bcl-2 family by binding within the BH 3 domain. Moreover, the proapoptotic activity of Bax is also regulated by the BH 3 domain [Giam et al., 2008; Hunter & Parslow, 1996].

17

The three-dimensional structure of Bax was revealed by the study of Suzuki et al.. 9 α-helices are the backbone of the molecular structure of Bax, which are connected by flexible loops (Fig. 5) [Suzuki et al., 2000]. The two hydrophobic helices α5 and α6 are located in the central position of Bax while the other hydrophilic helices (all helices except α5, α6, and α9) are located at the surface of Bax encompassing the α5 and α6 helices [Antonsson, 2001]. The conserved domains (BH 1-3) of Bax are also located at the surface of Bax, and are accessible for interaction with other proteins (Fig. 5) [Antonsson, 2001]. Moreover, the C-terminus of Bax is constituted of the α9 helix located in the hydrophobic pocket. The α9 helix could regulate the activity of Bax through the disclosure of α5 and α6 helices [Suzuki et al., 2000; Antonsson, 2001].
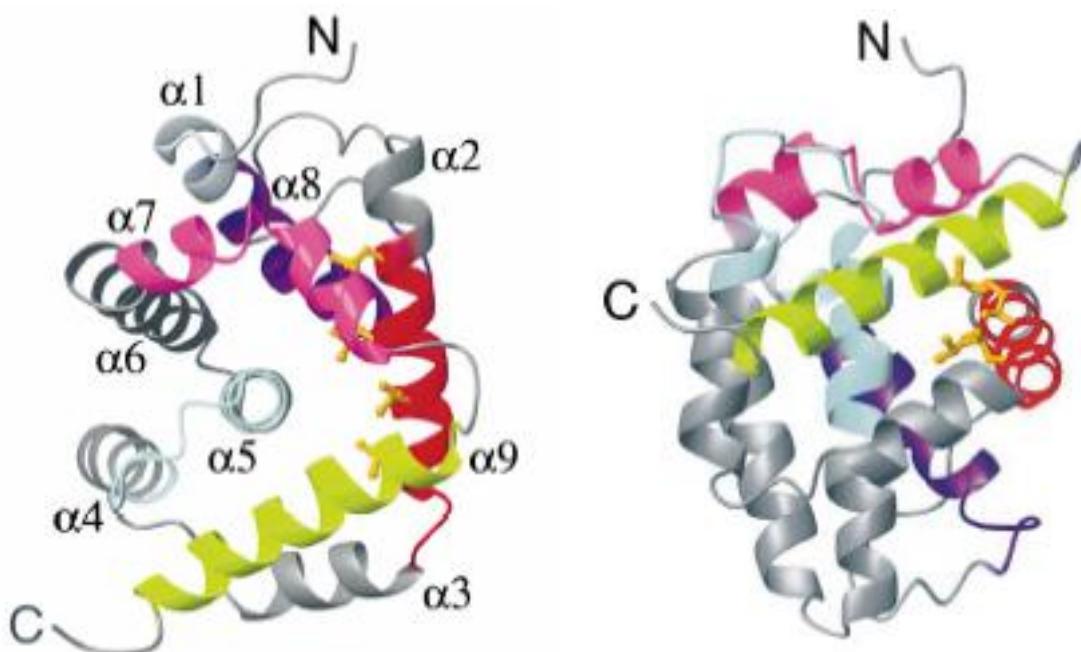
Fig. 5: Structure of Bax [from Suzuki et al., 2000]. 2 different views of Bax are demonstrated, a view straight down the central hydrophobic helix α5 (left panel) and a view from side of Bax (right panel). The conserved sequence of BH 1, BH 2, and BH 3 are demonstrated in cyan, magenta, and red, respectively. Helix α1 and the C-terminus helix in Bax are shown in purple and green [Suzuki et al., 2000].

1.4.3 Bcl-XL

Bcl-XL (B-cell lymphoma-extra large) is an antiapoptotic member of the Bcl-2 family and possesses all BH domains (BH 1–4). The BH 4 domain, which is present in every antiapoptotic member of the Bcl-2 family, is necessary and sufficient for its antiapoptotic activity [Cittelly et al., 2007; Gill & Perez-Polo, 2008]. This was proved by inhibition of apoptosis by the isolated BH 4 peptide from Bcl-XL [Soto & Smith, 2009]. Except for some minor differences, the structure of Bcl-XL is similar to the structure of Bax, although their

function is opposite. Bcl-$_{XL}$ possesses the BH 4 domains in helix α1, which is absent in helix α1 of Bax. Another difference is that there is no helix α9 in Bcl-$_{XL}$, which forms the C-terminus in Bax [Suzuki et al., 2000].
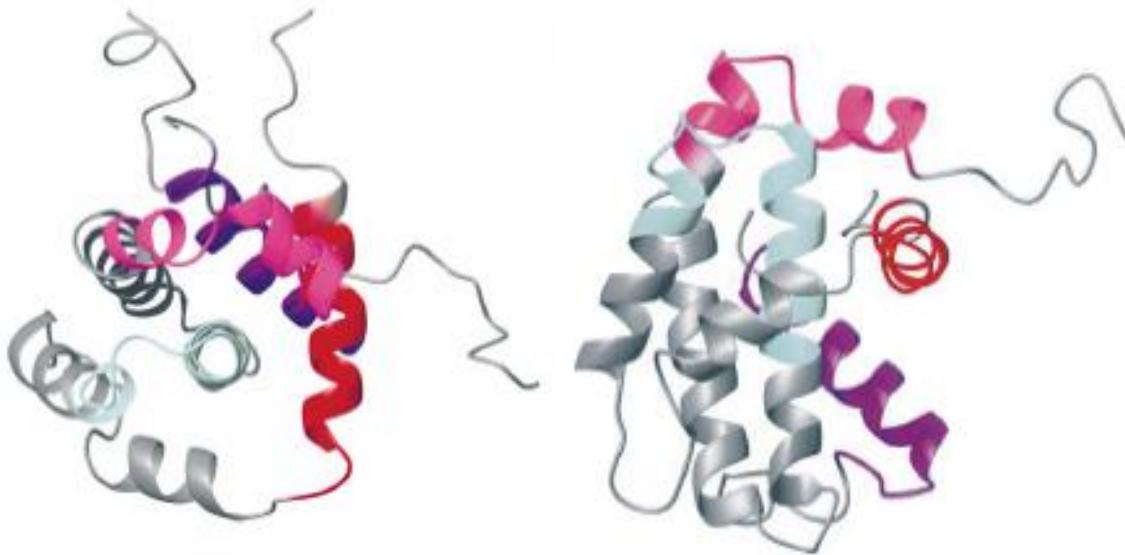
Fig. 6: Structure of Bcl-$_{XL}$ [from Suzuki et al., 2000]. The view is straight down the central hydrophobic helix (left panel) and from the side of Bcl-$_{XL}$ (right panel). The BH 1, BH 2, and BH 3 domain are shown in cyan, magenta, and red, respectively. The BH 4 containing helix in Bcl-$_{XL}$ is shown in purple [Suzuki et al., 2000].

1.5 The role of Bax, Bcl-$_{XL}$, and the PTP in apoptosis

1.5.1 Fundamentals of apoptosis

Apoptosis is the programmed cell death that plays an important role in a variety of biological processes [Kerr et al., 1972; Prindull, 1995]. Condensation of nuclear chromatin, cell membrane blebbing, cell shrinkage, and formation of the apoptotic bodies were described as morphological characteristics of apoptosis [Saraste & Pulkki, 2000]. The apoptotic bodies, which are enclosed by plasma membrane, contain cytosolic organelles and enzymes. They are phagocytosed by macrophages and by the parenchyma cells. This mechanism prevents the release of intracellular contents into the extracellular milieu, which could initiate inflammation [Kerr et al., 1972; Saraste & Pulkki, 2000; Gill & Perez-Polo, 2008]. Under the molecular-biological aspect, a chain of signaling cascades is activated within the process of apoptosis. Most important is the activation of caspase 7 (cysteine-aspartic acid protease) resulting in the activation of other enzymes finally fragmentating the nuclear DNA [Stefanis, 2005].

Apoptosis plays an important role in various physiological and pathophysiological processes. It contributes to the regulation of tissue homeostasis. Those cells, which are not required during the development, are eliminated by apoptosis [Meier et al., 2000; Jin & El-Deiry, 2005]. A number of diseases seem to be associated with a failing regulation of apoptosis. Several neurodegenerative and autoimmunological diseases are thought to be due to an excess of apoptosis. On the other hand, the tumorigenesis and some developmental defects are thought to be associated with the downregulation of the programmed cell death [Thompson, 1995; Jin & El-Deiry, 2005].

Although the signaling cascade of apoptosis involves a great number of cellular factors and forms a complicated network, the process of apoptosis is generally classed into two main pathways: the extrinsic- and the intrinsic apoptotic pathway. By these two pathways, caspases are activated eventually resulting in initiation of DNA fragmentation and in morphological changes of the cell [Aggarwal et al., 1999; Bender et al., 2005; Stefanis, 2005].

In the extrinsic apoptotic pathway, the signaling cascade is initiated by the activation of the TNF-α receptor or the Fas/CD95 receptor. The cell death receptors (TNF-α receptor or Fas/CD95 receptor) are triggered by extracellular factors (Fas ligand or TNF-α) leading to the recruitment of the TNF receptor-associated death domain (TRADD) or the Fas-associated death domain protein (FADD) forming a protein complex to activate the initiator caspase, caspase 8. The activated caspase 8 triggers downstream caspases (caspase 3, 7) through protein cleavage. The activated caspase 7 then activates enzymes, which can carry out the cellular degradation [Bender et al., 2005; Gill & Perez-Polo, 2008; Saraste & Pulkki, 2000]. The intrinsic apoptotic pathway involves opening of the PTP by Ca^{2+}, ROS, or by proapoptotic factors resulting in the release of cytochrome c into the cytosol. This release plays a key role in the intrinsic apoptotic pathway. Pro-caspase 9, dATP, and cytochrome c form the apoptosome in the cytosol leading to the activation of caspase 9. Further, the activated caspase 9 exerts its proteolytic activity to activate caspase 3 and 7 resulting in cellular degradation [Antonsson, 2001; Rao et al., 2002; Gill & Perez-Polo, 2008].

1.5.2 Bax, Bcl-$_{XL}$, and the PTP in intrinsic apoptotic pathway

Within the intrinsic apoptotic pathway, the release of cytochrome c from the mitochondria into the cytosol is the central process that activates the downstream cascade finally leading to cell death. Although the details of the release of cytochrome c from the mitochondria are not

very clear, opening of the PTP is considered to play a determinative role in the release of cytochrome c. The opening of the PTP leads to a series of consequences: increased permeability of the IMM e.g. to Ca^{2+}, increased matrix volume, loss of $\Delta\Psi$, rupture of the OMM, release of mitochondrial proteins including cytochrome c and apoptosis-inducing factor (AIF) into the cytosol [Kluck et al., 1997; Susin et al., 1996]. Therefore, inhibition of the PTP could interrupt the intrinsic apoptotic pathway resulting in cell survival. It is thought that some drugs exert their neuroprotective function by the inhibition of the PTP. Thus, the PTP could be a promising drug target for cell protection [Sayeed et al., 2006].

Opening of the PTP can be induced by Ca^{2+}, ROS, and proapoptotic factors such as Bax that result in the release of cytochrome c. The proapoptotic factor Bax is synthesized and localized in the cytosol. Bax is activated by the BH 3-interacting-domain death agonist (Bid) [Jin & El-Deiry, 2005]. After its activation, Bax is transported to its target, the mitochondrion [Hsu et al., 1997; Gross et al., 1998; Antonsson, 2001]. Bax can lead to the release of cytochrome c, however, it is still under debate how Bax induces the release of cytochrome c from the mitochondria [Li et al., 1997; Zhang et al., 1998]. There are several hypotheses provided in the study of Antonsson: "1) Bax itself may form channels, 2) Bax may destabilize the mitochondrial membrane inducing "lipic holes", 3) Bax may form chimeric channels with the VDAC or the ANT, or 4) Bax may trigger opening of the PTP" [Basañez et al., 1999; Antonsson, 2001].

Bcl-$_{XL}$ is known as a member of the Bcl-2 family and plays an antiapoptotic role in apoptotic signaling. It was demonstrated in some studies that Bcl-$_{XL}$ can interrupt the intrinsic apoptotic pathway by prevention of the release of apoptotic factors such as cytochrome c and AIF from the mitochondria into the cytosol [Liu et al., 1996; Kluck et al., 1997; Yang et al., 1997]. Moreover, Bcl-$_{XL}$ is able to inhibit apoptotic proteins including Bax and caspases [Gill & Perez-Polo, 2008]. The mechanisms of interruption of the apoptotic pathway by Bcl-$_{XL}$ are still under debate. In some studies, it was believed that Bcl-$_{XL}$ inhibits the proapoptotic factor Bax by forming of a heterodimer that prevents the activation of downstream signaling [Aritomi et al., 1997; Takada et al., 2005]. Another explanation of the antiapoptotic activity of Bcl-$_{XL}$ is that Bcl-$_{XL}$ interacts with cytochrome c thus avoiding the formation of the apoptosome [Kharbanda et al., 1997]. Furthermore, the PTP could be a target of Bcl-$_{XL}$. The latter point will be subject of this study.

1.6 The aims of this study

The cerebrovascular diseases are the third leading cause of death after heart attack and cancer in the United States (150074 cases in 2004) and in Germany (67117 cases in 2005) [National Center for Health Statistics, 2004; Statistische Bundesamt Deutschland, 2005]. About one third of the patients will die, and about half of the surviving patients will be left with severe and permanent disability, which has profound negative social and economic effects [Dugan & Kim-Han, 2006].

In stroke, ischemia and hypoxia may cause cell death in the brain. In the core region, where blood supply is interrupted, cell death occurs mostly by necrosis. In the penumbra, cell death occurs by a combination of necrosis and hypoxia-induced apoptosis. Here, neuroprotection could contribute to survival and reduced disability of the patients [Fadeel & Orrenius, 2005; Dugan & Kim-Han, 2006]. Mitochondrial ion channels play a substantial role in apoptosis. The PTP is thought to be responsible for the release of cytochrome c from the mitochondria resulting in apoptosis while the mitochondrial potassium channels, such as the BK-channel and K_{ATP}-channel, contribute to cell survival [Garlid, 2000; Xu et al., 2002]. Therefore, studying the responses of the mitochondrial ion channels to hypoxia and to apoptotic factors will help to understand the pathophysiological process during hypoxia induced apoptosis [Cheng et al., 2008].

In this study, the following problems will be addressed: 1) testing if hypoxia has effects on the mtBK-channel of astrocytes and identifying the kinetic component responsible for the channel activity; 2) testing for effects of hypoxia on the PTP of rat liver at the level of the single-channel and on the PTP of rat brain at the level of the intact mitochondrion; 3) exploring the interaction of the mtBK-channel and the PTP in intact rat-brain mitochondria; and 4) investigating the effects of Bax and Bcl-$_{XL}$ on the mtBK-channel and the PTP for a better understanding of the role of the apoptotic factors and of the mitochondrial ion channels in apoptosis.

2 Materials and methods

2.1 Materials

2.1.1 Instruments

Carl Zeiss	Microscope Axiovert 10
(Jena, Germany)	
CompuMess Elektronik	4-pole-lowpass/highpass filter 902
(Unterschleißheim, Germany)	
Eppendorf	Centrifuge 5417 R
(Hamburg, Germany)	
Harvard Apparatus	Borosilicate glass GC150-10
(Kent, UK)	
HEKA electronics	Amplifier EPC-7
(Lambrecht, Germany)	
Heraeus	Cell culture incubator
(Hanau, Germany)	
Hermle Labortechnik	Centrifuge z-382K
(Gosheim, Germany)	
Ismatec SA	Peristaltic pump REGLO analog; Tygon tubing
(Glattbrug, Switzerland)	
Jahnke und Kunkel	Thermomixer Basic
(Staufen, Germany)	
Knick	Portamess ®751 pH-meter
(Berlin, Germany)	
Märzhauser Wetzlar	Manipulator STM-3
(Wetzlar, Germany)	
Molecular Devices	AD/DA converter Digidata 1322A; pClamp software
(Sunnyvale, CA, USA)	
Nicolet Instrument	Oscilloscope 310
(Madison, WI, USA)	
Olympus	Microscope IMT-2; IX70
(Tokyo, Japan)	
Oroboros	Oxygraph-2k High-resolution respirometry
(Innsbruck, Austria)	
Sartorius AG	Balance MC BB 100

(Goettingen, Germany)

Barry Controls GmbH (Raunheim, Germany)	Shock-absorbing table
University of Giessen, **Machine shop of** **the Dept. of Physiology** (Giessen, Germany)	Pipette puller
Varian Instruments (Walnut Creek, CA, USA)	Cary 100 Conc UV-visible spectrophotometer; Cary Eclipse Fluorescence spectrophotometer

2.1.2 Chemicals and reagents

ICN Biochemicals (Cleveland, OH, USA)	Agar
Merck KGaA (Darmstadt, Germany)	Calcium chloride-dihydrate ($CaCl_2.2H_2O$); Magnesium chloride-hexahydrate ($MgCl_2.6H_2O$); Potassium chloride (KCl); Buffer solution for pH-meter; Dithionite (DTN); Potassium dihydrogen phosphate (KH_2PO_4); Disodium hydrogen phosphate (Na_2HPO_4); Sacrose; Mannitol; Sodium potassium tartrate; Sodium hydroxide (NaOH); Potassium iodiade; Cyclosporin A (CsA)
PAA Laboratories (Pasching, Austria)	Dulbecco's modified Eagle medium (DMEM) (with L-glutamine and sodium pyruvate); Hank's BSS medium
Roche (Indianapolis, IN, USA)	Penicillin; Streptomycin
SERVA (Heidelberg, Germany)	Bovine serum albumin (BSA); Digitonin; Triton X 100
Sigma (Deisenhofen, Germany)	Iberiotoxin; Protease type I; Sodium deoxycholate; Trizma base; Tylosin; Ethylene glycol tetraacetic acid (EGTA); Ethylenediaminetetraacetic acid (EDTA); Malic acid; Safranine O; L-glutamic acid; Cupric sulfate-pentahydrate ($CuSO_4.5H_2O$); 4-(2-hydroxyethyl)-1-piperazineethanesulfonic acid (Hepes)

2.1.3 Buffers

Hypotonic solution	5 mM Hepes, pH=7.2
Hypertonic solution	750 mM KCl, 30 mM Hepes, pH=7.2
Isotonic solution	150 mM KCl, 10 mM Hepes, pH=7.2
Hypotonic solution with 1 µM Ca^{2+}	5 mM Hepes, 1 mM EGTA, 0.952 mM $CaCl_2$, pH=7.2
Hypertonic solution with 1 µM Ca^{2+}	750 mM KCl, 30 mM Hepes, 1 mM EGTA, 0.852 mM $CaCl_2$, pH=7.2
Isotonic solution with 1 µM Ca^{2+}	150 mM KCl, 10 mM Hepes, 1 mM EGTA, 0.875 mM $CaCl_2$, pH=7.2
Hypotonic solution with 200 µM Ca^{2+}	5 mM Hepes, 200 µM $CaCl_2$, pH=7.2
Hypertonic solution with 200 µM Ca^{2+}	750 mM KCl, 30 mM Hepes, 200 µM $CaCl_2$, pH=7.2
Isotonic solution with 200 µM Ca^{2+}	150 mM KCl, 10 mM Hepes, 200 µM $CaCl_2$, pH=7.2
MSE-medium	225 mM mannitol, 75 mM sucrose, 1mM EGTA, 5 mM Hepes, pH=7.4
Hansson medium	125 mM KCl, 20 mM Trizma base, 1 mM $MgCl_2$, 1 µM EGTA, 0.3 mM KH_2PO_4, 0.7 mM NaH_2PO_4, pH=7.4
Biuret reagent (1000 ml)	1.5 g cupric sulfate-pentahydrate, 6 g sodium potassium tartrate, 30 g NaOH and 5 g potassium iodide

2.2 Methods

2.2.1 Preparation of mitochondria from rat liver (RLM)

Wistar rats weighing 250-350 g (about 7 weeks old) were killed by decapitation. The liver was rapidly removed and washed twice in ice-cold isolation medium containing 250 mM sucrose (pH=7.4). After removing blood vessels and clumps, the liver was minced with scissors in a petri dish. The resulting small pieces of liver were homogenized in a solution of 250 mM sucrose and 1 mM EDTA (pH=7.4) and centrifuged for 5 min at 800 × g. The supernatant was filtered by sterile gauze and centrifuged for 4 min at 5100 × g. The pellet was resuspended in isolation medium, homogenized again by hand in a 2-ml tight glass homogenizer, and centrifuged for 2 min at 12300 × g. Resuspension of the pellet in isolation

medium and centrifugation were repeated for 10 min at 12300 × g. The final pellet was resuspended in 1-2 ml solution with 250 mM sucrose and 0.5 mM EDTA (pH=7.4). All procedures were performed at 4 ℃.

2.2.2 Preparation of mitochondria from rat brain (RBM)

Brain mitochondria were prepared from Wistar rats (7 weeks, 250-350 g) for measurement of the $\Delta\Psi$. The rats were killed by decapitation, and the brain was rapidly removed and washed in ice-cold MSE-medium containing 225 mM mannitol, 75 mM sucrose, 1 mM EGTA and 5 mM HEPES (pH=7.4). After removing meninges and major blood vessels, the brain was minced with scissors, homogenized in 10 ml MSE medium with 10 mg protease type I and 0.1% BSA. After homogenization, the medium was diluted by 20 ml MSE-medium with 0.1% BSA. The suspension was centrifuged for 3 min at 2000 × g and the supernatant was centrifuged for 8 min at 12000 × g. The pellet was resuspended in 10 ml MSE-medium with 6 mg digitonin and homogenized by hand in a 2-ml tight homogenizer. After 10 min incubation at 4 ℃ and centrifugation for 10 min at 12000 × g, the final pellet was resuspended in 1-1.5 ml MSE-medium. All procedures were performed at 4 ℃.

2.2.3 Determination of protein concentration of RLM and RBM

The protein concentrations of RLM and RBM were determined by the Biuret method [Layne, 1957]. The Biuret reagent and 0.1% sodium deoxycholate solution were required for the measurement. The formula for the Biuret reagent is (per 1000 ml final volume) 1.5 g cupric sulfate pentahydrate, 6 g sodium potassium tartrate, 30 g sodium hydroxide, and 5 g potassium iodide. One day before use of the Biuret reagent, 3 ml emulgator was added per 100 ml Biuret reagent. 750 µl Biuret reagent, 250 µl 0.1% sodium deoxycholate, and 500 µl distilled water were added in a tube as the blank sample. The standard samples contained 750 µl Biuret reagent, 250 µl 0.1% sodium deoxycholate, 495 µl distilled water, and 5 µl bovine serum albumin (protein concentration: 200 mg/ml) for each of 3 tubes. The test samples A were constituted of 750 µl Biuret reagent, 250 µl 0.1% sodium deoxycholate, 495 µl distilled water, and 5 µl isolated mitochondria for 3 tubes, while test samples B were constituted of 750 µl Biuret reagent, 250 µl 0.1% sodium deoxycholate, 490 µl distilled water and 10 µl isolated mitochondria for each of 3 tubes.

All samples were heated at 95 ºC for 4 min. After vortexing the ultraviolet absorption of the sample was measured by a spectrometer at a wavelength of 540 nm. The values of ΔA_{540nm} of standard samples and of mitochondria were calculated by the following formulas:

$$\Delta A_{540nm} \text{ standard} = A_{540nm} \text{ standard} - A_{540nm} \text{ blank} \tag{1}$$

$$\Delta A_{540nm} \text{ mitochondria sample A} = A_{540nm} \text{ mitochondria sample A} - A_{540nm} \text{ blank} \tag{2}$$

$$\Delta A_{540nm} \text{ mitochondria sample B} = A_{540nm} \text{ mitochondria sample B} - A_{540nm} \text{ blank} \tag{3}$$

$$\Delta A_{540nm} \text{ mitochondria} = \frac{\Delta A_{540nm} \text{ mitochondria sample A} + \Delta A_{540nm} \text{ mitochondria sample B}}{3}$$

$$\tag{4}$$

(A_{540nm} blank: absorbance of blank sample at the wavelength of 540 nm; A_{540nm} standard: absorbance of standard sample at the wavelength of 540 nm; A_{540nm} mitochondria: absorbance of mitochondria sample at the wavelength of 540 nm).

The protein concentration of the isolated mitochondria was calculated as follows:

$$\text{Protein concentration of mitochondria (mg/ml)} = \frac{200 \, (\text{mg/ml}) \times \Delta A_{540nm} \text{ mitochondria}}{\Delta A_{540nm} \text{ standard}}$$

$$\tag{5}$$

The protein concentration of the isolated mitochondria was mostly ranging between 30 and 50 mg/ml.

2.2.4 Cell culture of astrocytes

Mitoplasts for patch-clamp experiments were prepared from astrocytes of the embryonal rat brain [Chamaon et al., 2005]. The cells were cultured in DMEM medium supplemented with 10% FCS, 2 mM L-glutamine, 100 U/ml penicillin, 100 μg/ml streptomycin, and 10 μg/ml tylosin at 37 ºC in a humidified atmosphere with 5% CO_2. The cells were fed and reseeded every third day.

2.2.5 Preparation of mitochondria from astrocytes

After removing of the culture medium from the culture flask, the astrocytes at the bottom of the flask were washed with Hank's BSS (1×) medium twice (first time with 5 ml, second time with 2 ml). Astrocytes were harvested from the bottom of the flask by a sterile cell scraper. Astrocytes from 4-6 culture flasks were collected in about 20 ml Hank's BSS (1×) medium and centrifuged at 800 × g for 10 min. The pellet was resuspended in 1 ml isolation solution (250 mM sucrose and 5 mM HEPES, pH=7.2) and homogenized by hand in a 2-ml tight glass

homogenizer. One fast (9200 ×g, 10 min) and one slow (800 × g, 10 min) centrifugation were performed to separate the fraction of other cellular organelles from mitochondria. Mitochondria from astrocytes were centrifuged at 9200 × g for 10 min again. The pellet was resuspended in 1 ml storage solution (150 mM KCl and 10 mM HEPES pH=7.2) in order to remove the sucrose. All procedures were performed at 4 ºC.

2.2.6 GST-Bax, GST-Bcl-$_{XL}$, and GST protein

GST-Bax, GST-Bcl-$_{XL}$, and GST (Glutathionyl-S-Transferase) protein were kindly provided by Prof. Dr. E. Gulbins (University of Essen, Essen, Germany). Bax (amino acids 1-170) and Bcl-$_{XL}$ were cloned, expressed, and purified as the GST recombinant proteins (GST-Bax and GST-Bcl-$_{XL}$) [Szabo et al., 2008].

2.2.7 Patch-clamp experiments

2.2.7.1 Introduction and history

The patch-clamp technique was developed by Sakman and Neher in 1976 at the University of Göttingen and became a powerful tool in the research of the electrophysiological characteristics of ion channels [Neher et al., 1976; Hamill et al., 1981; Sakmann & Neher, 1995]. By support of the patch-clamp technique, it became possible for the first time to measure the current through single ion channels in the plasma membrane. By means of the patch-clamp technique, the responses of the ion channels to changes of the voltage and the solution at either side of the membrane can be studied throughout the experiments [Safronov & Vogel, 1999]. Several years later, the patch-clamp technique was also applied for studying the ion channels of the mitochondrial membranes [Kinnally et al., 1987; Sorgato et al., 1987; Tedeschi et al., 1987].

2.2.7.2 The patch-clamp setup

The patch-clamp setup is constituted of patch-clamp amplifier, AD/DA converter, and a computer. Additionally, the built-in filter of the amplifier, a separate low-pass filter (8 pole Bessel), an independent pulse generator, and an oscilloscope are required for a patch-clamp setup [Safronov & Vogel, 1999].

Besides these essential devices, further materials are necessary. A pneumatic shock-absorbing table is required to reduce mechanical noise. In order to reduce electrical noise, a Faraday cage was built around the measuring chamber. Moreover, all instruments near measuring

chamber including the Faraday cage are grounded [Safronov & Vogel, 1999]. An inverted microscope is necessary for visual control of catching the mitoplasts by means of the patch pipettes. The mitoplasts are observed with the microscope through the bottom of the dish and are accessible for the measuring pipette from above [Safronov & Vogel, 1999]. An objective of $40 \times$ is employed when the patch pipette is used to access the mitoplasts; an objective of $10 \times$ is employed when the testing solution is applied by the flow system. With a stable hand- and motor-driven micromanipulator, the pipette holder on top of the preamplifier can be flexibly moved to access the mitoplast [Safronov & Vogel, 1999]. The flow system is constituted of a peristaltic pump, tygon tubing, and sewer pipes. A constant stream of test solution is driven by the pump and is provided for the patch by the so-called "sewer pipes". The ion channels within the mitoplast membrane patch can be moved into the openings of the different sewer pipes and thus be tested with different solutions.

2.2.7.3 Fabrication, polishing, and filling of pipettes

Borosilicate glass capillaries were used for pulling the measuring pipettes. Its external and internal diameters were 1.5 mm and 0.86 mm, respectively. In order to prevent scraping the electrode holder, the two ends of the glass capillary were smoothened by means of a flame. The surface of the glass capillary was cleaned with ethanol before the pulling.

The capillary was pulled into two pipettes in two steps. For the first step the current of heating filament was about 16.5 A, for the second step the current was 12.5 A. Sometimes the current was adjusted to get a better geometry and an improved reproducibility of the patch pipettes.

The geometry and the width of the opening of the tip are critical parameters of a patch pipette. The opening of the tip could be tested by reading the bubbling number [Sakmann & Neher, 1995]. A positive pressure was applied in the patch pipette by a 10 ml syringe. The tip of the patch pipette was inserted into methanol solution and air bubbles were observed. The pressure of the syringe was decreased gradually until the small bubbles appeared in the methanol. The reading on the syringe at this moment was the bubble number of the patch pipette [Corey & Stevens, 1983; Safronov & Vogel, 1999]. Mostly the bubble number of the patch pipettes ranged from 4.5 to 5.5 and pipette resistance ranged from 10 to 20 mΩ.

The pipettes were filled with the isotonic solution in 2 steps. First, the tip of the pipette was filled with the isotonic solution by negative pressure provided by a 10 ml syringe. Before the

pipette tip was withdrawn from the isotonic solution, the negative pressure was replaced by positive pressure to prevent clogging by dust at the surface of the isotonic solution. As the second step, the pipette was back filled. Thereafter, it was gently flicked to remove the air bubbles [Safronov & Vogel, 1999]. The filled part of the pipette was about one-third of the whole patch pipette and excess solution was removed from the pipette in order to reduce electrical noise [Safronov & Vogel, 1999]. When the test solution should be applied from pipette inside, the pipette was filled from back side with test solution and from tip side with control solution. It is called back filling. The test solution reaches the tip of pipette accessing the patch membrane by diffusion.

0.1% Agar bridges were made from pipettes after breaking their tips to increase the diameter of the opening. The pipettes were stored in a hypertonic solution at 4 ºC. Before using the pipettes for the patch-clamp experiments, the rear part of the pipette was filled with isotonic solution.

2.2.7.4 Treatment of mitochondria by hypotonic solution

In order to access the IMM, the mitochondria were first treated by a hypotonic solution (150 mM KCl, 10 mM Hepes, pH=7.2) for 30 seconds. The mitochondria swelled because of the osmotic gradient between matrix and hypotonic solution [Siemen et al., 1999]. Finally, the outer membrane broke and the cristae of the inner membrane unfolded. The round and fragile vesicles of IMM called mitoplasts were clearly visible by phase contrast. To some of them remnants of the OMM were still attached. One or several black spots at the surface of the vesicles were observed frequently. They are thought to be the contact points of the inner and the outer membrane and are called caps (Fig.7) [Siemen et al., 1999]. The mitoplasts from astrocytes (radius about 5 µm) were larger than the mitoplasts from liver cells (radius about 2 µm). According to the formula

$$A = 4\pi r^2 \tag{6}$$

the surface areas of mitoplasts from astrocytes and from liver cells were calculated as 314 μm^2 and 50 μm^2, respectively (A: area; r: radius; π: mathematical constant). A mitoplast that was floating close to the bottom of the experimental chamber was the best target for the patch pipette [Siemen et al., 1999].
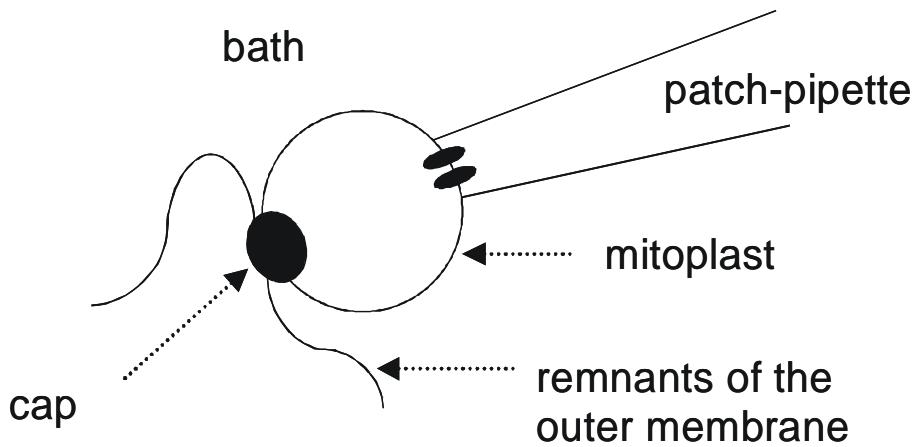
Fig. 7: Scheme of a patch pipette with a mitoplast in the mitoplast-attached mode [from Siemen et al., 1999].

2.2.7.5 Formation of a seal and current recording in patch-clamp experiments

The pipette was mounted tightly to a pipette holder and was connected to the pressure system. The pressure was applied by a water column from a U-shaped glass tube connected to the holder [Safronov & Vogel, 1999]. Positive pressure was applied to the system causing a constant stream of solution out of the pipette tip to push the unwanted particles away. Negative pressure (*i.e.* suction by mouth) was applied when the pipette was near to the target mitoplast [Safronov & Vogel, 1999]. Occasionally, seals were formed without any suction, however, normally, very gentle suction was necessary. Usually, it took 1 to 10 min to form a reliable seal with a resistance that was commonly in the range of 800 MΩ to 2 GΩ.

In single-channel experiments with mitoplasts from astrocytes, a good seal resistance (> 0.5 GΩ) was obtained in 5 out of about 10 patches. In 1 out of them current through the mtBK-channel was present and was recorded. With a probability of about 20%, two or more mtBK-channels could be measured in a single patch. This means that 20% of the good patches (1 out of 5 patches with a good seal resistance) possessed one or more activated mtBK-channels; 20% of these patches showed 2 mtBK-channels. Thus, the probability of the presence of one mtBK-channel in a good patch was calculated as:

$$(80\% * 1 + 20\% * 2) / 5 = 24\% \tag{7}$$

Occasionally, a patch was obtained with remnants of the OMM instead of the IMM. Under this condition, a large single-channel current with a conductance of 400 pS was recorded. According to its voltage-dependence and conductance, this channel was identified as the VDAC, which is present in the OMM, only. This result further supports that the patches were obtained from mitochondrial membrane rather than the plasma membrane.

Usually, I obtained a patch in the cell-attached mode. Thereafter, the gain was increased to 20 mV/pA for single-channel recording of the PTP and to 50 mV/pA for single-channel recording of the mtBK-channel. The currents through the channels were low-pass filtered at a corner frequency of 0.5 kHz and sampled at a frequency of 2.5 kHz by means of the software Clampex 9.2. I chose a recording duration of 1 min and mostly measured at holding potentials (E_H) ranging from -60 mV to +60 mV.

2.2.7.6 Data analysis

Data were analyzed using the pClamp 9.2 software, as well. Voltages in text and figures were given as at the inner side of the mitoplasts, throughout. Inward currents were defined downward. The open probability (P_o) means the probability of the channel in the open state.

P_o of the mtBK-channel was calculated by means of the single-channel search mode of the pClamp software. In this mode, the open state and the closed state of the individual channels were determined automatically with high speed. Events shorter than 0.5 ms were ignored as they consisted of one sample only. Thus, their amplitude could not be properly determined. Currents exceeding 50% of fully open currents (including obvious substates) were considered as the open state of the channel, while substates currents smaller than 50% of the fully open currents were counted as closed state. After detection of the events, open probability, dwell times of the open state and of the closed state were determined by Clampfit. Furthermore, the open time constant and the closed time constant were calculated from the dwell times of the open state and of the closed state.

The open probability of the PTP was determined by means of an all-points analysis. For this purpose, currents were recorded for one minute and analyzed point by point for the amplitudes which were drawn as histograms [Loupatatzis et al., 2002]. Occupation of the open or the closed states was determined as the area (A_n) below the corresponding Gauss-curve and weighed by their corresponding current amplitude (B_n) [Andrabi et al., 2004]. Occupation of the weighed open-state area divided by the total area weighed by the maximum-current amplitude gave the P_o, which was calculated by the following formula:

$$P_o = \frac{(A_1 \times B_1) + (A_2 \times B_2) + ... + (A_n \times B_n)}{B_{max}(A_0 + A_1 + A_2 + ... A_n)} \tag{8}$$

P_o is the probability of the PTP in the open state. A_0 is the area under the Gaussian curve of closed state and A_n is area under the Gaussian curves of open state and different substates. B_n are the different amplitudes of the substates. B_{max} is the largest one of them [Loupatatzis et al., 2002].

2.2.8 Measurements of the ΔΨ

ΔΨ was estimated by the safranine O method [Åkerman et al., 1976]. Safranine O is a biological dye that is used in histology and cytology. Its chemical structure is $C_{20}H_{19}N_4Cl$ (Fig.8). It was used at a concentration of 5 µM in experiments performed in Hansson medium. Accumulation of safranine O inside the mitochondria was driven by ΔΨ and subsequently results in a decrease of fluorescence intensity. If the mitochondria depolarize, safranine O will be released and the intensity of the fluorescence will increase. Changes of safranine O fluorescence were recorded using a CARY Eclipse fluorescence spectrophotometer operating at excitation and emission wavelengths of 525 nm and 587 nm, respectively.
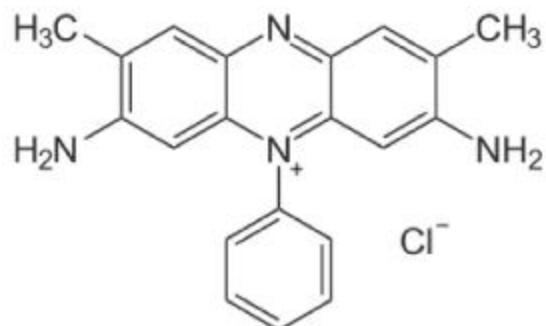
Fig. 8: The chemical structure of safranine O

2.3 Statistical analysis

Statistical evaluation was carried out by t-test with Microsoft Excel 2000. Data were given as means ± SEM or SD by means of software OriginPro 7.5. $p < 0.05$ was considered significant, $p < 0.01$ was considered highly significant, and $p < 0.001$ was considered extremely significant.

3 Results

3.1 Identification of the BK-channel in mitochondria of astrocytes

The mtBK-channel had been identified in brain-glioma cells and in cardiac cells, but not in astrocytes yet [Siemen et al., 1999; Xu et al., 2002]. In order to test for the presence of the BK-channel also in the mitochondria of astrocytes, I started recording current from mitoplasts from rat astrocytes by means of the patch-clamp technique. In about 60 out of 300 patches with good seal resistance, the single-channel current was present and recorded. Two or more mtBK-channels were present in a single patch with a probability of about 20%. That means that 20% of the good patches (60 out of 300 patches with a good seal resistance) possessed one or more activated mtBK-channels; 20% of these patches showed 2 mtBK-channels. Thus, the probability of the presence of one mtBK-channel in a good patch was 24% (equation 7). Occasionally, a substate of the channel showed a smaller current than that of the fully open state.

The mean amplitude of the single-channel current was 13.1 ± 1.3 pA (n=7) at +40 mV and -4.6 ± 1.3 pA at –20 mV. To identify this channel in the mitoplasts of astrocytes, I used the BK-channel selective inhibitor Ibtx. As the toxin was applied from the pipette side, I had to use the method of "backfilling". At first, the tip of the pipette was filled with isotonic solution, then 100 nM Ibtx was filled in from the backside of the pipette. The concentration of Ibtx in the tip of the pipette was increasing gradually by the diffusion. After about 90 min, Ibtx reached the patch membrane and blocked the mtBK-channel.
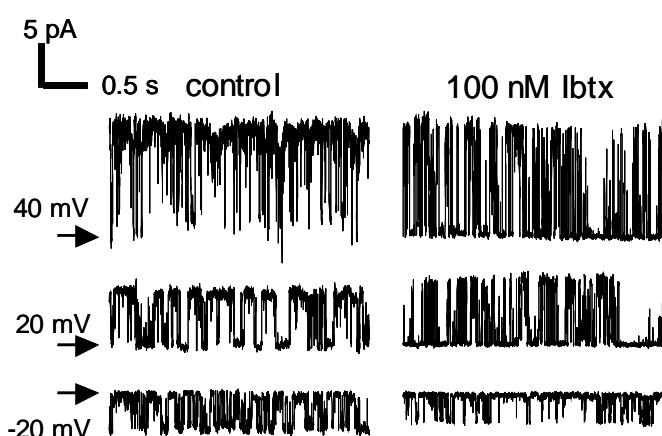
Fig. 9: Blockade of the mtBK-channel by Ibtx. The current through the mtBK-channel from astrocyte mitochondria was recorded at –20 mV, +20 mV, and +40 mV in symmetrical isotonic KCl solution (control, left panel, closed state always marked by arrows). After 93 min, when the diffusion of 100 nm Ibtx to the patch was assumed to be complete, records were taken again (right panel).

The open probability (P_o) of the mtBK-channel in control and after diffusion of 100 nM Ibtx was determined by single-channel search (see: Methods). The mean P_o at potentials ranging between -40 mV and +40 mV was calculated from 3 independent experiments and is shown in Fig. 10. A mostly significant decrease of the mean P_o was demonstrated under the influence of 100 nM Ibtx.
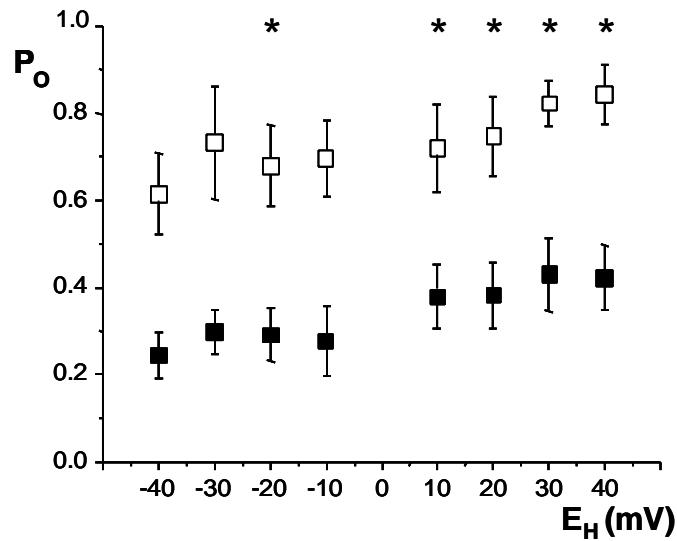
Fig. 10: Decrease of P_o of the mtBK-channel by 100 nM Ibtx. The P_o of the mtBK-channel at potentials ranging from -40 mV to +40 mV is shown. The P_o before (open squares) and after diffusion (filled squares) of 100 nM Ibtx indicated reduced activity of the mtBK-channel. P_o was decreased at all potentials and the mean P_o was decreased by 54.2 ± 1.9% (significantly at -20 mV, +10 mV, +20 mV, +30 mV, and +40 mV; $p<0.05$), error bars give SD.
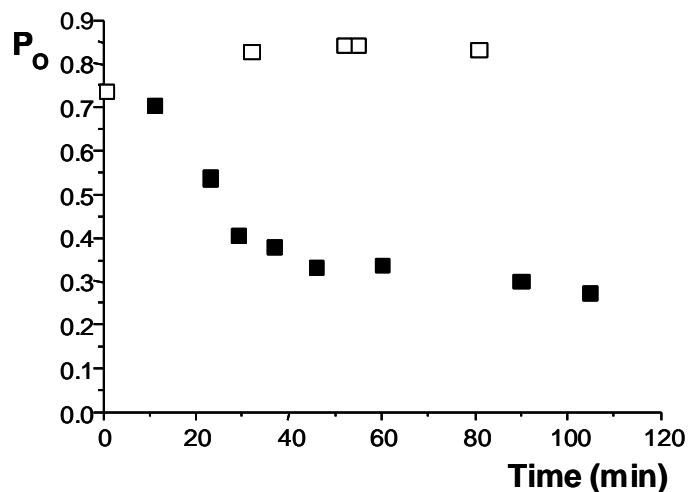
Fig. 11: Time course of P_o of the mtBK-channel during diffusion of Ibtx. Same experiment as in Fig. 9, Ibtx was back filled into the pipette. The control experiment without added Ibtx (open squares) did not show any decrease of P_o. The experiment with 100 nM Ibtx (filled squares) reflects the progress of Ibtx. During diffusion, P_o decreased gradually corresponding to the increase of the Ibtx concentration at the patch membrane.

The characteristics of the described single-channel activity are namely 1) a single-channel conductance of 296 ± 18 pS (n=7, determined from the current-voltage relation in Fig. 13), 2) a voltage dependence of P_o at least at depolarizing potentials, 3) Ca^{2+} dependence (shown in next part), and 4) sensitivity to the BK-channel selective inhibitor Ibtx. These characteristics make it very likely that the observed channel activity is caused by a mitochondrial $K_{(Ca)}$-channel of the BK-type, a so-called mtBK-channel, which was described earlier [Siemen et al., 1999; Gu et al., 2007].

3.2 Activation of the mtBK-channel by hypoxia

3.2.1 Activation of the mtBK-channel by nitrogen (N_2)-induced hypoxia

Hypoxia-induced apoptosis is the reason for cell death in stroke. Therefore, it is of high interest to study the response of the mitochondrial ion channels to hypoxia. In order to induce hypoxia at the mtBK-channel, the isotonic solution (containing 1 µM Ca^{2+}) was bubbled with 100% N_2 for two hours. The oxygen content of the hypoxic solution was measured in the closed chamber of the Clark-electrode of an OROBOROS respirometer. The oxygen content of the N_2-bubbled solution was determined to be 21.1 ± 1.2 nmol/ml (n=5), as compared with 222.3 ± 13.1 nmol/ml after stirring the same solution for 17 min in the open chamber.

The single-channel recording of the mtBK-channel in Fig. 12 demonstrated a considerable increase of P_o measured in the hypoxic solution as compared with the control solution (both containing 1 µM Ca^{2+}). After testing in hypoxic solution, the patch with the mtBK-channel was switched into control solution again. It was observed that the activity of the mtBK-channel recovered and was even smaller than before hypoxia indicating that the effect of hypoxia on the mtBK-channel is reversible.
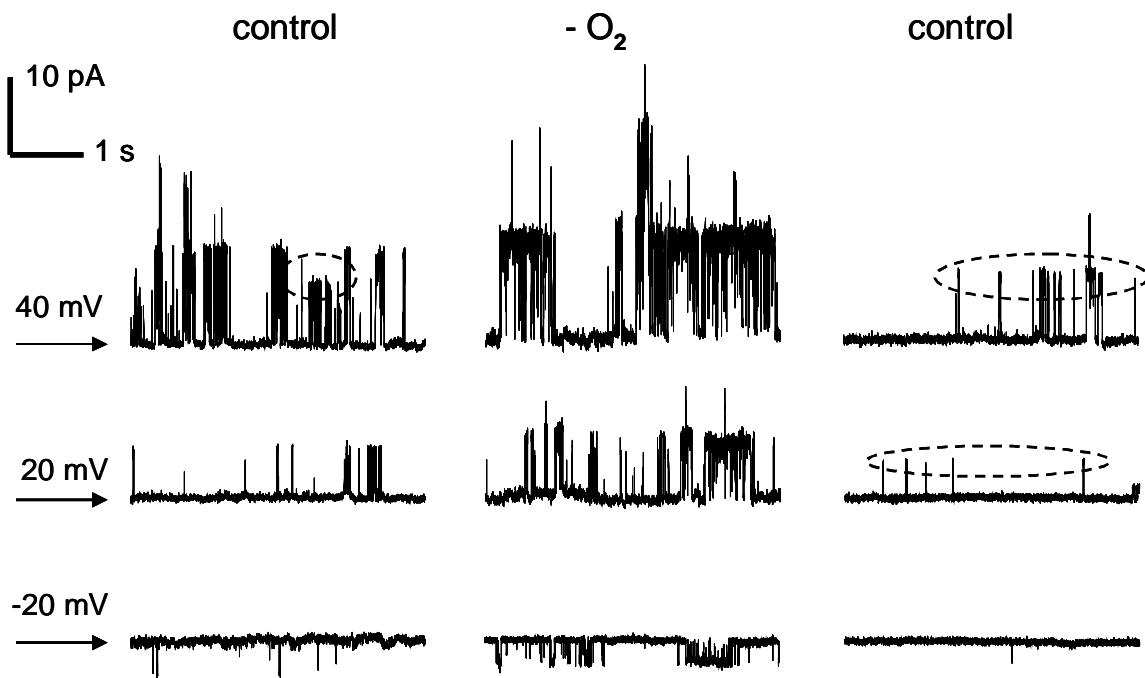
control   - O$_2$ control

Fig. 12: Increased activity of the mtBK-channel under N$_2$-induced hypoxia. For testing the effect of hypoxia, a control solution (containing 1 µM Ca^{2+}, which may not be too far from the physiological cellular Ca^{2+} concentration) and a hypoxic solution (control solution bubbled by 100% N$_2$ for 2 hours) were used. Single-channel recordings at three different potentials demonstrated an increased activity of the mtBK-channel. Arrows mark the closed state of the mtBK-channel. At least 2 mtBK-channels were present in this patch. The mtBK-channel occasionally switched to substates of smaller conductance (marked by circles), which were more frequent in the control after hypoxia in this patch.
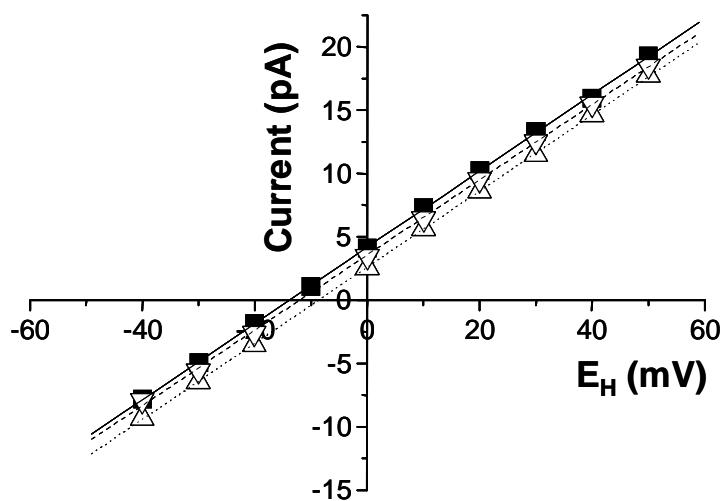
Fig. 13: Current-voltage relations of the mtBK-channel under hypoxia. The slope of the current-voltage relations showed that the full conductance of the mtBK-channel was not changed by hypoxia (one out of 3 experiments). The mean reversal potential is -5.5 ± 2.2 mV (n=3) in control solution (open triangle, tip up). Hypoxia shifted the reversal potential by 5.0 ± 0.4 mV (n=3) into the negative direction (filled squares). This shift was

partially reversible in control solution after hypoxia (open triangle, tip down). Straight drawn by linear regression.

The increase of the mean P_o (n=3) by N_2-induced hypoxia is quantified in Fig. 14. Additionally, panel A (with the absolute P_o values) and panel B (with the normalized P_o values) demonstrate an increased activity of the mtBK-channel at depolarizing potentials, which matches the voltage dependence of the mtBK-channel that was described in earlier studies [Gu et al., 2007; Siemen et al., 1999]. Even at very small P_o values, the P_o values measured in hypoxic solutions tend to be insignificantly larger than the controls. This becomes clearer if P_o is drawn on a logarithmic scale (not shown, but compare Fig. 16B). P_o was always smaller in the control after hypoxia than that in the control before.
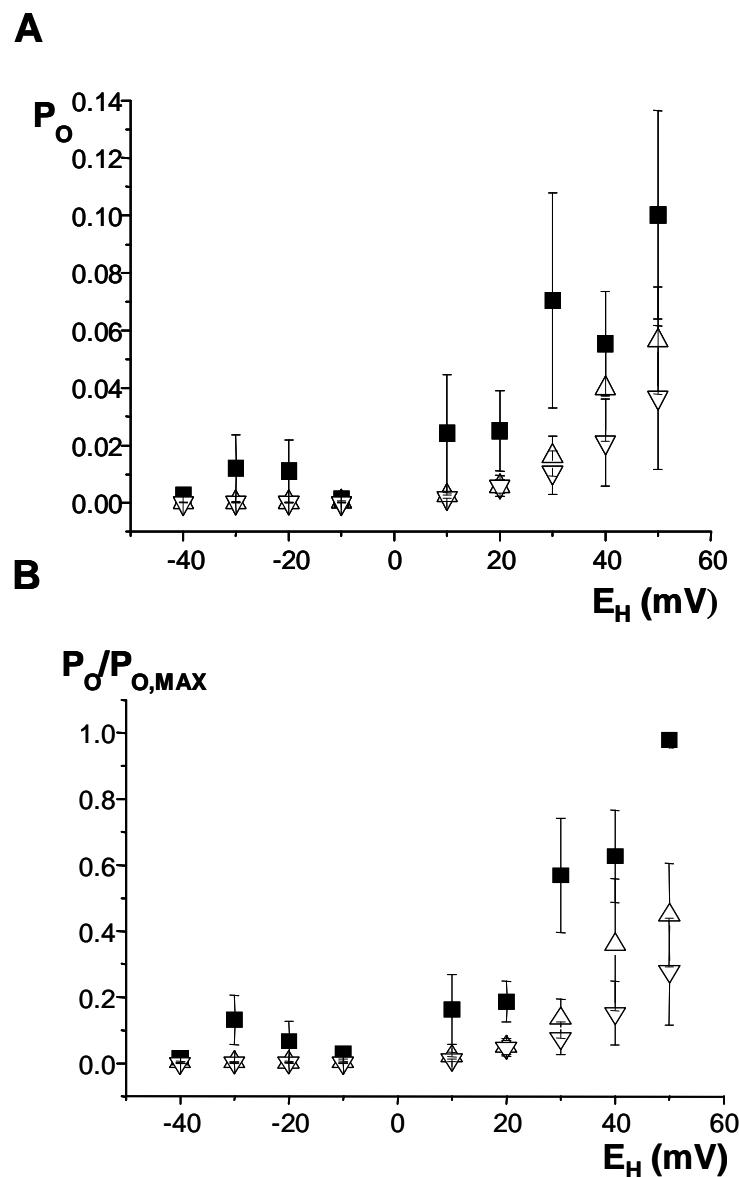
Fig. 14: Increased P_o of the mtBK-channel by N_2-induced hypoxia. The increase of P_o by N_2-induced hypoxia becomes more obvious at larger P_o values, *i.e.* at more positive potentials. **A)** Increased P_o in hypoxic solution (filled squares) as compared with control solution (before hypoxia: open triangle, tip up, and after hypoxia: open triangle, tip down, n=3). Control solution and hypoxic solution contained 1 μM Ca^{2+} so that the Ca^{2+}-activated mtBK-channel showed little activity only ($P_o < 0.15$ at all potentials and almost 0 at negative potentials). (Note: larger P_o induced by 200 μM Ca^{2+} in Fig. 9 for comparison). **B)** P_o normalized to largest P_o of the experiment ($P_o/P_{o,max}$). Values during hypoxia differed significantly from control values before hypoxia at +30 mV and at +50 mV (p<0.05) and from control values after hypoxia at +20 mV and +30 mV (p<0.05), at +40 mV (p<0.02), and at +50 mV (p<0.01, error bars give SD).

3.2.2 Increased activity of the mtBK-channel by DTN-induced hypoxia

Dithionite (DTN) is well-known for removing oxygen from solutions. Since I found that hypoxia induced by N_2 modified the ion channel activity, I tested furthermore whether 1 mM sodium-dithionite containing solutions had the same effect. When checking the pH after DTN-application small amounts of O_2 leaked into solution causing hypoxia instead of anoxia.
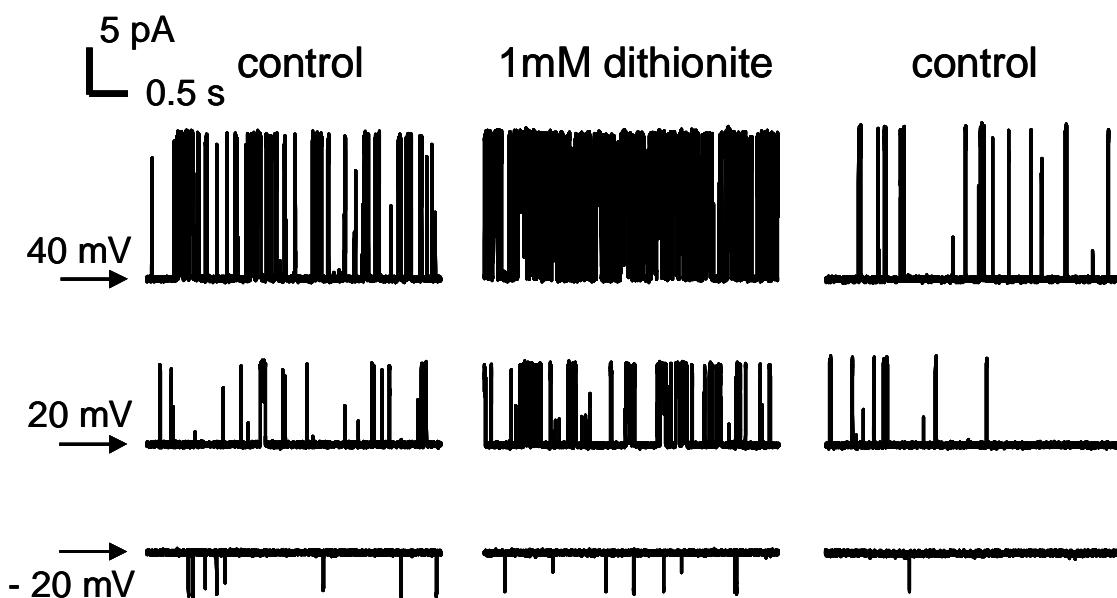
Fig. 15: DTN-induced hypoxia increased the activity of the mtBK-channel. Single-channel recordings of the mtBK-channel before, during, and after application of 1 mM DTN solution are shown at -20 mV, +20 mV, and +40 mV. The activity of the channel was remarkably increased in DTN solution and recovered in control solution (closed state marked by arrows).

It turned out that the P_o of the mtBK-channel was reversibly increased by 1 mM DTN (Fig. 15). P_o was larger in 1 mM DTN-solution as compared to control solutions without DTN (n=4; absolute values in Fig. 16A). Again the P_o values were larger in the depolarizing range showing the voltage dependence of the mtBK-channel. The P_o values in the controls after DTN were smaller than the controls before. Thus, the activity of the mtBK-channel was

regulated by DTN-induced hypoxia in the same way as it was regulated by N_2-induced hypoxia. In order to demonstrate the difference clearer, the P_o was drawn on a logarithmic scale in Fig. 16B. Data could be fitted by a straight line, whose steepness did not change in DTN. An e-fold change of P_o was caused by a change of holding potential of 13.2 mV (control before), 13.6 mV (1 mM DTN), and 9.9 mV (control after) to the depolarizing direction, of which an e-fold increase of P_o is achieved by a depolarization (e: base of natural logarithm ≈ 2.718).
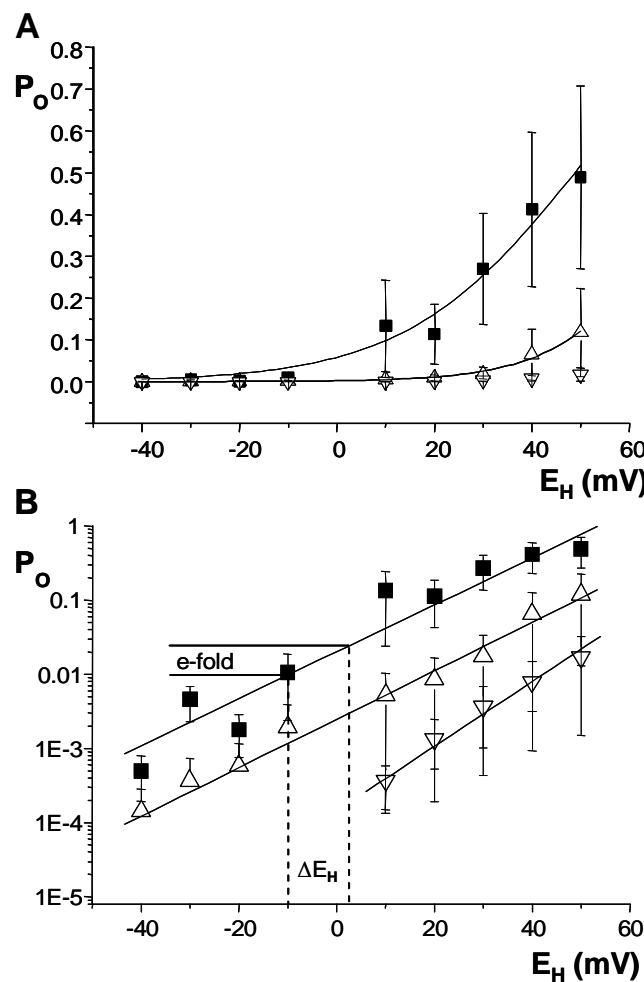
Fig. 16: P_o of the mtBK-channel was increased by DTN-induced hypoxia (n=4). A) P_o in 1 mM DTN solution (filled squares) was larger than in control solution (before hypoxia: open triangle, tip up, and after hypoxia: open triangle, tip down) at the potentials ranging from -40 mV to +50 mV (continuous curve fitted by Boltzmann equation). **B)** Same data on logarithmic scale demonstrate an increase of P_o also at negative potentials. Data can be fitted by a straight line. Increase of the holding potential that induces an e-fold change of P_o is a measure for the voltage dependence of the channel, which is unchanged by DTN. Shift of the fits for control data (before) and for DTN data was -25 mV (determined at $P_o = 0.5$; fits differed slightly in steepness) in A and -29 mV in B, respectively (error bars give SD).

Fig. 17 demonstrates the results of a dwell-time analysis for the experiment of Fig. 15 as histograms of a one-minute segment. The left panel shows the open-time distribution while the right panel demonstrates the closed-time distribution. A least-square fit (the red curve) of the histogram gives best results with two exponentials for the open times and three exponentials for the closed times. The resulting time constants (τ-values) are collected in Table 1. The DTN-induced hypoxia increases the second open-time constant and it increases the slowest closed time constant. The detailed time constants are given in Table 1.
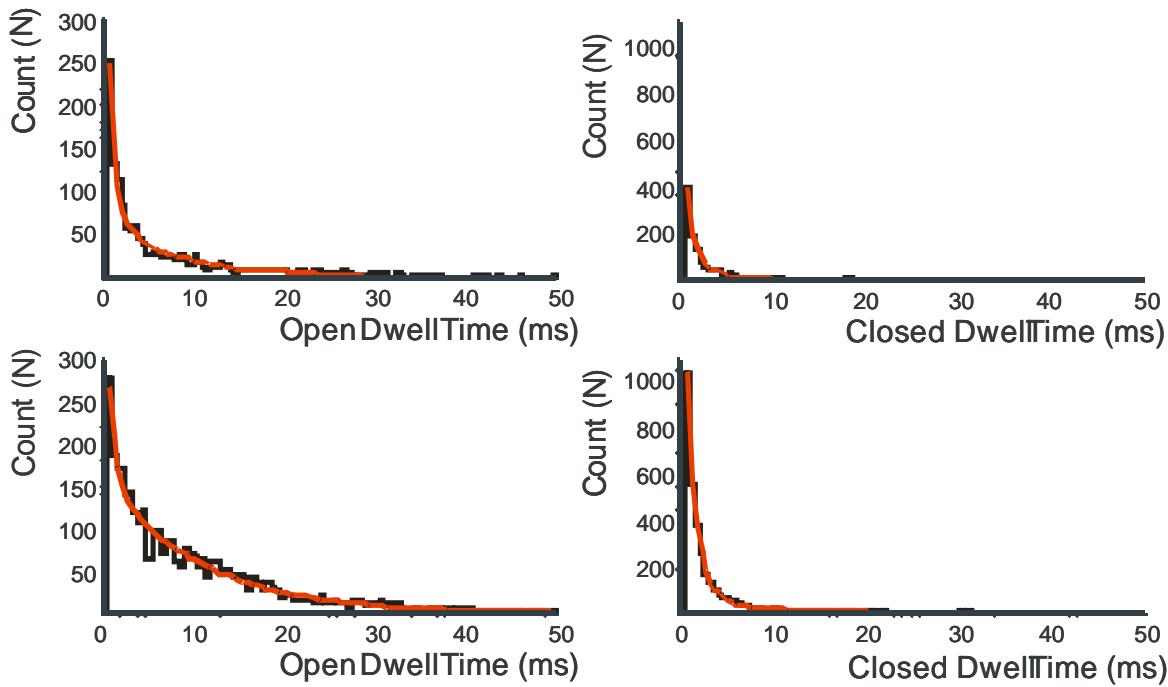
Fig. 17: Histograms of open and closed times of the mtBK-channel. Open–time histograms (left) and closed-time histograms (right) of the experiment of Fig. 15 at +40 mV before (upper panel) and during (lower panel) application of DTN solution as determined by all-points analysis. The distributions of open-time histogram and of closed time histogram were fitted by the exponential curves. Distributions of open-time histograms were fitted by two exponentials (the red curves), distributions of closed-time histograms by three exponentials (the red curves, the time constants are given in Table 1).

	control before	1 mM DTN
Open time constants (τ_O)	$\tau_{O,1} = 0.70$ ms	$\tau_{O,1} = 0.82$ ms
	$\tau_{O,2} = 7.63$ ms	$\tau_{O,2} = 10.80$ ms
	$\tau_{C,1} = 0.06$ ms	$\tau_{C,1} = 0.24$ ms
Closed time constants (τ_C)	$\tau_{C,2} = 1.05$ ms	$\tau_{C,2} = 1.27$ ms
	$\tau_{C,3} = 6.68$ ms	$\tau_{C,3} = 8.16$ ms

Tab. 1: Time constants of the mtBK in control and under DTN (at +40 mV).

3.3 Inhibition of the PTP by hypoxia

It is our working hypothesis deduced from earlier experiments that mitochondrial potassium channels are keeping the PTP closed [Garlid et al., 1997]. Therefore, I tested if hypoxia has an effect on the PTP itself. The single-channel current through the PTP from RLM was measured in control solutions and in test solutions in which hypoxia was induced by 1 mM DTN. In these experiments inhibition of the PTP was observed (Fig. 18).
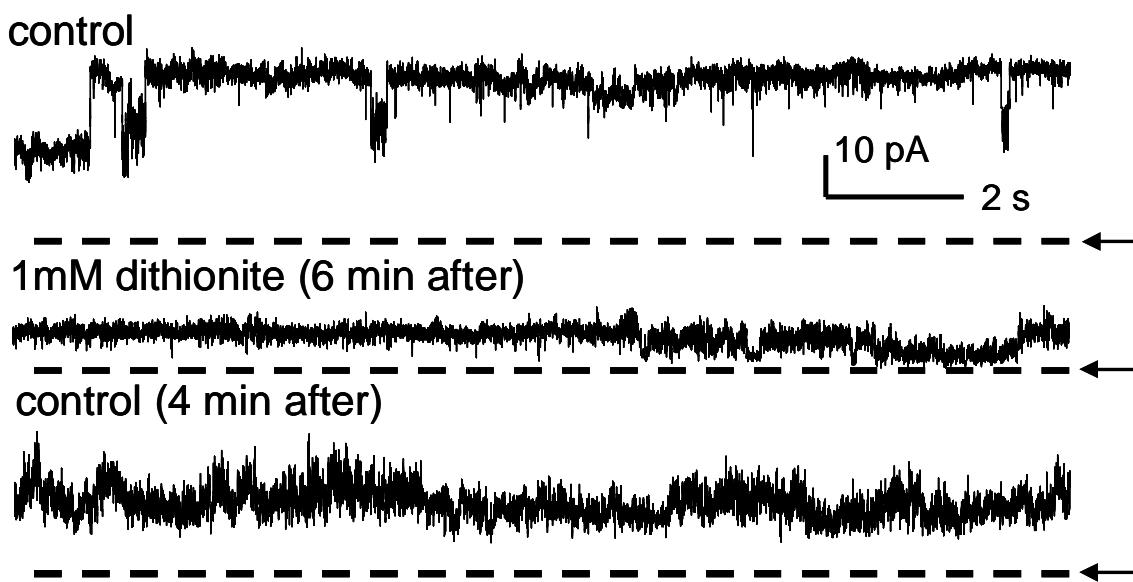
Fig. 18: DTN-induced hypoxia inhibits the PTP of RLM. The single-channel current through the PTP was recorded in the mitoplasts from rat liver at +20 mV. Control records showed a large conductance (> 1 nS) with multiconductance substates (upper panel). During application of 1 mM DTN, the activity of the PTP is remarkably decreased (central panel). During washout of DTN in control solution, the current did not recover (lower panel). Closed states of the channel are marked by dashed lines and arrows.

Moreover, the PTP was also tested in a solution, which was bubbled with 100% N_2 for 2 hours. As was seen when inhibiting the PTP by 1 mM DTN containing solutions, the N_2-induced hypoxia reduced the activity of the PTP irreversibly. The P_o of the PTP before, during, and after hypoxia induced by 1 mM DTN and by N_2-bubbling are shown in Fig. 19 (n=4).
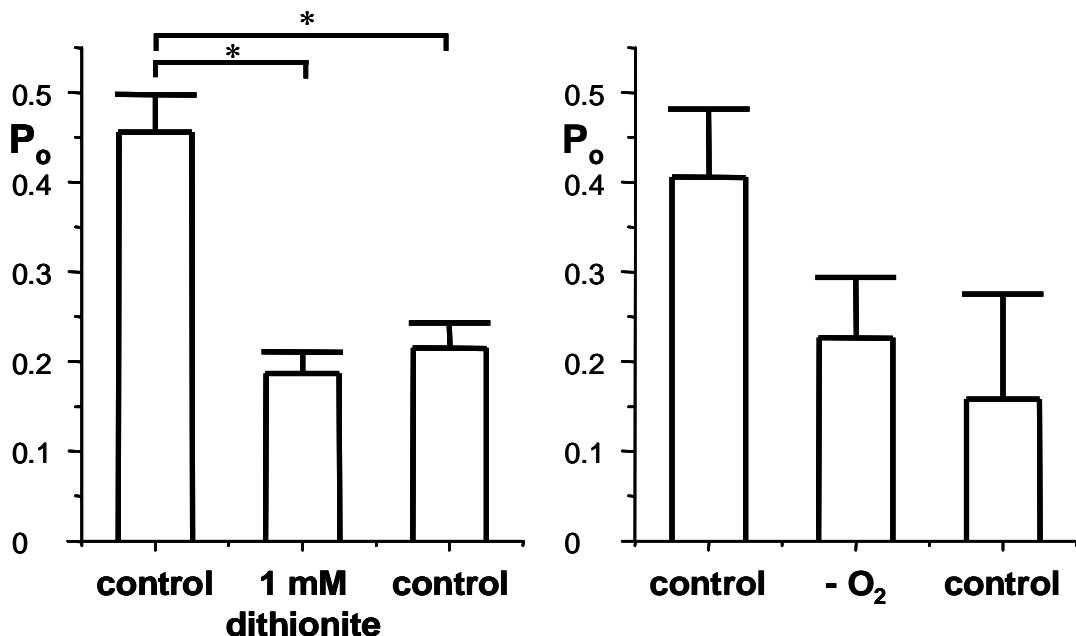
Fig. 19: Reduced P_o of the PTP by hypoxia. In the left panel, the mean P_o of the PTP was 0.45 ± 0.04 in the control solution at +20 mV. Under hypoxia induced by 1 mM DTN, P_o was significantly decreased by 57% to 0.19 ± 0.02 (n=4). After 1 mM DTN, the mean P_o was 0.22 ± 0.03 (p<0.05, left panel, significance marked by *). The right panel demonstrates that the mean P_o was insignificantly decreased by 44% in a N_2-bubbled solution (n=4, P=0.07). The mean P_o before, during, and after N_2-induced hypoxia was 0.41 ± 0.08, 0.23 ± 0.07, and 0.16 ± 0.12, respectively (error bars give SEM).

3.4 Interaction of the mtBK-channel and the PTP

In order to check if the effects of hypoxia on mitochondrial ion channels of rat liver cells and rat astrocytes measured in the patch-clamp experiments were trustworthy, I repeated the experiments in intact RBM. For this purpose, $\Delta\Psi$ was measured by means of application of safranine O to intact RBM. The experiments were carried out in Hansson medium containing 5 µM safranine O, whose fluorescence intensity was measured using a fluorescence spectrophotometer. After addition of the mitochondria to the Hansson medium, safranine O was accumulated in the mitochondria by their negative $\Delta\Psi$ resulting in a decrease of the fluorescence intensity. When the mitochondrial membrane depolarized, safranine O lost its driving force into mitochondria and was released into the medium leading to an increase of fluorescence intensity.
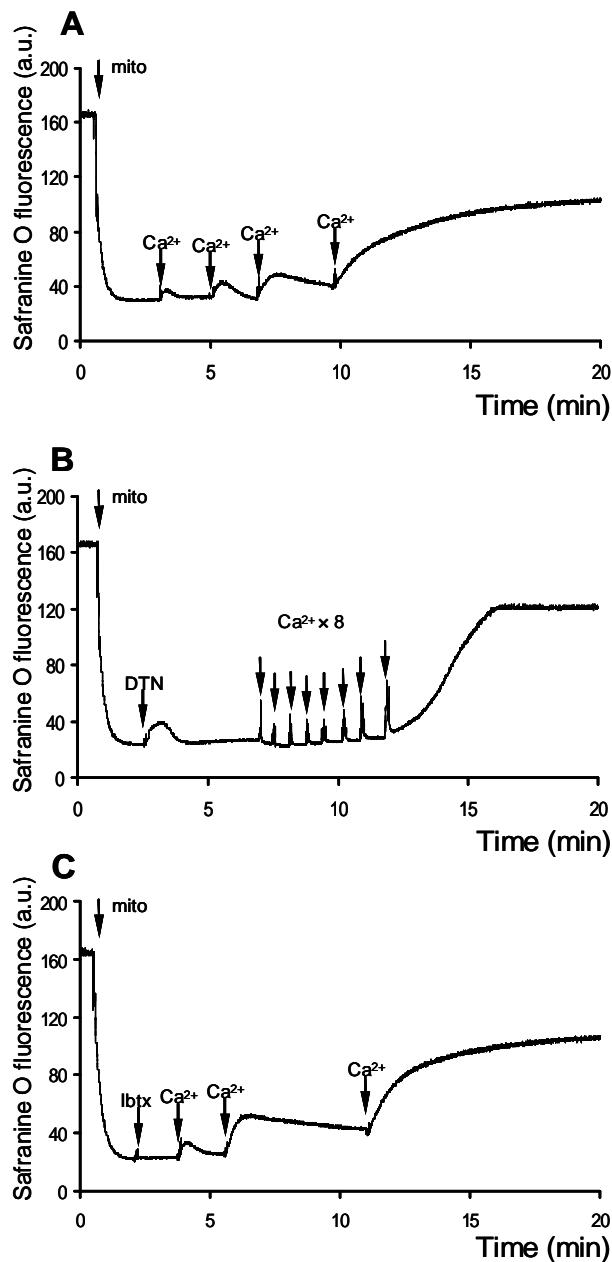
Fig. 20: ΔΨ measurements with intact RBM. Recordings of potential-dependent safranine O uptake (in arbitrary units) demonstrate impaired opening of the PTP in DTN and improved opening after Ibtx-blockade of the mtBK-channel. Increased extramito-chondrial dye corresponds to a depolarization. **A)** In control experiment depolarization of the mitochondrial membrane was induced by 4 times application of 50 μM Ca^{2+}. **B)** After addition of 1 mM DTN more Ca^{2+} (8 times application of 50 μM) was required to induce depolarization. **C)** After addition of the BK-channel inhibitor Ibtx (100 nM) less Ca^{2+} (3 times application of 50 μM) was required to induce depolarization. Each panel stands for 5 comparable experiments from different preparations with similar results.

Addition of Ca^{2+} induced opening of the PTP, which causes depolarization of the mitochondrial membrane. By titration with aliquots of 50 μM Ca^{2+} in Hansson medium, it turned out that 200 μM Ca^{2+} were able to induce depolarization of the mitochondrial membrane (Fig. 20A). In control experiments with 10 μM CsA, application of 400 μM Ca^{2+}

was necessary to induce a depolarization making it likely that the decline in membrane potential was due to Ca^{2+}-activation of the PTP. After addition of 1 mM DTN also 8 aliquots of Ca^{2+} corresponding to 400 µM were required to induce a continuing depolarization (Fig. 20B). After application of the BK-channel inhibitor Ibtx (100 nM), only 150 µM Ca^{2+} were required to induce depolarization of mitochondrial membrane (Fig. 20C). The corresponding mean values of Ca^{2+} requirement of 5 experiments from 5 independent preparations were 190 ± 10 µM, 280 ± 33 µM, and 140 ± 10 µM for the controls, 1 mM DTN, and 100 nM Ibtx, respectively (means ± SD). As compared with the Ca^{2+} requirement for controls, a significant increase was observed with 1 mM DTN ($p<0.05$) and a highly significant decrease with 100 nM Ibtx ($p<0.01$). In summary, DTN increased the concentration of Ca^{2+} required for opening of the PTP and the BK-channel inhibitor Ibtx reduced the Ca^{2+} required for opening of the PTP.

3.5 The effects of Bax and Bcl-$_{XL}$ on the mtBK-channel

3.5.1 Absence of "rundown" of the mtBK-channel

In order to test the effects of GST-Bax on the mtBK-channel from the cytosolic side, GST-Bax was filled into the pipette from backside. After diffusion, GST-Bax reached the tip of the pipette and there its concentration increased over time. However, GST-Bax is a large molecule with a molecular weight of about 50 kDa. Thus, diffusion went slowly. Therefore, the spontaneous change of the mtBK-channel activity during the diffusion was checked.

A typical phenomenon of several types of ion channels is called "rundown". It means that the activity of the ion channels decreases, and they may even disappear over time [Hille, 2001]. In order to find out whether there exists a rundown of the mtBK-channel activity during diffusion of GST-Bax, a control experiment was carried out. A patch with mtBK-channel was made and recorded for about two hours at different potentials. Comparing the P_o of the mtBK-channel at the start and two hours later, there was almost no change of the activity of the mtBK-channel at all potentials (Fig. 21).
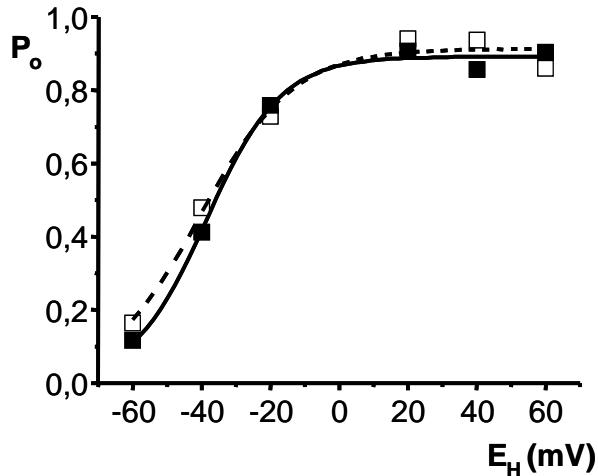
Fig. 21: P_o of the mtBK-channel at the start of the experiment and two hours later.
A patch with mtBK-channel was obtained with a mitoplast from rat astrocytes. The Patch lasted for more than two hours. The mtBK-channel was recorded at the start (open squares, fitted by dashed curve) and 2 hours later (filled squares, continuous curve) at -60 mV, -40 mV, -20 mV, +20 mV, +40 mV, and +60 mV. Voltage dependence of the mtBK-channel is demonstrated. Comparing P_o at the start of the experiment and after two hours showed almost no difference between the fitted curves.

3.5.2 GST-Bax in pipette blocks the mtBK-channel

Since in the earlier study the mitochondrial $K_{V1.3}$ channel was modulated by GST-Bax with a concentration of 1 nM, I firstly tested the mtBK-channel also with 1 nM GST-Bax [Szabo et al., 2008]. For the patch-clamp experiments testing GST-Bax, the tip of the pipettes was filled with isotonic solution without GST-Bax and isotonic solution with 1 nM GST-Bax was filled into the pipette from the backside. Thereby, the concentration of GST-Bax in the tip increased slowly (Fig. 22A). 6 experiments were carried out. These 6 experiments lasted in the range of 40 minutes to 2 hours and the mean value of their duration was 80 minutes. After diffusion of GST-Bax to the patch membrane, the activity of the mtBK-channel was decreased at all potentials measured. However, after diffusion the conductance of the fully open state of the mtBK-channel was unchanged.

A

diffusion

1 nM GST-Bax

mitoplast

no bax

B **before diffusion** **after diffusion**

40 mV

-40 mV

10 pA

1 s

(reversal potential at −17 mV)

C P_o

* * * ** *

1,0

0,8

0,6

0,4

0,2

0,0

-60 -40 -20 0 20 40 60

E_H (mV)
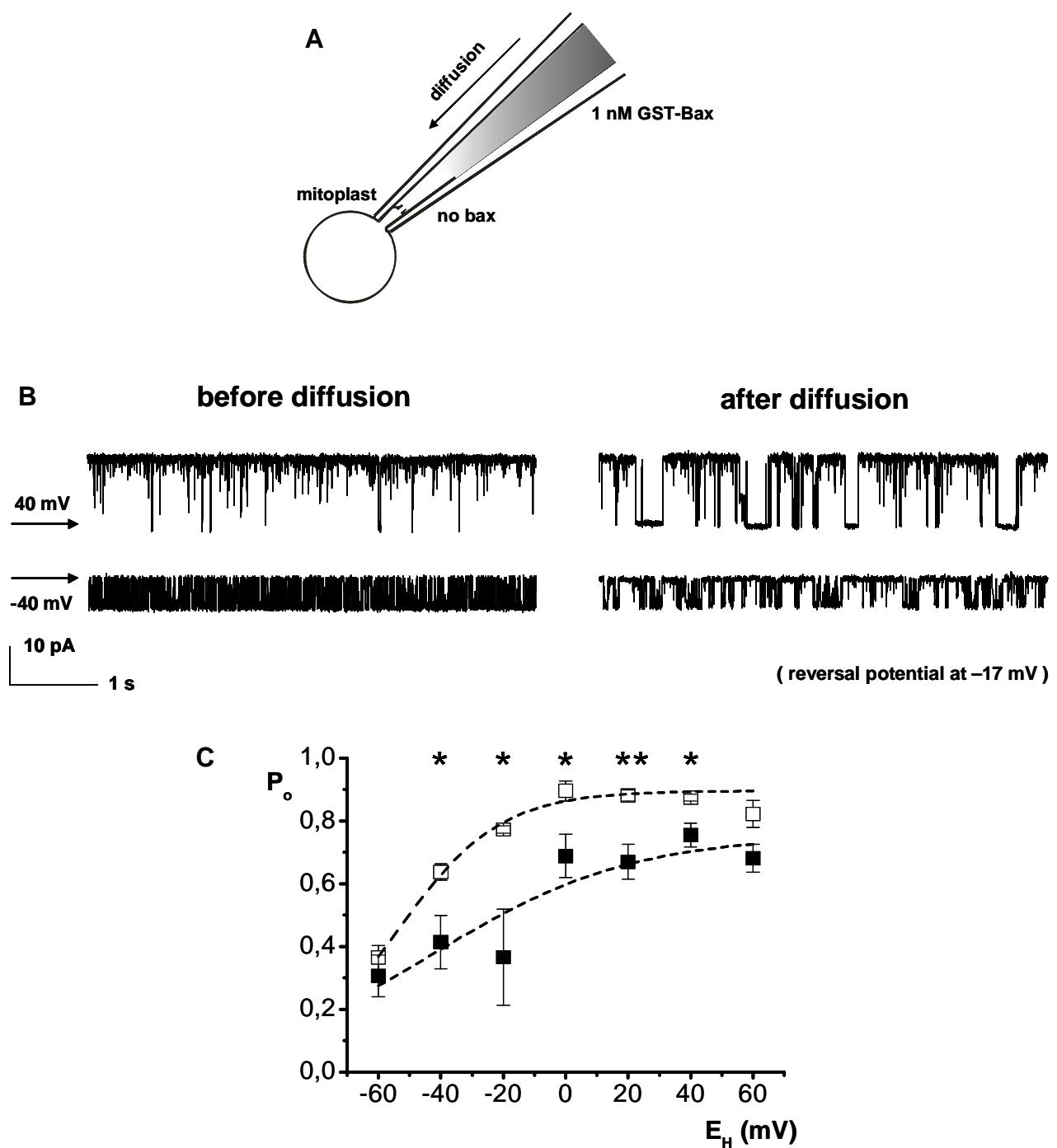
Fig. 22: Inhibition of the mtBK-channel by GST-Bax. A) The sketch shows back filling of the measuring pipette by GST-Bax. **B)** Single-channel recordings of the mtBK-channel before and after diffusion are demonstrated at -40 mV and +40 mV (closed state marked by arrows). It was obvious that the closed state of the mtBK-channel was more occupied after the diffusion than before the diffusion. However, the amplitudes of the currents did not change. They were asymmetrical in these recordings at -40 mV and +40 mV, because the reversal potential was -17 mV. **C)** P_o of the mtBK-channel before and after diffusion is shown as open and filled squares, respectively. At all potentials measured, the P_o was decreased. At -40 mV, -20 mV, 0 mV, and +40 mV, the decrease was significant ($p < 0.05$) and at +20 mV, it was highly significant ($p < 0.01$, error bars give SEM).

47

3.5.3 GST-Bax blocks the mtBK-channel from the membrane inside

After showing inhibition of the mtBK-channel by GST-Bax from the outside of the membrane *i.e.* the pipette side, I tested the effects of GST-Bax on the mtBK-channel from the membrane inside. The mtBK-channel was first recorded in the control sewer pipe applying the isotonic solution. At the next step, the activity of the mtBK-channel was measured in an isotonic solution containing 1 nM GST-Bax. Finally, the patch with the mtBK-channel was moved into control sewer pipe again.

Similar to the results with GST-Bax applied from the membrane outside, the activity of the mtBK-channel was decreased as well, if the isotonic solution containing 1 nM GST-Bax was applied from the bath side, *i.e.* the inside of the patch, recorded from (see discussion). The full conductance of the mtBK-channel was unchanged (Fig. 23C). However, the blocking effect was not like the inhibition by the other toxins, whose effects were partially reversible during washout. The activity of the mtBK-channel went on decreasing, even under control conditions.

The mean time constants of the mtBK-channel from 3 experiments at +40 mV were calculated and collected in Tab. 2. Two exponentials for the open times and two exponentials for closed time were found. Under the influence of 1 nM GST-Bax the open time constants were decreased and the closed time constants were increased. These effects continued during washout of GST-Bax. In particular, the slower open time constants of the mtBK-channel in 1 nM GST-Bax and of the control after were significantly decreased as compared to the control before ($p<0.05$). The other changes of both time constants in 1 nM GST-Bax and of the control after were not significant as compared with the control before.

	control before	1 nM GST-Bax	control after
Open time constants	$\tau_{O,1} = 10.0 \pm 6.8$ ms	$\tau_{O,1} = 8.1 \pm 0.9$ ms	$\tau_{O,1} = 7.5 \pm 0.2$ ms
(τ_O)	$\tau_{O,2} = 161.2 \pm 56.2$ ms	$\tau_{O,2} = 41.5 \pm 14.8$ ms	$\tau_{O,2} = 26.3 \pm 4.7$ ms
Closed time constants	$\tau_{C,1} = 2.7 \pm 1.3$ ms	$\tau_{C,1} = 4.2 \pm 0.3$ ms	$\tau_{C,1} = 5.6 \pm 1.4$ ms
(τ_C)	$\tau_{C,2} = 176.4 \pm 102.8$ ms	$\tau_{C,2} = 193.2 \pm 119.2$ ms	$\tau_{C,2} = 169.6 \pm 71.4$ ms

Tab. 2: Time constants of the mtBK in control before, 1 nM GST-Bax, and control after (E_H = +40 mV, means ± SEM).

A

10 pA

0.5 s

control   1 nM GST-Bax   washout

60 mV

40 mV

20 mV

-20 mV

-40 mV

-60 mV
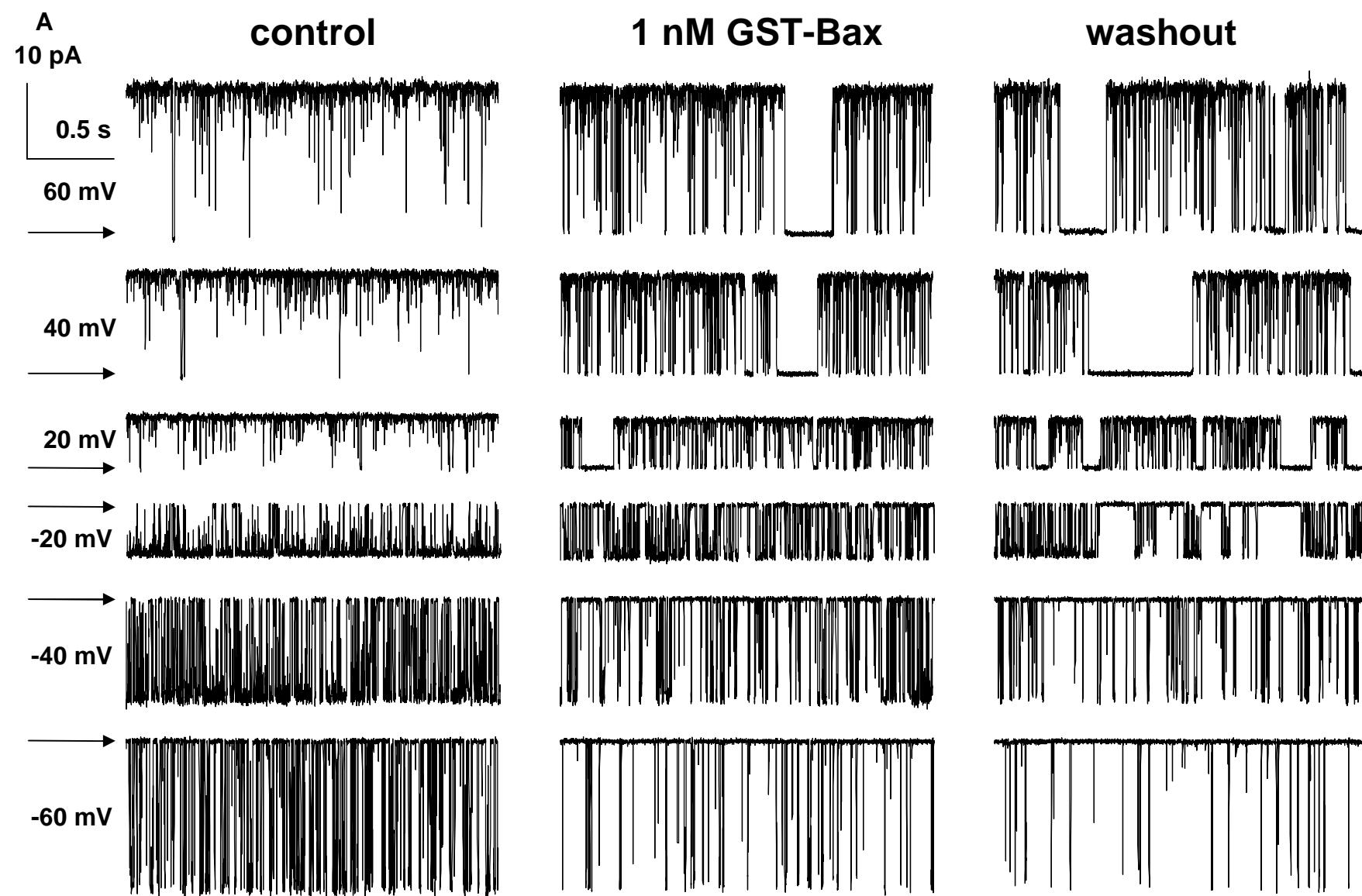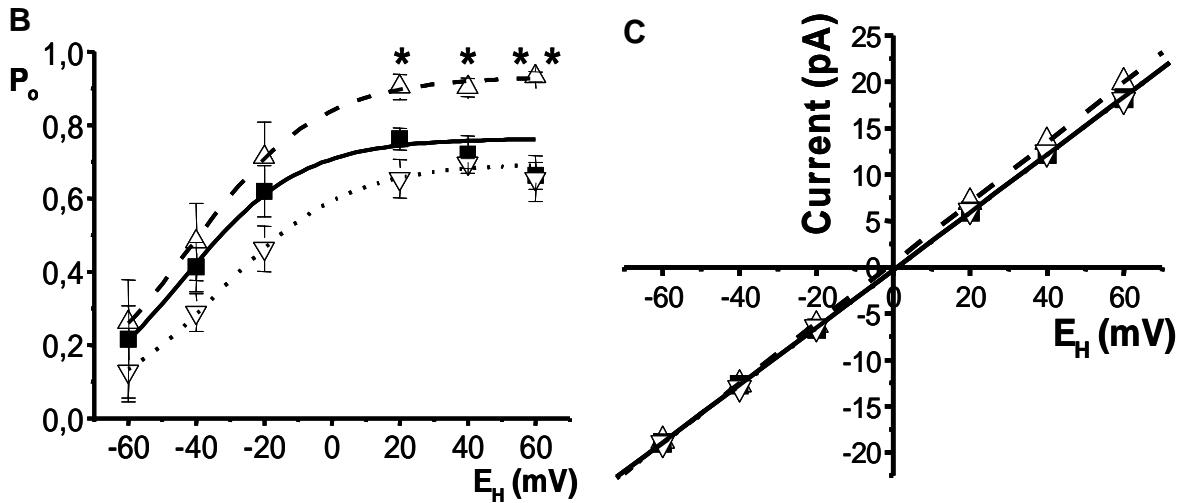
Fig. 23: Inhibition of the mtBK-channel by GST-Bax from the membrane inside. A) Single-channel currents of the mtBK-channel in control solution **(left panel)**, a solution with 1 nM GST-Bax **(central panel)**, and in control solution again (washout, **right panel)** were recorded at -60 mV, -40 mV, -20 mV, 20 mV, 40 mV, and 60 mV. The P_o of the mtBK-channel under control conditions before was larger than in GST-Bax solution and during washout. For example, the open state of the mtBK-channel was almost constantly occupied at +40 mV in the control solution (P_o about 0.9) and the interval between two events was very short, whereas there were the longer intervals in the GST-Bax solution and during washout the intervals were longest (closed state marked by arrows). **B)** The P_o of the mtBK-channel at different potentials demonstrates the decrease of the channel activity. P_o in control solution (open triangle, tip up, dashed curve) was larger than P_o in GST-Bax solution (filled squares, continuous curve). The decrease is significant at +20 mV, +40 mV and highly significant at +60 mV. During washout, the P_o (open triangle, tip down, dotted curve) became even smaller than that in GST-Bax. This suggests that the blockade of the mtBK-channel by GST-Bax was irreversible and the process of blockade continued during the time (error bars give SEM). **C)** The current-voltage relation showed no change of conductance or reversal potential. The current amplitudes at different potentials (control before: open triangle, tip up; GST-Bax: filled squares; and control after: open triangle, tip down) did not differ significantly and the slopes of the regression lines were almost identical (control before: dashed; GST-Bax: continuous; control after: dotted).

Moreover, I tested for concentration dependence of the blockade of the mtBK-channel by GST-Bax. An isotonic solution with 3 nM GST-Bax was applied by sewer pipe. Like in the experiments with 1 nM GST-Bax, the activity of the mtBK-channel was first measured in isotonic solution, then in a solution with 3 nM GST-Bax and finally in isotonic solution again. It turned out that the activity of the mtBK-channel was inhibited by 3 nM GST-Bax (Fig. 24A). Under the influence of 3 nM GST-Bax, the decrease of P_o was in the range from 7.2% to 26.4% at different potentials with a mean value of 16.8 ± 7.8%. However, under the influence of 1 nM GST-Bax, it was in the range from 12.9% to 28.9% with a mean value of 18.3 ± 5.8%, which was even slightly larger than that with 3 nM GST-Bax. The difference between the blockade by 1 nM and by 3 nM GST-Bax was insignificant. During washout with

3 nM GST-Bax, P_o continued to decrease by between 22.1% and 41.9% at different potentials with a mean value of 30.2 ± 7.8% as compared to the control before. During washout with 1 nM GST-Bax, P_o was decreased by between 22.5% and 51.0% at different potentials with a mean value of 34.3 ± 10.1%. Comparing the decrease of P_o during and after 1 nM GST-Bax and 3 nM GST-Bax, however, there was no significant difference of the inhibition by 1 nM GST-Bax and by 3 nM GST-Bax pointing to the absence of concentration dependence in this concentration range.
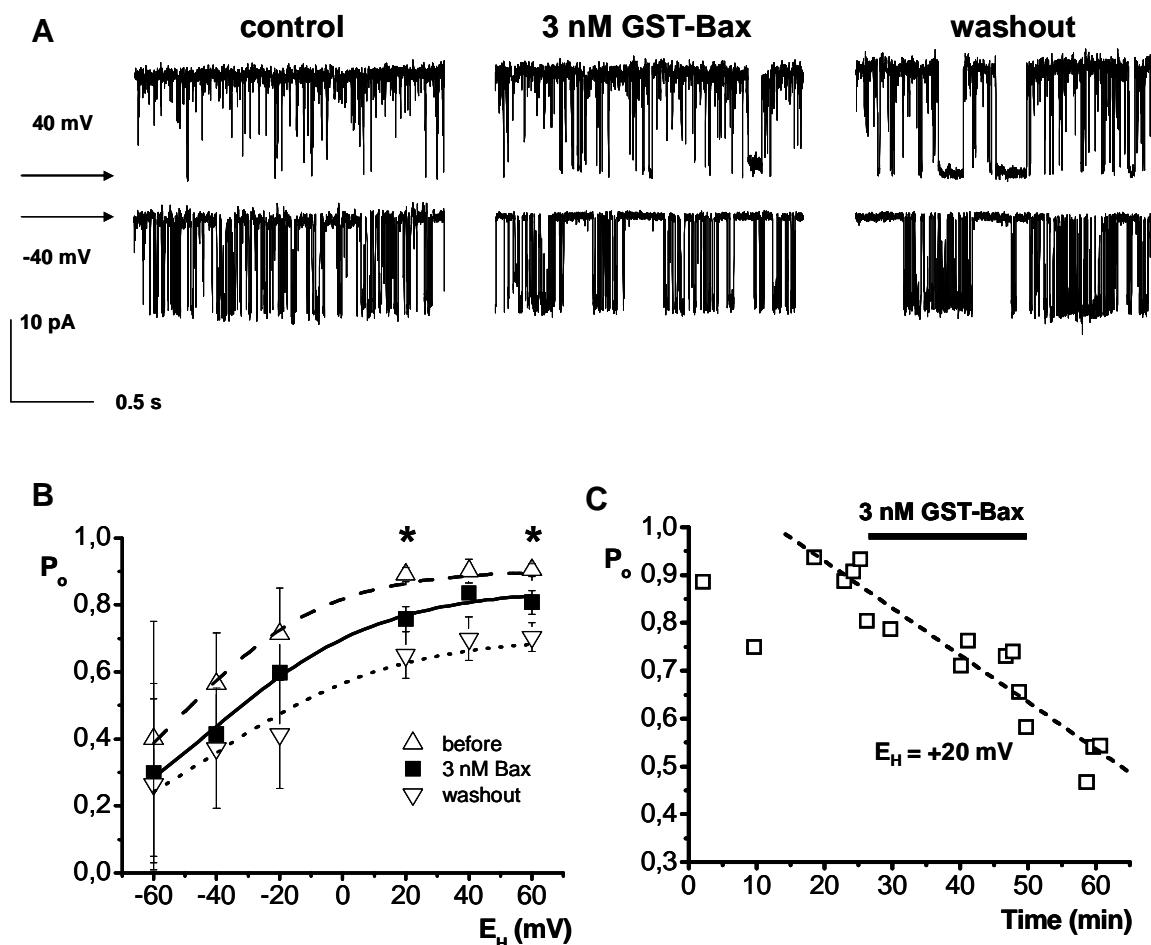
Fig. 24: Inhibition of the mtBK-channel by 3 nM GST-Bax. A) Single-channel recordings of the mtBK-channel are shown before, during, and after application of 3 nM GST-Bax at -40 mV and +40 mV. The activity of the mtBK-channel was decreased under and after 3 nM GST-Bax in the same way as it was with 1 nM GST-Bax. **B)** The P_o of the mtBK-channel was decreased by 10.6% to 26.4% with a mean value of 16.8 ± 7.8% with 3 nM GST-Bax. The decrease was significant at +20 mV and +60 mV. The mean value of the decrease of P_o during washout was 30.2 ± 7.8% ranging between 22.1% and 41.9% as compared with control before. It was significant at +20 mV, +40 mV, and +60 mV (error bars give SEM). **C)** The time course of the decrease of the P_o (open squares) is demonstrated at a holding potential of +20 mV. The inhibition by 3 nM GST-Bax was progressing over time. The steepness of the regression line (dotted) was about -0.01 meaning that P_o decreased by 1% per minute under the influence of 3 nM GST-Bax and during washout.

3.5.4 GST-Bcl-$_{XL}$ activates the mtBK-channel at hyperpolarizing potentials insignificantly

Bax is a proapoptotic member of the Bcl-2 family, while another member of the Bcl-2 family, Bcl-$_{XL}$, exerts an antiapoptotic activity. As I showed the inhibition of the mtBK-channel by GST-Bax before, I now wanted to understand the influence of GST-Bcl-$_{XL}$ on the mtBK-channel.

5 nM GST-Bcl-$_{XL}$ was applied by the sewer pipe in order to test its effect on the mtBK-channel from the membrane inside. The channel activity was recorded before, during, and after applying 5 nM GST-Bcl-$_{XL}$ at holding potentials ranging between -60 mV and +60 mV.
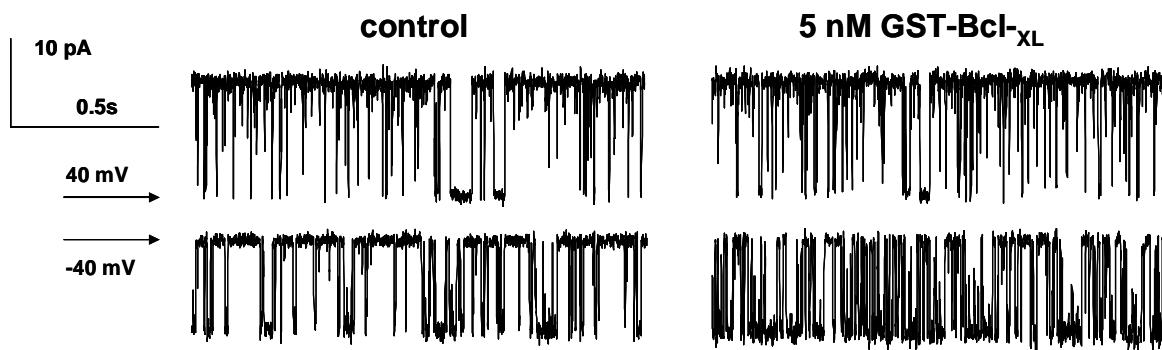
Fig. 25: Effect of 5 nM GST-Bcl-$_{XL}$ on the single-channel current through the mtBK-channel. Recordings before and during 5 nM GST-Bcl-$_{XL}$ are demonstrated at -40 mV and +40 mV. According to the voltage dependence of the channel, its open state was more occupied at +40 mV than at -40 mV. Comparing the recordings under control conditions (left panel) and in 5 nM GST-Bcl-$_{XL}$ (right panel) there was no change of channel activity at +40 mV, whereas the channel was activated by 5 nM GST-Bcl-$_{XL}$ at -40 mV. The closed state is marked by arrows.

The P_o of the mtBK-channel before, during, and after 5 nM GST-Bcl-$_{XL}$ was determined by Clamfit 9.2 in single-channel search mode. The change of the P_o was very small (<10%) at depolarizing holding potentials (+20 mV, +40 mV, and +60 mV) during and after 5 nM GST-Bcl-$_{XL}$. However, a larger P_o at hyperpolarizing holding potentials during, and after GST-Bcl-$_{XL}$ could be seen (Fig. 26A). The activation of the mtBK-channel by 5 nM GST-Bcl-$_{XL}$ was partially reversible. For example, the mean P_o at -60 mV (n=4) before, during and after 5 nM GST-Bcl-$_{XL}$ was 0.078 ± 0.06, 0.233 ± 0.14, and 0.166 ± 0.12, respectively. P_o at -60 mV was increased by 199% under the influence of 5 nM GST-Bcl-$_{XL}$ and by 113% in the control after. This increase of P_o by GST-Bcl-$_{XL}$ was small and statistically insignificant (t-test). As in the case of GST-Bax, the full conductance of the mtBK-channel was not changed by 5 nM GST-Bcl-$_{XL}$ (Fig. 26B).
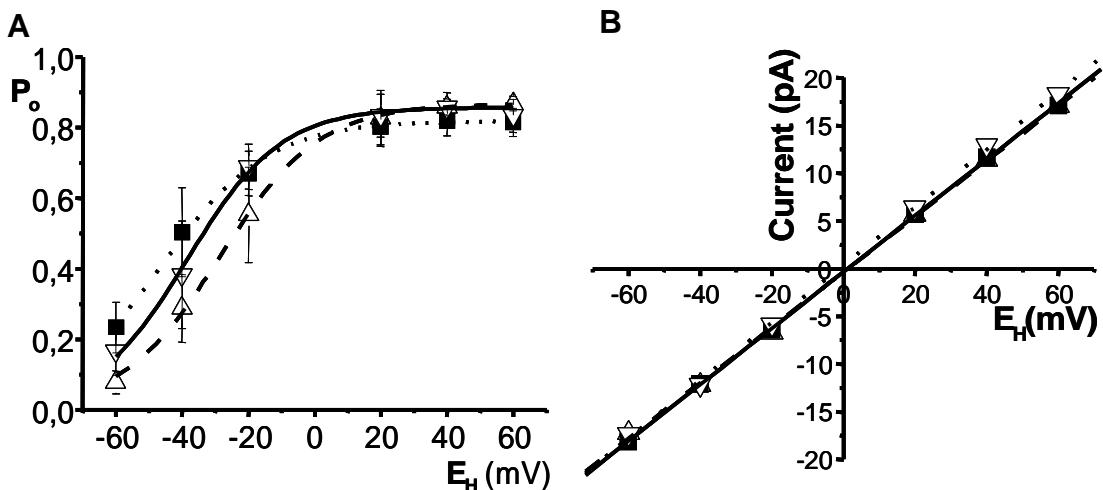
Fig. 26: Activation of the mtBK-channel by 5 nM GST-Bcl-$_{XL}$ at hyperpolarization.
A) At depolarizing holding potentials (+20 mV, +40 mV, and +60 mV), the change of P_o was very small before (open triangles, tip up), during (filled squares), and after (open triangles, tip down) 5 nM GST-Bcl-$_{XL}$. At hyperpolarizing potentials, P_o during 5 nM GST-Bcl-$_{XL}$ was increased by 21% at -20 mV, 87.5% at -40 mV, and 199% at -60 mV, respectively. After 5 nM GST-Bcl-$_{XL}$, P_o became smaller than during GST-Bcl-$_{XL}$, however, was still increased by 24.6% at -20 mV, 33% at -40 mV, and 113% at -60 mV as compared with the controls before (error bars give SEM). **B)** The current-voltage relation was not changed during and after 5 nM GST-Bcl-$_{XL}$, which indicates that there is no effect of Bcl-$_{XL}$ on the full conductance and on the reversal potential.

3.5.5 Effect of the combination of GST-Bax and Bcl-$_{XL}$ on the mtBK-channel

Though Bax and Bcl-$_{XL}$ are both members of the Bcl-2 family, their function is opposite. Bax induces the opening of the PTP and reduces the activity of the mtBK-channel while Bcl-$_{XL}$ prevents the release of cytochrome c and activates the mtBK-channel at hyperpolarizing potentials. It is suggested that Bcl-$_{XL}$ is able to inhibit the activity of Bax [Green-DR, 2006]. Therefore, I tested the effect of the combination of Bax and Bcl-$_{XL}$ on the mtBK-channel.

The test solution containing 5 nM GST-Bcl-$_{XL}$ and 3 nM GST-Bax was applied by sewer pipe, and the currents through the channel before, during, and after test solution were recorded at different potentials. The results of these experiments (n=3) showed that there was no significant change of the P_o and of the full single-channel conductance (Fig. 27A, B), although P_o was slightly increased at hyperpolarizing potentials. The explanation of the tiny increase of P_o could be that the concentration of GST-Bcl-$_{XL}$ (5 nM) was higher than of GST-Bax (3 nM). The reversal potential of the mtBK-channel was not shifted by the test solution, either (Fig. 27C).

A
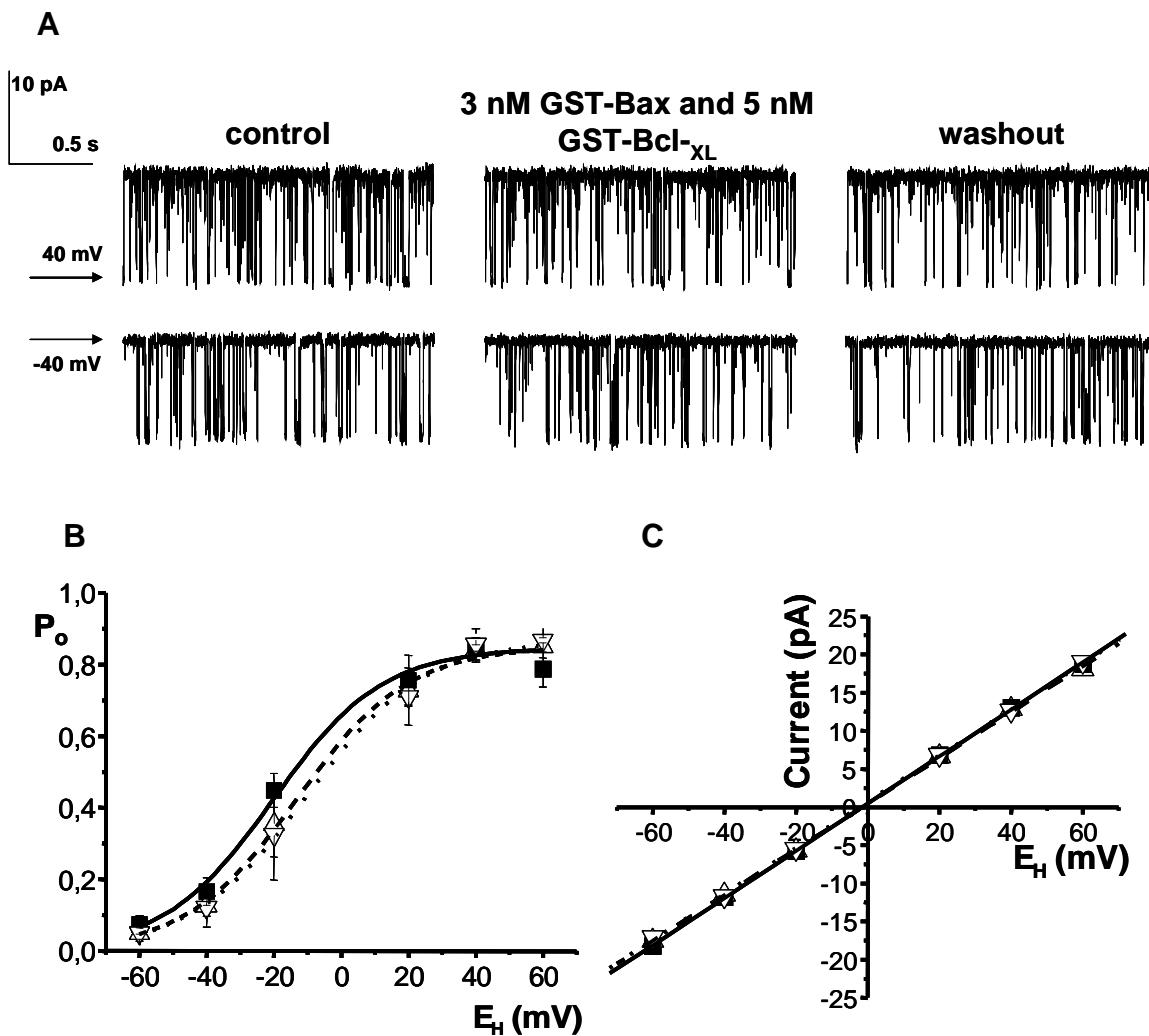
Fig. 27: Effect of combined GST-Bax and GST-Bcl-$_{XL}$ on the mtBK-channel. A) Single-channel recordings are shown at +40 mV and -40 mV (closed state marked by arrows). No significant change of P_o before, during, and after the solution containing 5 nM GST-Bcl-$_{XL}$ and 3 nM GST-Bax was detected. **B)** The P_o in test solution (filled squares) was insignificantly increased by 27.2%, 31.7%, and 54.2% at +20 mV, +40 mV, and +60 mV, respectively, as compared with the control before (open triangles, tip up). The differences of P_o at the other potentials between the test solution and either the control before or the control after (open triangles, tip down) were not more than 8% (error bars give SEM). **C)** The full single-channel conductance of the channel was unchanged under the influence of 5 nM GST-Bcl-$_{XL}$ and 3 nM GST-Bax.

3.5.6 Control experiment of GST protein

Glutathione-S-transferase (GST) protein is an effective tool to study the function of protein and protein-protein interaction [Vikis & Guan, 2004]. In this study, the proteins Bax and Bcl-$_{XL}$ were isolated as combination protein with GST protein. In order to ensure the effects of Bax and Bcl-$_{XL}$ on the mtBK-channel, I tested the effect of GST protein on the mtBK-channel.

An isotonic solution containing 5 nM GST protein was applied by sewer pipe. The mtBK-channel did not show any change of activity or conductance induced by GST protein as compared to control. This result ensures that the proteins Bax and Bcl-$_{XL}$ and not the GST protein caused the effects of GST-Bax and GST-Bcl-$_{XL}$ on the mtBK-channel.
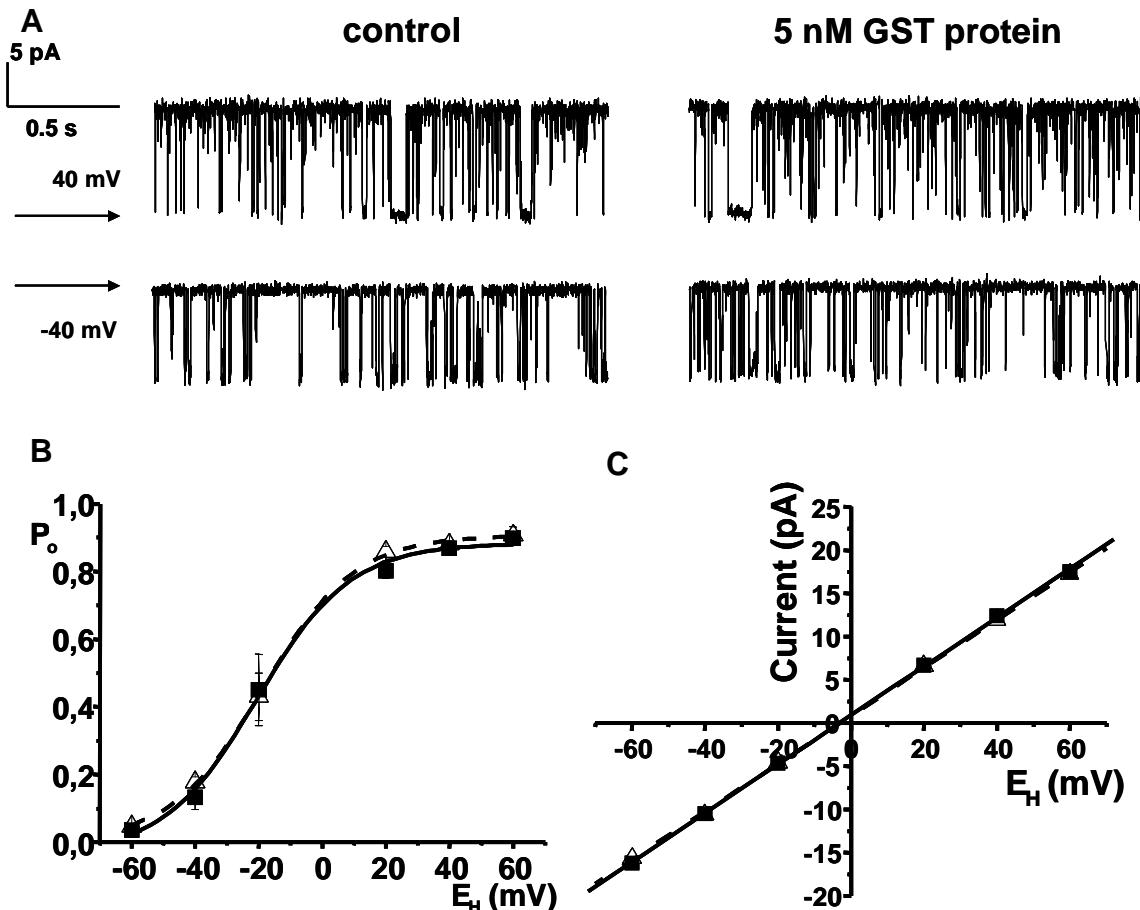
Fig. 28: GST protein does not modify the mtBK-channel. P_o of the channel (panel **A** and **B**) and single-channel conductance (panel **C**) were unchanged under the influence of 5 nM GST-protein (error bars give SEM).

3.6 Effects of Bax and Bcl-$_{XL}$ on the PTP

3.6.1 GST-Bax does not induce any currents irrespectively of the presence of the PTP

Bax was shown to induce the mitochondrial permeability transition resulting in the release of cytochrome c, which promotes apoptosis. There are several models existing, which explain the mechanisms of the opening of the PTP by Bax. One hypothesis assumes that Bax itself is inserted into the mitochondrial membrane to form an ion selective pore [Antignani & Youle, 2006]. Another theory assumes that Bax triggers the opening of the PTP [Antonsson, 2001]. A single-channel experiment with the PTP was thought to lead to a decision between these

two theories. Therefore, I tried to record current through the PTP after stimulation by Bax by means of the patch-clamp technique.

Mitoplasts from astrocytes were tested in isotonic solution with 200 µM Ca^{2+}, in which 3 nM GST-Bax was added either by back filling or in sewer pipe. More than 140 pipettes were tested, however, no large channel current matching the PTP was observed. Only the mtBK-channel with a full conductance of about 300 pS was present.

Moreover, mitochondria from rat liver cells, in which the PTP induced by Ca^{2+} was commonly recorded, were incubated in isotonic solution containing 3 nM Bax and 1 µM Ca^{2+}. 1 µM Ca^{2+} is not enough to trigger the opening of the PTP. After more than 1 hour incubation, patches with liver mitochondria were formed in a solution containing 1 µM Ca^{2+}. However, the single-channel current of the PTP was not present, either. The absence of the PTP could either due to the combination of Bax with the GST protein or due to the absence of some putative cellular factors, which are obligatory for Bax-triggering of the PTP.

3.6.2 Inhibition of the PTP by GST-Bcl-$_{XL}$

The antiapoptotic protein Bcl-$_{XL}$ plays a roll in the intrinsic apoptosis pathway through the prevention of the release of cytochrome c [Tsujimoto, 1998]. The underlying mechanism could be the inactivation of Bax and caspases [Tsujimoto, 1998; Green-DR, 2006]. Another possible mechanism would be its ability to inhibit opening of the PTP.

In order to solve this open question, the PTP was tested in an isotonic solution, to which 5 nM GST-Bcl-$_{XL}$ were added. An irreversible inhibition of the PTP by Bcl-$_{XL}$ was demonstrated by the patch clamp experiments (Fig. 29), which proved the antiapoptotic ability of Bcl-$_{XL}$. The mean P_o of the PTP was 0.51 ± 0.04 in the control solution. The P_o of the PTP was decreased extremely significant by 5 nM GST-Bcl-$_{XL}$ (n=6, p<0.001) and significantly in the control after (n=6, p<0.05)

A

Control

5 nM GST-Bcl-XL 30s after

10 pA

0.2s

5 nM GST-Bcl-XL 60s after

Washout

B
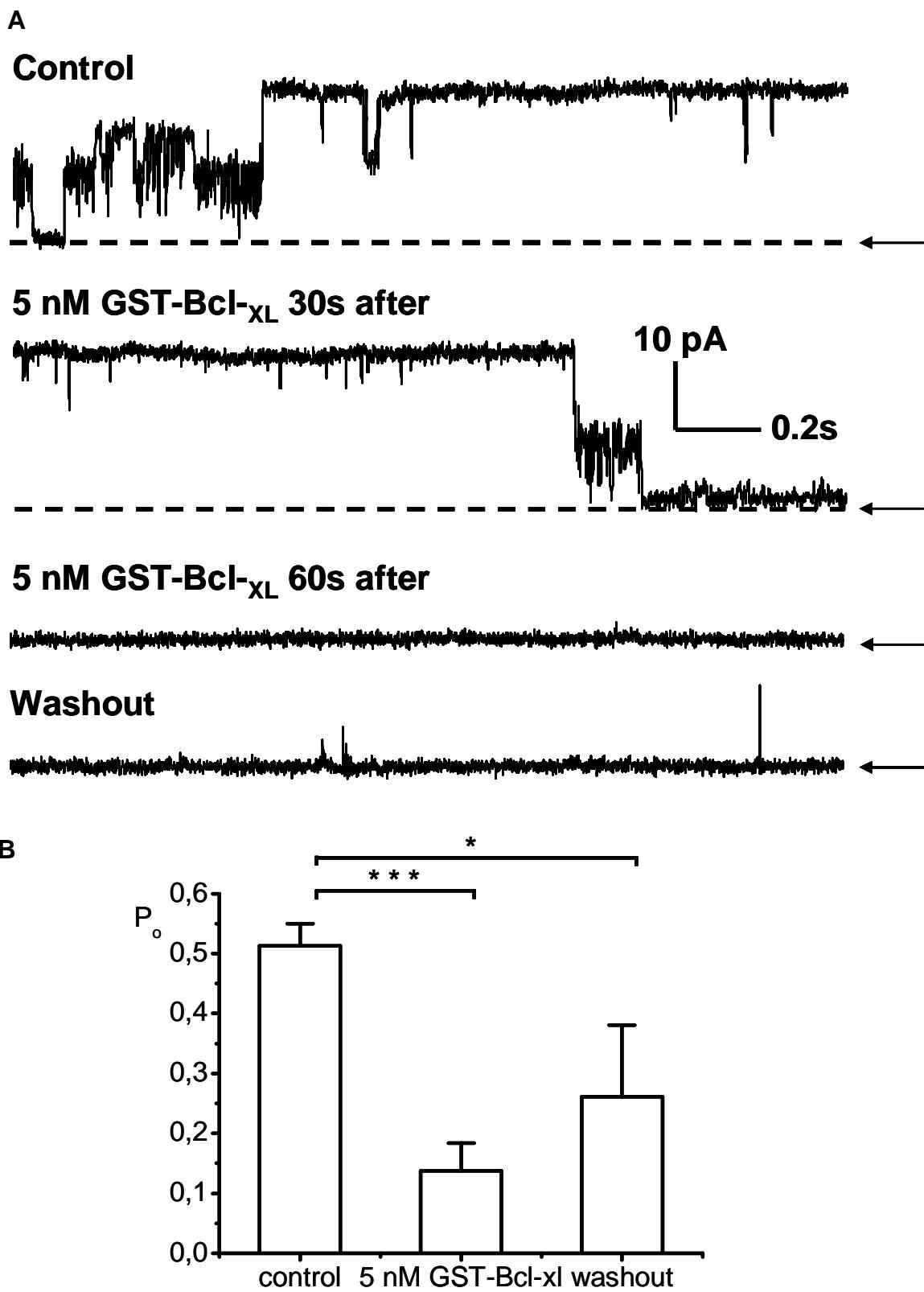
Fig. 29: **Inhibition of the PTP by 5 nM GST-Bcl-XL. A)** The single-channel recording demonstrates the irreversibly decreased activity of the PTP by 5 nM GST-Bcl-XL. The closed state of the channel is marked by dashed lines and arrows. **B)** The mean P_o of the PTP before, during, and after 5 nM Bcl-XL was 0.51 ± 0.04, 013 ± 0.05, and 0.26 ± 0.12, respectively (error bars give SEM).

4 Discussion

4.1 Estimation of the number of the mtBK-channel in a mitoplast

As described in results, in patch-clamp experiments with mitoplasts of astrocytes, the probability of the presence of a mtBK-channel in a good patch was 24%. The mean radius of a medium-sized mitoplast of astrocytes was about 5 µm and its surface area was calculated as 314 µm^2. In the pipette, the free membrane of the mitoplasts for single-channel recording was about 2.9 µm^2 (Fig. 30). I obtained one mtBK-channel from 2.9 µm^2 membrane with a probability of 24%. It was estimated that there was one mtBK-channel in every 12.1 µm^2 and the area of a mitoplast was about 314 µm^2, thus I roughly estimate that there were at minimum 26 mtBK-channels activated in a medium-sized mitoplast. Moreover, taking account the "silent" mtBK-channels, which were inactivated and could not be detected during the experiments, the number of the mtBK-channels in a mitoplasts in fact may have been higher than 26, possibly up to 50.
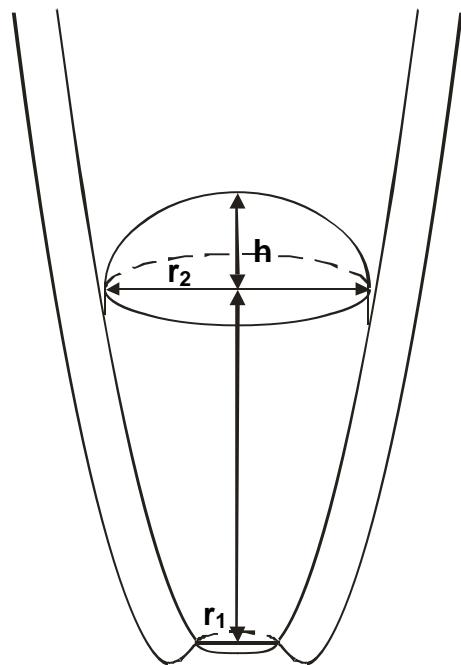
Fig. 30: Geometry of the membrane within the tip of a pipette. A schematic diagram of the geometry of a patch membrane from mitoplast is shown. The free membrane, which is the upper spherical part of the patch membrane, is facing the solution and available for the channel-current recording. The radius of the opening of the pipette (r_1) is 0.25 µm that corresponds to a resistance of 15 – 20 mΩ of the pipette. The height (h) and radius (r_2) of the spherical part is 0.375 µm and 0.625 µm, respectively. From these values, the area of the free membrane A = π (h^2 + 2 r$_2^2$) = 2.9 µm^2 (equation 9) [Sakmann & Neher, 1995].

4.2 Activation of the mtBK-channel by hypoxia

Maintenance of O_2 homeostasis and utilization of O_2 to generate ATP are essential for cell survival. A deprivation of O_2 and hypoxia–induced energy failure will lead to disruption of pH and ionic homeostasis. On the other hand, a change of O_2 concentration will be sensed and will induce cellular responses, including the expression of the hypoxia-inducible factor 1 (HIF-1) [Semenza, 2007]. However, little is understood about the molecular mechanism of O_2 sensing. The active transport of the ions and metabolites, which consumes the energy, will be attenuated under hypoxia contributing to energy deficiency. Besides, according to the results of the earlier studies and of this study, the ion channels themselves are also modulated by hypoxia [Liu et al., 1999; Gu et al., 2007; Cheng et al., 2008].

A possible effect of hypoxia on the BK-channel in the plasma membrane was tested in earlier studies of Liu et al. and of Williams et al. Liu et al. found an inhibition of the BK-channel by argon-induced hypoxia in mice neocortical neurons [Liu et al., 1999]. Moreover, in the study of Williams et al., the BK-channel was reversibly inhibited by hypoxia in rat carotid body glomus cells [Williams et al., 2004]. However, according to the results of Gu et al. and of this study, the effect of hypoxia on the mtBK-channel and on the BK-channel in plasma membrane is opposite. An activation of the mtBK-channel by hypoxia was demonstrated in the study of Gu et al. for the IMM of the human glioma cell and in this study for the IMM of rat astrocytes [Gu et al., 2007; Cheng et al., 2008].

In the study of Liu et al., it was claimed that "a low-O_2 medium markedly inhibited the BK-channel open probability in a voltage-dependent manner in cell-attached patches, but not in inside-out patches, indicating that the effect of O_2 deprivation on the BK-channels of mice neocortical neurons was mediated via cytosol-dependent processes" [Liu et al., 1999]. From this conclusion, the inhibition of the BK-channel is not directly induced by low O_2 concentration, but by hypoxia-induced cytosolic processes. These processes could be the change of the intracellular pH value, which is modified by hypoxia-induced energy deficiency. Another underlying mechanism is the regulation of the activity of the cAMP-dependent protein kinase A (PKA) and of phosphatases by hypoxia. Phosphorylation and dephosphorylation at the C-terminus of the α-subunit of the BK-channel can regulate the Ca^{2+} sensitivity of the BK-channel or can modify the activity of the BK-channel directly [Reinhart et al., 1991; Bietefeldt & Jackson, 1994; Liu et al., 1999]. However, this BK-channel activating mechanism might not be present in the mitochondria. The response of mitochondria

to hypoxia might be different from the responses of the cytosol. Thus, the mtBK-channel could be activated by other hypoxia-induced mitochondrial processes.

In the study of Williams et al., the activity of the BK-channel in the plasma membrane was decreased under hypoxia. Moreover, the BK-channel was also inhibited under normoxia when the gene of hemoxygenase-2 was knocked out. However, the activity of the BK-channel was rescued by the application of carbon monoxide (CO) itself, a product of hemoxygenase-2 from O_2 [Williams et al., 2004]. It is suggested that the hemoxygenase-2 is a part of the BK-channel complex and its product CO could maintain the activity of the BK-channel in the plasma membrane [Williams et al., 2004]. Under hypoxia, the BK-channel is inhibited because of the absence of CO, the product of hemoxygenase-2. This theory might explain the hypoxia-induced cytosolic process, which can activate the BK-channel in the plasma membrane. However, hemoxygenase-2 was not identified in mitochondria so far. Thus, this mechanism is not likely to be carried out in mitochondria under hypoxia.

In this study, the activation of the mtBK-channel might be induced by the increase of mitochondrial Ca^{2+} uptake induced by hypoxia [Ruiz-Meana et al., 2006]. Ruiz-Meana et al. discovered such an increase of the mitochondrial Ca^{2+} uptake in cardiac myocytes under hypoxia by means of Ca^{2+} microelectrodes. It was considered that the mitochondrial Ca^{2+} uniporter could contribute to this increase, because it could be attenuated by the application of a selective inhibitor [Ruiz-Meana et al., 2006].

$\Delta\Psi$ (about -150 mV) is a driving force for the mitochondrial Ca^{2+} uptake. In our case, isolated mitoplasts are losing their membrane potential during isolation and during treatment in hypotonic solution. However, they do not lose their membrane potential completely which is proved by the fact that the mean reversal potential of the mtBK-channel was shifted from -5.5 mV to -10.5 mV under hypoxia in symmetrical isotonic solutions (Fig. 13). This negative shift indicates a hyperpolarization *i.e.* an increased potential difference between the inside and outside of the membrane enhancing the driving force for the influx of Ca^{2+}. The increase of the matrix Ca^{2+}-concentration then activates the mtBK-channel. Consequently, an increase of P_o was observed. After hypoxia, the reversal potential of the mtBK-channel was partially shifted back indicating depolarization of the mitoplasts membrane. This depolarization attenuates the driving force for the Ca^{2+} uptake again. It thus has a consequence

corresponding to that of the decreased P_o of the mtBK-channel after hypoxia, though the P_o is determined by a Ca^{2+}-independent mechanism namely kinetics of the channel gate.

Furthermore, taking into account the shift of the mean reversal potential of the mtBK-channel into the hyperpolarizing direction from -5 mV to -10 mV, I calculated the Ca^{2+} concentration in the mitoplasts by the Nernst equation:

$$E_{Ca} = \frac{RT}{2F} \ln \frac{[Ca]_o}{[Ca]_i} \tag{10}$$

(E_{ca}: equilibrium potential for Ca^{2+}; R: gas constant, 8.31 J/mol K; T: absolute temperature, 298 T; F: Faraday's constant, 9.65×10^4 C/mol; $[Ca]_o$: Ca^{2+} concentration membrane outside, 1 µM ; $[Ca]_i$: Ca^{2+} concentration membrane inside) [Hille, 2001]. The Ca^{2+} concentration was slightly increased from 1.5 µM to 2.2 µM during hypoxia. In earlier study, when the Ca^{2+} concentration was increased from 1 µM to 5 µM, the increase of the P_o of the plasmalemmal BK-channel was very small at hyperpolarizing potentials and was relatively large at depolarizing potentials [Barrett et al., 1982; Hille, 2001]. A similar change of the P_o of the mtBK-channel was observed in this study that supports the estimation of the Ca^{2+} increase.

Moreover, I assume that the increase of the Ca^{2+}-uptake could not be accounted for by the shift of the membrane potential of the mitoplasts alone. In the study of Ruiz-Meana, $\Delta\Psi$ was progressively lost under hypoxia [Ruiz-Meana et al., 2006]. However, the mitochondrial Ca^{2+} uptake was increased when its driving force was progressively attenuated. This indicates there may be another underlying mechanism that increases the Ca^{2+} uptake. A possible explanation is that the Ca^{2+} uniporter itself is activated by hypoxia in some way.

Additionally, we found indications for a further possible mechanism of activation of the mtBK-channel under hypoxia. It was demonstrated that the channel is modified when the state of the mitochondrial respiratory chain is modified by substrates (Data not shown here). Under hypoxia, the state of the respiratory chain is changed because of O_2 deficiency in complex IV resulting in a change of the state of the upstream complexes. Therefore, it may be assumed that the mtBK-channel could be regulated by hypoxia via the state of the mitochondrial respiratory chain.

The increase of the P_o of the mtBK-channel under DTN-induced hypoxia was larger than under N_2-induced hypoxia. A possible explanation could be that there is less O_2 in the

solution containing 1 mM DTN than in the N_2 solution. At room temperature (20 °C) the solubility of oxygen in water is 7.6 mg/l which is 0.24 mM so that one would need at least 0.48 mM DTN to bind the O_2 present in the solution (I used 1 mM DTN). Another possibility is that not only the lack of O_2 but also DTN itself can activate the mtBK-channel by chemical interaction. DTN is known as a reducing agent, which could influence the properties of the proteins within the membrane. Therefore, the single-channel experiments were always performed in both ways, using N_2-bubbled solutions and applying DTN.

Taking together, there are three possible mechanisms for activation of the mtBK-channel under hypoxia: 1) an increase of the mitochondrial Ca^{2+} uptake through the enhancement of the driving force, 2) an increase of the mitochondrial Ca^{2+} uptake through the activation of the mitochondrial Ca^{2+} uniporter, and 3) an altered state of the mitochondrial respiratory chain by hypoxia.

4.3 Inhibition of the PTP by hypoxia and interaction of the PTP and the mtBK-channel

Under low O_2 concentration in the tissue, there is not enough O_2 provided for complex IV of the mitochondrial respiratory chain for the production of ATP. Hypoxia could induce an array of cellular consequences including energy deficit, disruption of pH value, necrosis, and apoptosis [Benjelloun et al., 2003]. Hypoxia-induced neuronal apoptosis was observed in stroke [Choi, 1996; Pulera et al., 1998].

The PTP plays a central role within the intrinsic pathway of apoptosis, by the release of cytochrome c resulting in the activation of the downstream caspases. An opening of the PTP under hypoxia was expected. However, according to earlier studies, an opening of the PTP under hypoxia was not observed. It is thought that in response to the hypoxia-induced cellular changes the PTP does not open during hypoxia, but opens during reperfusion [Burwell et al., 2009; Morin et al., 2004; Ruiz-Meana et al., 2006]. In this patch-clamp study, an inhibition of the PTP by hypoxia was demonstrated supporting the earlier studies.

As an explanation for the inhibition of the PTP by hypoxia, it was considered that it is regulated by the status of the mitochondrial respiratory chain [Brokemeier et al., 1998; Fontaine et al., 1998]. Under hypoxia, there is a lack of O_2 for conversion into H_2O in complex IV of the respiratory chain. If the electron transport is disrupted in complex IV, the

electron flow from complex I to complex IV could be stopped or be impaired so that the respiratory chain stays in the reduced form. It is suggested that the PTP is coupled to one of the respiratory chain complexes, which in their reduced form could keep the PTP in the closed state [Brokemeier et al., 1998]. In further studies, complex I was assumed to regulate the PTP. A decreased electron flow through complex I could inhibit the opening of the PTP while an increased electron flow could lower the threshold of the PTP for opening [Fontaine et al., 1998]. According to this theory, an electron flow in the respiratory chain attenuated or disrupted by hypoxia would lead to a reduced form of complex I that could inhibit the PTP.

Another explanation of the inhibition of the PTP by hypoxia was thought to happen via activation of the mtBK-channel. It had been proved to be a cytoprotective channel against hypoxia/ischemia-induced apoptosis before [Ohya et al., 2005; Xu et al., 2002]. Activation of the mtBK-channel by hypoxia was demonstrated earlier and this study [Gu et al., 2007; Cheng et al., 2008]. The activation of the mtBK-channel would cause the increase of potassium influx from the cytosol into the mitochondrial matrix. An increase of the potassium concentration in the matrix would then lead to an increase of the mitochondrial volume, which in turn would cause a dilution of the matrix Ca^{2+} [Garlid & Paucek, 2003; Xu et al., 2002].

In experiments on intact mitochondria (Fig. 21), the interaction of mtBK-channel and the PTP is shown. In these experiments, about 200 µM Ca^{2+} were required to induce opening of the PTP, which was measured as the increase of the fluorescence intensity outside the mitochondria caused by their depolarization. Under the influence of hypoxia, more Ca^{2+} (about 400 µM) was required to open the PTP. This indicates that hypoxia inhibited the PTP and the activated mtBK-channel contributed to this inhibition. In the experiments with the BK-channel selective inhibitor Ibtx the Ca^{2+} requirement to open the PTP was decreased. In other words, when the mtBK-channel was blocked, the PTP was more sensitive to Ca^{2+} and easier to open. This result is further substantial evidence for our working hypothesis that an activated mtBK-channel keeps the PTP closed. Furthermore, inhibition of the PTP by hypoxia is mediated by activation of the mtBK-channel and most likely by reduction of complex I of the mitochondrial respiratory chain by an inhibited electron flow [Fontaine et al., 1998].

4.4 The effects of GST-Bax and GST-Bcl-$_{XL}$ on the mtBK-channel

Bax is considered a proapoptotic cellular factor, which is involved in the opening of the PTP and the release of cytochrome c from mitochondria [Pouliquen et al., 2006]. In a recent study,

the effect of Bax on a mitochondrial ion channel was revealed. The inhibition of $K_{v1.3}$ by Bax was thought to be a part of Bax-induced apoptosis [Szabo et al., 2008]. In this thesis, it is shown that also the mtBK-channel is inhibited by GST-Bax in which Bax is connected to the GST protein. It is intriguing to speculate that Bax may exert a general inhibitory effect on mitochondrial potassium channels.

GST-Bax inhibits the mtBK-channel not regarding whether it is applied from the sewer pipe and from the patch pipette. This indicates that GST-Bax blocks the mtBK-channel from both, extra- and intracellular side. However, when GST-Bax was applied from the sewer pipe, how can GST-Bax access to the BK-channel from membrane inside? I hypothesize that GST-Bax could be transported by TIM into matrix or there might be some small cracks in membranes of the mitoplasts, which might be the entrance for GST-Bax into matrix.

Usually the BK-channel is blocked by inhibitors such as Chtx and Ibtx only from extracellular side [Hirano et al., 2001]. According to the inhibition of the mtBK-channel by GST-Bax from both sides, I hypothesize that the GST-Bax blocks the mtBK-channel within the selectivity filter, the narrowest part of the pore, where GST-Bax could access from both sides. Alternatively, it could act on the channel through the membrane *i.e.* from the side of the channel molecule as was shown for lipophilic local anesthetics and voltage-dependent sodium channels [Braü et al., 1998].

1 nM GST-Bax and 3 nM GST-Bax were both applied by sewer pipe. A decrease of the P_o of the mtBK-channel was observed, however, a concentration dependence of this decrease was not present (Fig. 23B; 24B). The concentration dependence of the blockade is usually demonstrated as an S-shaped curve, which corresponds to a sigmoid function. According to such a curve, the effect of a blockade saturates at large concentrations of the inhibitor. It thus looks as if the inhibiting effect of GST-Bax saturates already at a concentration of 1 nM. This result suggests that GST-Bax could inhibit the mtBK-channel at a very low concentration, may be below 100 pM.

After testing the mtBK channel in GST-Bax solutions, the mitoplasts were returned to control solution where the P_o continued to decline rather than to recover. Thus, the inhibition of the mtBK-channel by GST-Bax was irreversible and progressive over time. Thus, the inhibition of the mtBK-channel by GST-Bax is different from inhibition by other inhibitors such as

Chtx, which blocks the BK-channel reversibly [Ye et al., 2000; Kehl & Wong, 1996; Denson et al., 1994]. The reason for this different behavior is not well understood. I assume that binding of GST-Bax to the mtBK-channel is very tight. The interaction between mtBK-channel and GST-Bax may continue progressively somehow affecting its gating mechanism. In any case, the site of action at the channel does not seem to be easily accessed, possibly because it is located within the membrane as mentioned above. The interaction could include that GST-Bax reduces the Ca^{2+} sensitivity of mtBK-channel or regulates the interaction of the α- and β-subunit of the mtBK-channel.

Bcl-$_{XL}$ is an antiapoptotic factor, which is thought to stabilize the mitochondrial membrane and to prevent the release of cytochrome c into the cytosol [Sung et al., 2009]. In this study, it was demonstrated that the mtBK-channel is insignificantly activated at hyperpolarizing potentials when GST-Bcl-$_{XL}$ was applied to the mtBK-channel from membrane inside (from the sewer pipe, Fig. 25; 26). This is particularly remarkable, as usually the channel is more difficult to activate at hyperpolarizing potentials. Under the influence of 5 nM GST-Bcl-$_{XL}$, the P_o of the mtBK-channel was increased by 21%, 88%, 199% at -20 mV, -40 mV, and -60 mV, respectively. From this result, it is considered that increase of the P_o of the mtBK-channel by GST-Bcl-$_{XL}$ is enhanced when $\Delta\Psi$ is shifted into the negative direction. Under physiological conditions, $\Delta\Psi$ is about -150 mV [Kauppinen, 1983; Wan et al., 1993]. I assume that GST-Bcl-$_{XL}$ could activate the mtBK-channel strongly and that the P_o of the channel is increased at least thrice under physiological conditions *i.e.* at a potential of about -150 mV. However, in patch-clamp experiments I could not measure the mtBK-channel at -150 mV because such a strong potential would break the fragile mitoplast-membrane patch in a jiffy.

Since it was possible to observe inhibition of the mtBK-channel by GST-Bax and activation of mtBK-channel by GST-Bcl-$_{XL}$, the effect of the combination of both, GST-Bax and GST-Bcl-$_{XL}$ on the mtBK-channel was also tested. It turned out, that in a solution containing 3 nM GST-Bax together with 5 nM GST-Bcl-$_{XL}$, P_o of the mtBK-channel was unchanged at depolarizing potentials, while it was slightly increased at hyperpolarizing potentials (Fig. 27). This indicates that GST-Bcl-$_{XL}$ can abolish the inhibitory effect of GST-Bax on the mtBK-channel. It has been still under debate how Bcl-$_{XL}$ could abolish the effects of Bax on the mitochondria including opening of the PTP and release of cytochrome c. In some studies, it was believed that Bcl-$_{XL}$ can form a heterodimer with Bax through the interaction of their BH

3 domains [Diaz et al., 1997; Aritomi et al., 1997; Takada et al., 2005]. This theory is supported by the results of my study. In solutions containing 5 nM GST-Bcl-$_{XL}$ and 3 nM GST-Bax, GST-Bcl-$_{XL}$ heterodimerizes GST-Bax in the proportion 1:1. Thus, there was almost no free GST-Bax to inhibit the mtBK-channel. As the concentration of the GST-Bcl-$_{XL}$ was higher than GST-Bax, the remaining GST-Bcl-$_{XL}$, which did not form heterodimers with GST-Bax, would be available to increase the activity of the mtBK-channel slightly.

4.5 Effects of GST-Bax and GST-Bcl-$_{XL}$ on the PTP

Bax is a well-known activator of the mitochondrial PTP. In some studies, the underlying mechanism was explained by insertion of Bax into the mitochondrial membrane where it may form part of the pore by itself. The PTP and even the Bax-formed ion channel were observed in bilayer experiments [Qian et al., 2008; Schlesinger & Saito, 2006; García-Sáez et al., 2006]. Mitoplasts from astrocytes, in which the PTP is not recorded under normal conditions, were incubated in a solution containing 1 nM GST-Bax. I assumed that if GST-Bax could form the pore of the PTP in the mitoplast membrane, it should be possible to record current through the PTP in a patch-clamp experiment. However, no GST-Bax induced current was recorded. Moreover, mitoplasts from liver were incubated in a 1 nM Bax solution with 1 μM Ca^{2+}. 1 μM Ca^{2+} alone could not induce opening of the PTP in mitoplasts from liver. If current through the PTP could be observed, it is supposed to be induced by GST-Bax. However, no current of the PTP from liver mitoplasts was recorded, either. The explanation could be that Bax is combined with the GST protein, which can prevent Bax from forming the pore. Another reason for the absence of a PTP current could be that in isolated mitoplasts some cellular factors were missing, which are necessary for Bax to form the pore.

Inhibition of the PTP by Bcl-$_{XL}$ had been demonstrated in experiments at intact mitochondria [Li et al., 2003]. The patch-clamp experiments described here now show on the single-channel level that the PTP induced by 200 μM Ca^{2+}, can be irreversibly inhibited by 5 nM GST-Bcl-$_{XL}$. Thus, Li's results could be directly proved by my experiments. Taking together these result and the results from earlier studies, it is stated that Bcl-$_{XL}$ exerts its antiapoptotic activity through inactivation of Bax, stabilization of the mitochondrial membrane, and inhibition of caspases [Tsujimoto, 1998; Suzuki et al., 2000].

4.6 Conclusion

The results of my thesis describing the effects of both, hypoxia and apoptotic factors on the mtBK-channel and on the PTP as well as the interaction of the channels are summarized in Fig. 31. Under the influence of hypoxia, the mtBK-channel is activated and the PTP is inhibited. Thus, the response of the mitochondrial ion channels to hypoxia is considered as antiapoptotic. Further, mtBK-channel and PTP interact in that activated mtBK-channels keep the PTP closed. The proapoptotic factor Bax inhibits the mtBK-channel irreversibly from the intra- and from the extracellular side of the channel, which enables opening of the PTP. The antiapoptotic factor Bcl-$_{XL}$ exerts its antiapoptotic activity through direct inhibition of the PTP, insignificant activation of the mtBK-channel at hyperpolarizing potentials, and abolishing the effect of Bax on the mtBK-channel.
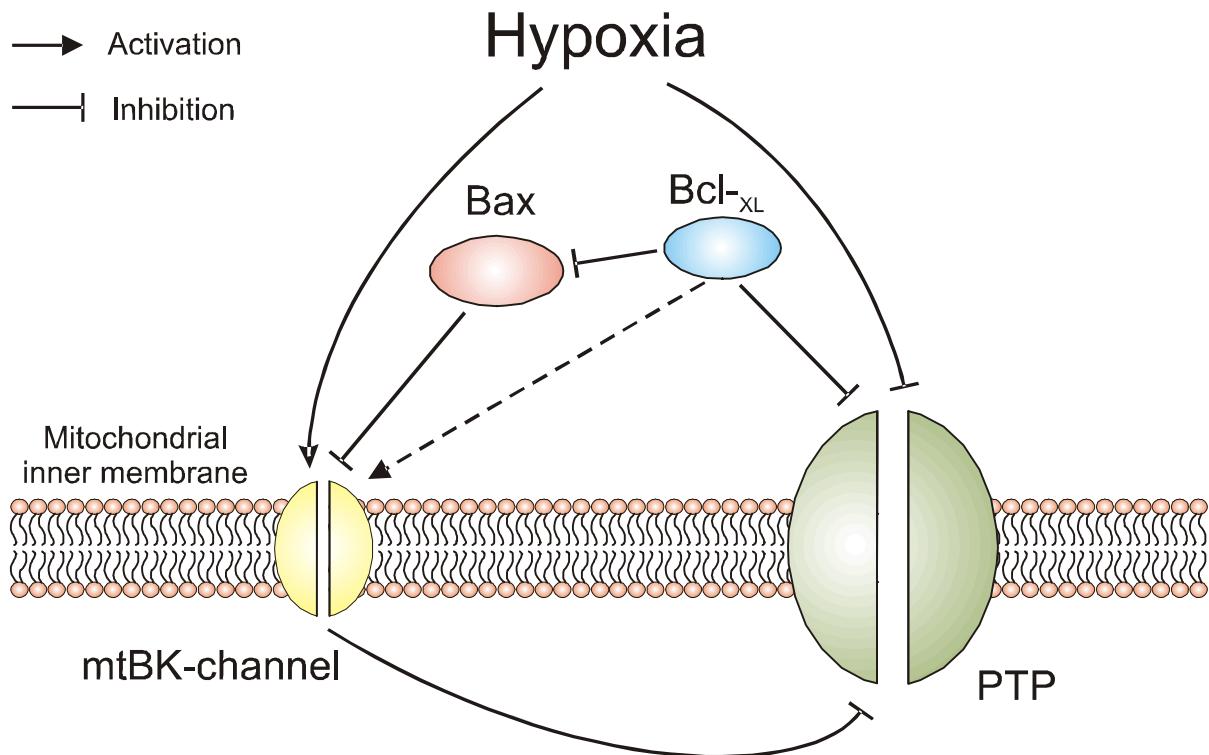
Fig. 31: Effects of hypoxia and of apoptotic factors on the mtBK-channel and on the PTP as well as interaction of the mtBK-channel and the PTP.

5 Abstract

Hypoxia causes severe damage to the cell by initiating signaling cascades that lead to cell death including necrosis and apoptosis. The apoptotic factors Bax and Bcl-$_{XL}$ can determine the destiny of the cell by their ability to influence the intrinsic pathway of apoptosis, which involves the mitochondria. Recently, there appeared evidence that mitochondrial ion channels are sensitive to low levels of oxygen and apoptotic factors. As our laboratory is interested in proving the interaction of the mtBK-channel and the PTP and their relation to apoptosis we assumed that studying hypoxia and cell death modulating substances would lead us to a better understanding of these mechanisms.

The effects of hypoxia induced by N_2 and DTN on the mtBK-channel from mitoplasts of rat astrocytes and at the PTP from mitoplasts of rat liver were studied by means of patch-clamp techniques. It is demonstrated here that hypoxia reversibly activated the mtBK-channel while the PTP was irreversibly inhibited. Experiments measuring $\Delta\Psi$ of intact rat brain mitochondria (using the fluorescence dye safranine O) exhibited an increased Ca^{2+}-retention capacity during hypoxia implying impaired opening of the PTP. Ca^{2+}-retention capacity was also reduced by 100 nM iberiotoxin, a selective BK-channel inhibitor. Thus, I show that an open mtBK-channel keeps the PTP closed. Moreover, I found that GST-Bax inhibited the mtBK-channel from both, intra- and extracellular side already at the very low concentration of 1 nM. This inhibition is progressively enhanced with time. The antiapoptotic factor GST-Bcl-$_{XL}$ had an insignificant tendency to activate the mtBK-channel at hyperpolarizing potentials. It inhibited the PTP, and abolished the effect of GST-Bax on the mtBK-channel.

The responses of the mtBK-channel and of the PTP to hypoxia could be considered as antiapoptotic and cytoprotective, because activation of the mtBK-channel contributes to cell survival and inhibition of the PTP disrupts the intrinsic apoptotic pathway. These effects might be mediated by the mitochondrial Ca^{2+} uptake and the oxygen sensitivity of the mitochondrial respiratory chain. Bax decreased the activity of the mtBK-channel so that opening of the PTP by Ca^{2+} is eased. This would result in activation of the downstream cascade of the intrinsic apoptotic pathway. Bcl-$_{XL}$ exerts its antiapoptotic activity through inhibition of Bax and the PTP.

6 Zusammenfassung

Hypoxie ist eine Ursache für die Auslösung der Signalkaskade, die zum Zelltod durch Apoptose oder Nekrose führen kann. Die apoptotischen Faktoren Bax und Bcl-$_{XL}$ können das Schicksal der Zelle durch ihre Wirkung im intrinsischen apoptotischen „Pathway" bestimmen, an dem die Mitochondrien beteiligt sind. In letzter Zeit gab es Beweise dafür, dass mitochondriale Ionenkanäle empfindlich gegen die Sauerstoffmangel und apoptotische Faktoren sind. Da unser Labor sich für die Interaktion des mtBK-Kanal und der PTP interessiert und ihre Bedeutung für die Apoptose, erwarten wir, dass die Untersuchung von Hypoxie und apoptotischen Faktoren uns zu einem besseren Verständnis dieser Mechanismen führen kann.

Mit Hilfe der Patch-Clamp Technik wurden die Effekte der durch N$_2$- und DTN-induzierten Hypoxie auf den mtBK-Kanal von Mitoplasten aus Rattenastrocyten und auf die PTP von Mitoplasten aus Rattenleber untersucht. Der mtBK-Kanal wurde durch Hypoxie reversibel aktiviert und die PTP irreversibel inhibiert. Die Messung des mitochondrialen Membran-potentials intakter Mitochondrien aus Rattenhirn mit fluoreszierendem Safranine O unter Hypoxie zeigte ein erhöhtes Ca^{2+}-Rückhaltvermögen der Mitochondrien, was eine beeinträchtigte Öffnung der PTP bedeutet. Es wurde ebenfalls ein reduziertes Ca^{2+}-Rückhaltvermögen der Mitochondrien mit 100 nM Ibtx, einem selektiven BK-Kanal Inhibitor, gefunden. Es ist deshalb davon auszugehen, dass ein offener mtBK-Kanal die PTP geschlossen hält. Außerdem inhibierte GST-Bax den mtBK-Kanal sehr wirksam von beiden Seiten der Membran. Diese Inhibition verstärkte sich nach dem Auswaschen weiter. GST-Bcl-$_{XL}$, ein antiapoptischer Faktor, konnte bei Hyperpolarisation den mtBK-Kanal nur insignifikant aktivieren, aber die PTP inhibieren und die Auswirkung von GST-Bax auf den mtBK-Kanal beseitigen.

Die Reaktion des mtBK-Kanals und der PTP auf Hypoxie könnte als antiapoptotisch und cytoprotektiv gesehen werden, weil Aktivierung des mtBK-Kanals zum Überleben der Zellen beiträgt und Inhibition der PTP den intrinsischen apoptotischen Pathway unterbricht. Die Reaktion der mitochondrialen Ionenkanäle könnte durch Zunahme der mitochondrialen Ca^{2+} Aufnahme und Empfindlichkeit der Atmungskette für Sauerstoff vermittelt werden. Bax kann die Aktivität des mtBK-Kanals inhibieren, was die Öffnung der PTP durch Ca^{2+} erleichtert. Die Öffnung der PTP führt zur Aktivierung der downstream Kaskaden in dem intrinsischen apoptotischen Pathway. Bcl-$_{XL}$ bewirkt seine antiapoptotische Tätigkeit nicht nur durch die

Inhibition der PTP sondern auch durch die Beseitigung des Inhibitionseffekts von Bax auf mtBK-Kanal.

7 Reference

Adams JM, Cory S (1998) The Bcl-2 protein family: arbiters of cell survival. *Science* 281:1322-1326.

Aggarwal S, Gollapudi S, Gupta S (1999) Increased TNF-alpha-induced apoptosis in lymphocytes from aged humans: changes in TNF-alpha receptor expression and activation of caspases. *J Immunol* 162:2154-2161.

Åkerman KE, Wikström MK (1976) Safranine as a probe of the mitochondrial membrane potential. *FEBS Lett* 68:191-197.

Andrabi SA, Sayeed I, Siemen D, Wolf G, Horn TF (2004) Direct inhibition of the mitochondrial permeability transition pore: a possible mechanism responsible for anti-apoptotic effects of melatonin. *FASEB J* 18:869-871.

Antignani A, Youle RJ (2006) How do Bax and Bak lead to permeabilization of the outer mitochondrial membrane? *Curr Opin Cell Biol* 18:685-689.

Antonsson B (2001) Bax and other pro-apoptotic Bcl-2 family "killer-proteins" and their victim the mitochondrion. *Cell Tissue Res* 306: 347-361.

Apte SS, Mattei MG, Olsen BR (1995) Mapping of the human BAX gene to chromosome 19q13.3-q13.4 and isolation of a novel alternatively spliced transcript, BAX delta. *Genomics* 26:592-594.

Aritomi M, Kunishima N, Inohara N, Ishibashi Y, Ohta S, Morikawa K (1997) Crystal structure of rat Bcl-xL. Implications for the function of the Bcl-2 protein family. *J Biol Chem* 272:27886-27892.

Barrett JN, Magleby KL, Pallotta BS (1982) Properties of single calcium-activated potassium channels in cultured rat muscle. *J Physiol* 331:311-230.

Basañez G, Nechushtan A, Drozhinin O, Chanturiya A, Choe E, Tutt S, Wood KA, Hsu Y, Zimmerberg J, Youle RJ (1999) Bax, but not Bcl-xL, decreases the lifetime of planar phospholipid bilayer membranes at subnanomolar concentrations. *Proc Natl Acad Sci USA* 96:5492-5497.

Bender LM, Morgan MJ, Thomas LR, Liu ZG, Thorburn A (2005) The adaptor protein TRADD activates distinct mechanisms of apoptosis from the nucleus and the cytoplasm. *Cell Death Differ* 12:473-481.

Benjelloun N, Joly LM, Palmier B, Plotkine M, Charriaut-Marlangue C (2003) Apoptotic mitochondrial pathway in neurones and astrocytes after neonatal hypoxia-ischaemia in the rat brain. *Neuropathol Appl Neurobiol* 29:350-360.

Bielefeldt K, Jackson MB (1994) Phosphorylation and dephosphorylation modulate a Ca^{2+}-activated K^+ channel in rat peptidergic nerve terminals. *J Physiol* 475:241-254.

Blatz AL, Magleby KL (1986) Single apamin-blocked Ca-activated K^+ channels of small conductance in cultured rat skeletal muscle. *Nature* 323:718-720.

Braun M, Ramracheya R, Bengtsson M, Zhang Q, Karanauskaite J, Partridge C, Johnson PR, Rorsman P (2008) Voltage-gated ion channels in human pancreatic beta-cells: electrophysiological characterization and role in insulin secretion. *Diabetes* 57:1618-1628.

Bräu ME, Vogel W, Hempelmann G (1998) Fundamental properties of local anesthetics: half-maximal blocking concentrations for tonic block of Na+ and K+ channels in peripheral nerve. *Anesth Analg* 87:885-889.

Broekemeier KM, Klocek CK, Pfeiffer DR (1998) Proton selective substate of the mitochondrial permeability transition pore: regulation by the redox state of the electron transport chain. *Biochemistry* 37:13059-13065.

Burwell LS, Nadtochiy SM, Brookes PS (2009) Cardioprotection by metabolic shut-down and gradual wake-up. *J Mol Cell Cardiol* 46:804-810.

Butler A, Tsunoda S, McCobb DP, Wei A, Salkoff L (1993) mSlo, a complex mouse gene encoding "maxi" calcium-activated potassium channels. *Science* 261:221-224.

Chamaon K, Kirches E, Kanakis D, Braeuninger S, Dietzmann K, Mawrin C (2005) Regulation of the pituitary tumor transforming gene by insulin-like-growth factor-I and insulin differs between malignant and non-neoplastic astrocytes. *Biochem Biophys Res Commun* 331:86-92.

Chan DC (2006) Mitochondria: dynamic organelles in disease, aging, and development. *Cell* 125:1241-1252.

Chance B (1964) The energy-linked reaction of calcium with mitochondria. *J Biol Chem* 240:2729-2748.

Cheng Y, Gu XQ, Bednarczyk P, Wiedemann FR, Haddad GG, Siemen D (2008) Hypoxia increases activity of the BK-channel in the inner mitochondrial membrane and reduces activity of the permeability transition pore. *Cell Physiol Biochem* 22:127-136.

Choi DW (1996) Ischemia-induced neuronal apoptosis. *Curr Opin Neurobiol* 6:667-672.

Cittelly DM, Nesic O, Johnson K, Hulsebosch C, Perez-Polo JR (2007) Detrimental effects of antiapoptotic treatments in spinal cord injury. *Exp Neurol* 210:295-307.

Cohen MV, Baines CP, Downey JM (2000) Ischemic preconditioning: from adenosine receptor to K_{ATP} channel. *Annu Rev Physiol* 62:79-109.

Connern CP, Halestrap AP (1992) Purification and N-terminal sequencing of peptidyl-prolyl cis-trans-isomerase from rat liver mitochondrial matrix reveals the existence of a distinct mitochondrial cyclophilin. *Biochem J* 284:381-385.

Corey DP, Stevens GF (1983) Science and technology of patchrecording electrodes. In: Sakmann B, Neher E (eds) *Singlechannel recording*. Plenum, NY, USA, pp 66-67.

Crompton M, Ellinger H, Costi A (1988) Inhibition by cyclosporin A of a Ca^{2+}-dependent pore in heart mitochondria activated by inorganic phosphate and oxidative stress. *Biochem J* 255:357-360.

Dale TJ, Cryan JE, Chen MX, Trezise DJ (2002) Partial apamin sensitivity of human small conductance Ca^{2+}-activated K^+ channels stably expressed in Chinese hamster ovary cells. *Naunyn Schmiedebergs Arch Pharmacol* 366:470-477.

Denson DD, Duchatelle P, Eaton DC (1994) The effect of racemic ketamine on the large conductance Ca^{2+}-activated potassium (BK) channels in GH3 cells. *Brain res* 638:61-68.

Dermietzel R, Hwang TK, Buettner R, Hofer A, Dotzler E, Kremer M, Deutzmann R, Thinnes FP, Fishman GI, Spray DC, Siemen D (1994) Cloning and in situ localization of a brain-derived porin that constitutes a large-conductance anion channel in astrocytic plasma membranes. Proc Natl Acad Sci USA 91:499-503.

Di Lisa F, Kaludercic N, Carpi A, Menabò R, Giorgio M (2009) Mitochondrial pathways for ROS formation and myocardial injury: the relevance of p66 (Shc) and monoamine oxidase. *Basic Res Cardiol* 104:131-139.

Diaz JL, Oltersdorf T, Horne W, McConnell M, Wilson G, Weeks S, Garcia T, Fritz LC (1997) A common binding site mediates heterodimerization and homodimerization of Bcl-2 family members. *J Biol Chem* 272:11350-11355.

Douglas RM, Lai JC, Bian S, Cummins L, Moczydlowski E, Haddad GG (2006) The calcium-sensitive large-conductance potassium channel (BK/MAXI K) is present in the inner mitochondrial membrane of rat brain. *Neuroscience* 139:1249-1261.

Dugan LL, Kim-Han JS (2006) Hypoxic-ischemic brain injury and oxidative stress. In: Siegel GJ, Wayne Albers R, Brady ST, Price DL (eds.) *Basic neurochemistry: molecular, cellular, and medical aspects.* 7th edition Elsevier Academic Press, MA, USA, pp 559.

Dworetzky SI, Trojnacki JT, Gribkoff VK (1994) Cloning and expression of a human large-conductance calcium-activated potassium channel. *Brain Res Mol Brain Res* 27:189-193.

Fadeel B, Orrenius S (2005) Apoptosis: a basic biological phenomenon with wide-ranging implications in human disease. *J Intern Med.* 258:479-517.

Fontaine E, Eriksson O, Ichas F, Bernardi P (1998) Regulation of the permeability transition pore in skeletal muscle mitochondria. Modulation By electron flow through the respiratory chain complex I. *J Biol Chem* 273:12262-12268.

Fournier N, Ducet G, Crevat A (1987) Action of cyclosporine on mitochondrial calcium fluxes. *J Bioenerg Biomembr* 19:297-303.

Garcia ML, Galvez A, Garcia-Calvo M, King VF, Vazquez J, Kaczorowski GJ (1991) Use of toxins to study potassium channels. *J Bioenerg Biomembr* 23:615-646.

García-Sáez AJ, Coraiola M, Serra MD, Mingarro I, Müller P, Salgado J (2006) Peptides corresponding to helices 5 and 6 of Bax can independently form large lipid pores. *FEBS J* 273:971-981.

Gardos G (1958) The function of calcium in the potassium permeability of human erythrocytes. *Biochim Biophys Acta* 30:653-654.

Garlid KD (2000) Opening mitochondrial K_{ATP} in the heart--what happens, and what does not happen. *Basic Res Cardiol.* 95:275-279.

Garlid KD, Paucek P (2003) Mitochondrial potassium transport: the K^+ cycle. *Biochim Biophys Acta* 1606:23-41.

Garlid KD, Paucek P, Yarov-Yarovoy V, Murray HN, Darbenzio RB, D'Alonzo AJ, Lodge NJ, Smith MA, Grover GJ (1997) Cardioprotective effect of diazoxide and its interaction with mitochondrial ATP-sensitive K^+ channels. Possible mechanism of cardioprotection. *Circ Res* 81: 1072-1082.

Ghatta S, Nimmagadda D, Xu X, O'Rourke ST (2006) Large-conductance, calcium-activated potassium channels: structural and functional implications. *Pharmacol Ther* 110:103-116.

Giam M, Huang DC, Bouillet P (2008) BH3-only proteins and their roles in programmed cell death. *Oncogene* 27:128-136.

Gill MB, Perez-Polo JR (2008) Hypoxia ischemia-mediated cell death in neonatal rat brain. *Neurochem Res* 33:2379-2389.

Green DR (2006) At the gates of death. *Cancer Cell* 9:328-330.

Grigoriev SM, Muro C, Dejean LM, Campo ML, Martinez-Caballero S, Kinnally KW (2004) Electrophysiological approaches to the study of protein translocation in mitochondria. *Int Rev Cytol* 238:227-274.

Gross A, Jockel J, Wei MC, Korsmeyer SJ (1998) Enforced dimerization of BAX results in its translocation, mitochondrial dysfunction and apoptosis. *EMBO J* 17:3878-3885.

Gu XQ, Siemen D, Parvez S, Cheng Y, Xue J, Zhou D, Sun X, Jonas EA, Haddad GG (2007) Hypoxia increases BK channel activity in the inner mitochondrial membrane. *Biochem Biophys Res Commun* 358:311-316.

Gunter TE, Buntinas L, Sparagna G, Eliseev R, Gunter K (2000) Mitochondrial calcium transport: mechanisms and functions. *Cell Calcium* 28:285-296.

Gunter TE, Pfeiffer DR (1990) Mechanisms by which mitochondria transport calcium. *Am J Physiol* 258:C755-C786.

Halestrap AP, McStay GP, Clarke SJ (2002) The permeability transition pore complex: another view. *Biochem* 84:153-166.

Hamill OP, Marty A, Neher E, Sakmann B, Sigworth FJ (1981) Improved patch-clamp techniques for high-resolution current recording from cells and cell-free membrane patches. *Pflügers Archiv* 391:85-100.

Harris EJ, Al-Shaikhaly M, Baum H (1979) Stimulation of mitochondrial calcium ion efflux by thiol-specific reagents and by thyroxine. The relationship to adenosine diphosphate retention and to mitochondrial permeability. *Biochem J* 182:455-464.

Haworth RA, Hunter DR (1980) Allosteric inhibition of the Ca^{2+}-activated hydrophilic channel of the mitochondrial inner membrane by nucleotides. *J Membr Biol* 54:231-236.

Heginbotham L, Abramson T, MacKinnon R (1992) A functional connection between the pores of distantly related ion channels as revealed by mutant K^+ channels. *Science* 258:1152-1155.

Heginbotham L, Lu Z, Abramson T, MacKinnon R (1994) Mutations in the K^+ channel signature sequence. *Biophys J* 66:1061-1067.

Hille B (2001) *Ion channels of excitable membranes*. Sinauer Association, Sunderland, MA.

Hirano J, Nakamura K, Kubokawa M (2001) Properties of a Ca^{2+}-activated large conductance K^+ channel with ATP sensitivity in human renal proximal tubule cells. *Jpn J Physiol* 51:481-489.

Holland M, Langton PD, Standen NB, Boyle JP (1996) Effects of the BK_{Ca} channel activator, NS1619, on rat cerebral artery smooth muscle. *Br J Pharmacol* 117:119-129.

Hood DA, Adhihetty PJ, Colavecchia M, Gordon JW, Irrcher I, Joseph AM, Lowe ST, Rungi AA (2003) Mitochondrial biogenesis and the role of the protein import pathway. *Med Sci Sports Exerc* 35:86-94.

Hsu YT, Youle RJ (1997) Nonionic detergents induce dimerization among members of the Bcl-2 family. *J Biol Chem* 272:13829-13834.

Hudspeth AJ, Lewis RS (1988) Kinetic analysis of voltage- and ion-dependent conductances in saccular hair cells of the bull-frog, Rana catesbeiana. *J Physiol* 400:237-274.

Hunter DR, Haworth RA, Southard JH (1976) Relationship between configuration, function, and permeability in calcium-treated mitochondria. *J Biol Chem* 25:5069-5077.

Hunter JJ, Parslow TG (1996) A peptide sequence from Bax that converts Bcl-2 into an activator of apoptosis. *J Biol Chem* 271:8512-8514.

Inoue I, Nagase H, Kishi K, Higuti T (1991) ATP-sensitive K^+ channel in the mitochondrial inner membrane. *Nature* 352:244-247.

Ishii TM, Silvia C, Hirschberg B, Bond CT, Adelman JP, Maylie J (1997) A human intermediate conductance calcium-activated potassium channel. *Proc Natl Acad Sci USA* 94:11651-11656.

Jensen BS, Strøbaek D, Olesen SP, Christophersen P (2001) The Ca^{2+}-activated K^+ channel of intermediate conductance: a molecular target for novel treatments? *Curr Drug Targets* 2:401-422.

Jesenberger V, Jentsch S (2002) Deadly encounter: ubiquitin meets apoptosis. *Nat Rev Cell Biol* 3:112-131.

Jiang Y, Lee A, Chen J, Cadene M, Chait BT, MacKinnon R (2002) Crystal structure and mechanism of a calcium-gated potassium channel. *Nature* 417:515-522.

Jiang Y, Pico A, Cadene M, Chait BT, MacKinnon R (2001) Structure of the RCK domain from the E. coli K^+ channel and demonstration of its presence in the human BK channel. *Neuron* 29:593-601.

Jin Z, El-Deiry WS (2005) Overview of cell death signaling pathways. *Cancer Biol Ther* 4:139-163.

Kaczorowski GJ, Knaus HG, Leonard RJ, McManus OB, Garcia ML (1996) High-conductance calcium-activated potassium channels; structure, pharmacology, and function. *J Bioenerg Biomembr* 28:255-267.

Kauppinen R (1983) Proton electrochemical potential of the inner mitochondrial membrane in isolated perfused rat hearts, as measured by exogenous probes. *Biochim Biophys Acta* 725:131-137.

Kehl SJ, Wong K (1996) Large-conductance calcium-activated potassium channels of cultured rat melanotrophs. *J Membr Biol* 150:219-230.

Kerr JF, Wyllie AH, Currie AR (1972) Apoptosis: a basic biological phenomenon with wide-ranging implications in tissue kinetics. *Br J Cancer* 26:239-257.

Kharbanda S, Pandey P, Schofield L, Israels S, Roncinske R, Yoshida K, Bharti A, Yuan ZM, Saxena S, Weichselbaum R, Nalin C, Kufe D (1997) Role for Bcl-xL as an inhibitor of cytosolic cytochrome C accumulation in DNA damage-induced apoptosis. *Proc Natl Acad Sci USA* 94:6939-6942.

Kinnally KW, Tedeschi H, Mannella CA (1987) Evidence for a novel voltage-activated channel in the outer mitochondrial membrane. *FEBS Lett* 226:83-87.

Kleinsmith, LJ, Kish VM (1995) *Principles of cell and molecular biology.* Harper Collins College Publisher, NY, USA, pp 315-319.

Kluck RM, Bossy-Wetzel E, Green DR, Newmeyer DD (1997) The release of cytochrome c from mitochondria: a primary site for Bcl-2 regulation of apoptosis. *Science* 275:1132-1136.

Kokoszka JE, Waymire KG, Levy SE, Sligh JE, Cai J, Jones DP, MacGregor GR, Wallace DC (2004) The ADP/ATP translocator is not essential for the mitochondrial permeability transition pore. *Nature* 427:461-465.

Latorre R, Brauchi S (2006) Large conductance Ca^{2+}-activated K^+ (BK) channel: activation by Ca^{2+} and voltage. *Biol Res* 39:385-401.

Layne E (1957) Spectrophotometric and Turbidimetric Methods for Measuring Proteins. *Methods in Enzymology* 10:447-455.

Levadny V, Colombini M, Li XX, Aguilella VM (2002) Electrostatics explains the shift in VDAC gating with salt activity gradient. *Biophys J* 82:1773-1783.

Li M, Xia T, Jiang CS, Li LJ, Fu JL, Zhou ZC (2003) Cadmium directly induced the opening of membrane permeability pore of mitochondria which possibly involved in cadmium-triggered apoptosis. *Toxicology* 194:19-33.

Li P, Nijhawan D, Budihardjo I, Srinivasula SM, Ahmad M, Alnemri ES, Wang X (1997) Cytochrome c and dATP-dependent formation of Apaf-1/caspase-9 complex initiates an apoptotic protease cascade. *Cell* 91:479-489.

Li W, Aldrich RW (2004) Unique inner pore properties of BK channels revealed by quaternary ammonium block. *J Gen Physiol* 124:43-57.

Lingle CJ, Solaro CR, Prakriya M, Ding JP (1996) Calcium-activated potassium channels in adrenal chromaffin cells. *Ion Channels* 4:261-301.

Liu X, Kim CN, Yang J, Jemmerson R, Wang X (1996) Induction of apoptotic program in cell-free extracts: requirement for dATP and cytochrome c. *Cell* 86:147-157.

Liu H, Moczydlowski E, Haddad GG (1999) O_2 deprivation inhibits Ca^{2+}-activated K^+ channels via cytosolic factors in mice neocortical neurons. *J Clin Invest* 104:577-588.

Loupatatzis C, Seitz G, Schönfeld P, Lang F, Siemen D (2002) Single-channel currents of the permeability transition pore from the inner mitochondrial membrane of rat liver and of a human hepatoma cell line. *Cell Physiol Biochem* 12:269-278.

Mannella CA (2008) Structural diversity of mitochondria: functional implications. *Ann N Y Acad Sci* 1147:171-179.

Marty A (1981) Ca-dependent K channels with large unitary conductance in chromaffin cell membranes. *Nature* 291:497-500.

Meera P, Wallner M, Toro L (2000) A neuronal beta subunit (KCNMB4) makes the large conductance, voltage- and Ca^{2+}-activated K^+ channel resistant to charybdotoxin and iberiotoxin. *Proc Natl Acad Sci USA* 97:5562-5567.

Meier P, Finch A, Evan G (2000) Apoptosis in development. *Nature* 407:796-801.

Morin D, Pires F, Plin C, Tillement JP (2004) Role of the permeability transition pore in cytochrome C release from mitochondria during ischemia-reperfusion in rat liver. *Biochem Pharmacol* 68:2065-2073.

Nardi A, Calderone V, Chericoni S, Morelli I. (2003) Natural modulators of large-conductance calcium-activated potassium channels. *Planta Med* 69:885-892.

National Center for Health Statistics. Health, United States, 2004. Hyattsville, Maryland: *Public Health Service*.2004.

Neher E, Sakmann B (1976) Single-channel currents recorded from membrane of denervated frog muscle fibres. *Nature* 260:799-802.

Nelson MT, Cheng H, Rubart M, Santana LF, Bonev AD, Knot HJ, Lederer WJ (1995) Relaxation of arterial smooth muscle by calcium spark. *Science* 270:633-637.

Nicholls DG, Ferguson SJ (2002) *Bioenergetics 3*. London, Academic.

Nimigean CM, Magleby KL (1999) The beta subunit increases the Ca^{2+} sensitivity of large conductance Ca^{2+}-activated potassium channels by retaining the gating in the bursting states. *J Gen Physiol* 113:425-440.

Ohya S, Kuwata Y, Sakamoto K, Muraki K, Imaizumi Y(2005) Cardioprotective effects of estradiol include the activation of large-conductance Ca^{2+}-activated K^+ channels in cardiac mitochondria. *Am J Physiol Heart Circ Physiol* 289:H1635-H1642.

Oltvai ZN, Milliman CL, Korsmeyer SJ (1993) Bcl-2 heterodimerizes in vivo with a conserved homolog, Bax, that accelerates programmed cell death. *Cell* 74:609-619.

O'Rourke B (2006) Mitochondrial ion channels. *Annu Rev Physiol* 69:19-49.

Papazian DM, Shao XM, Seoh SA, Mock AF, Huang Y, Wainstock DH (1995) Electrostatic interactions of S4 voltage sensor in Shaker K^+ channel. *Neuron* 14:1293-1301.

Paquette JC, Guérin PJ, Gauthier ER (2005) Rapid induction of the intrinsic apoptotic pathway by L-glutamine starvation. *J Cell Physiol* 202:912-921.

Pluznick JL, Sansom SC (2006) BK channels in the kidney: role in K^+ secretion and localization of molecular components. *Am J Physiol Renal Physiol* 291:F517-F529.

Pouliquen D, Bellot G, Guihard G, Fichet P, Meflah K, Vallette FM (2006) Mitochondrial membrane permeabilization produced by PTP, Bax and apoptosis: a 1H-NMR relaxation study. *Cell Death Differ* 13:301-310.

Prindull G (1995) Apoptosis in the embryo and tumorigenesis. *Eur J Cancer* 31a:116-123.

Pulera MR, Adams LM, Liu H, Santos DG, Nishimura RN, Yang F, Cole GM, Wasterlain CG (1998) Apoptosis in a neonatal rat model of cerebral hypoxia-ischemia. *Stroke* 29:2622-2630.

Qian S, Wang W, Yang L, Huang HW (2008) Structure of transmembrane pore induced by Bax-derived peptide: evidence for lipidic pores. *Proc Natl Acad Sci USA* 105:17379-17383.

Ramanathan K, Michael TH, Jiang GJ, Hiel H, Fuchs PA (1999) A molecular mechanism for electrical tuning of cochlear hair cells. *Science* 283:215-217.

Rao RV, Castro-Obregon S, Frankowski H, Schuler M, Stoka V, del Rio G, Bredesen DE, Ellerby HM (2002) Coupling endoplasmic reticulum stress to the cell death program. An Apaf-1-independent intrinsic pathway. *J Biol Chem* 277:21836-21842.

Reinhart PH, Chung S, Martin BL, Brautigan DL, Levitan IB (1991) Modulation of calcium-activated potassium channels from rat brain by protein kinase A and phosphatase 2A. *J Neurosci* 11:1627-1635.

Robitaille R, Garcia ML, Kaczorowski GJ, Charlton MP (1993) Functional colocalization of calcium and calcium-gated potassium channels in control of transmitter release. *Neuron* 11:645-655.

Ruiz-Meana M, Garcia-Dorado D, Miró-Casas E, Abellán A, Soler-Soler J (2006) Mitochondrial Ca^{2+} uptake during simulated ischemia does not affect permeability transition pore opening upon simulated reperfusion. *Cardiovasc Res* 71:715-724.

Safronov BV & Vogel W (1999) Electrical activity of individual neurons: Patch-clamp techniques. In: Windhorst U, Johansson H (eds.) *Modern technique in neuroscience research.* Springer, Berlin, Germany, pp 173-192.

Sakmann B, Neher E (1995) *Single-channel recording 2nd.* A Division of Plenum Press, New York.

Saponara S, Testai L, Iozzi D, Martinotti E, Martelli A, Chericoni S, Sgaragli G, Fusi F, Calderone V (2006) (+/-)-Naringenin as large conductance Ca^{2+}-activated K^+ (BKCa) channel opener in vascular smooth muscle cells. *Br J Pharmacol* 149:1013-1021.

Saraste A, Pulkki K (2000) Morphologic and biochemical hallmarks of apoptosis. *Cardiovasc Res* 45:528-537.

Sayeed I, Parvez S, Winkler-Stuck K, Seitz G, Trieu I, Wallesch CW, Schönfeld P, Siemen D (2006) Patch clamp reveals powerful blockade of the mitochondrial permeability transition pore by the D2-receptor agonist pramipexole. *FASEB J* 20:556-558.

Scalettar BA, Abney JR, Hackenbrock CR (1991) Dynamics, structure, and function are coupled in the mitochondrial matrix. *Proc Natl Acad USA* 88:8057-8061.

Schein SJ, Colombini M, Finkelstein A (1975) Reconstitution in planar lipid bilayers of a voltage-dependent anion-selective channel obtained from paramecium mitochondria. *J Membr Biol* 30:99-120.

Schlesinger PH, Saito M (2006) The Bax pore in liposomes, Biophysics. *Cell Death Differ* 13:1403-1408.

Schreiber M, Salkoff L (1997) A novel calcium-sensing domain in the BK channel. *Biophys J* 73:1355-1363.

Semenza GL (2007) Life with oxygen. *Science* 318:62-64.

Shoshan-Barmatz V, Israelson A, Brdiczka D, Sheu SS (2006) The voltage-dependent anion channel (VDAC): function in intracellular signaling, cell life and cell death. *Curr Pham Des.* 12:2249-2270.

Siemen D, Loupatatzis C, Borecky J, Gulbins E, Lang F (1999) Ca^{2+}-activated K channel of the BK-type in the inner mitochondrial membrane of a human glioma cell line. *Biochem Biophys Res Commun* 257:549-554.

Sorgato MC, Keller BU, Stühmer W (1987) Patch-clamping of the inner mitochondrial membrane reveals a voltage-dependent ion channel. *Nature* 330:498-500.

Soto P, Smith LC (2009) BH4 peptide derived from Bcl-xL and Bax-inhibitor peptide suppresses apoptotic mitochondrial changes in heat stressed bovine oocytes. *Mol Reprod Dev* 76:637-646.

Statistische Bundesamt Deutschland. *Statistisches Jahrbuch Gesundheit 2005.* Wiesbaden, Germany, 2005.

Stefani E, Ottolia M, Noceti F, Olcese R, Wallner M, Latorre R, Toro L (1997) Voltage-controlled gating in a large conductance Ca^{2+}-sensitive K^+channel (hslo). *Proc Natl Acad Sci USA* 94:5427-5431.

Stefanis L (2005) Caspase-dependent and -independent neuronal death: two distinct pathways to neuronal injury. *Neuroscientist* 11:50-62.

Sung KF, Odinokova IV, Mareninova OA, Rakonczay Z Jr, Hegyi P, Pandol SJ, Gukovsky I, Gukovskaya AS (2009) Prosurvival Bcl-2 proteins stabilize pancreatic mitochondria and protect against necrosis in experimental pancreatitis. *Exp Cell Res* 315:1975-1989.

Susin SA, Zamzami N, Castedo M, Hirsch T, Marchetti P, Macho A, Daugas E, Geuskens M, Kroemer G (1996) Bcl-2 inhibits the mitochondrial release of an apoptogenic protease. *J Exp Med* 184:1331-1341.

Suzuki M, Youle RJ, Tjandra N (2000) Structure of Bax: coregulation of dimer formation and intracellular localization. *Cell* 103:645-654.

Szabó I, Bock J, Grassmé H, Soddemann M, Wilker B, Lang F, Zoratti M, Gulbins E (2008) Mitochondrial potassium channel $Kv_{1.3}$ mediates Bax-induced apoptosis in lymphocytes. *Proc Natl Acad Sci USA* 105:14861-14866.

Szabó I, Zoratti M (1991) The giant channel of the inner mitochondrial membrane is inhibited by cyclosporin A. *J Biol Chem* 266:3376-3379.

Szabó I, Zoratti M (1992) The mitochondrial megachannel is the permeability transition pore. *J Bioenerg Biomembr* 24:111-117.

Takada N, Yamaguchi H, Shida K, Terajima D, Satou Y, Kasuya A, Satoh N, Satake M, Wang HG (2005) The cell death machinery controlled by Bax and Bcl-XL is evolutionarily conserved in Ciona intestinalis. *Apoptosis* 10:1211-1220.

Tedeschi H, Kinnally KW (1987) Channels in the mitochondrial out membrane: evidence from patch-clamp studies. *J Bioenerg Biomembr* 19:321-327.

Thomas AL, Price C, Martin SG, Carmichael J, Murray JC (1999) Identification of two novel mRNA splice variants of bax. *Cell Death Differ* 6:97-98.

Thompson CB (1995) Apoptosis in the pathogenesis and treatment of disease. (1995) *Science* 267:1456-1462.

Toro L, Wallner M, Meera P, Tanaka Y (1998) Maxi-K_{Ca}, a unique member of the voltage-gated K channel superfamily. *News Physiol Sci* 13:112-117.

Tsujimoto Y, Nakagawa T, Shimizu S (2006) Mitochondrial membrane permeability transition and cell death. *Biochim Biophys Acta* 1757:1297-300.

Tsujimoto Y (1998) Role of Bcl-2 family proteins in apoptosis: apoptosomes or mitochondria? *Genes Cells* 3:697-707.

Vaux DL, Cory S, Adams JM (1988) Bcl-2 gene promotes haemopoietic cell survival and cooperates with c-myc to immortalize pre-B cells. *Nature* 335:440-442.

Vikis HG, Guan KL (2004) Glutathione-S-transferase-fusion based assays for studying protein-protein interactions. *Methods Mol Biol* 261:175-186.

Wallner M, Meera P, Ottolia M, Kaczorowski GJ, Latorre R, Garcia ML, Stefani E, Toro L (1995) Characterization of and modulation by a beta-subunit of a human maxi K_{Ca} channel cloned from myometrium. *Receptors Channels* 3:185-199.

Wan B, Doumen C, Duszynski J, Salama G, LaNoue KF (1993) A method of determining electrical potential gradient across mitochondrial membrane in perfused rat hearts. *Am J Physiol* 265:H445-452.

Wang X, Yin C, Xi L, Kukreja RC (2004) Opening of Ca^{2+}-activated K^+ channels triggers early and delayed preconditioning against I/R injury independent of NOS in mice. *Am J Physiol Heart Circ Physiol* 287:H2070-H2077.

Wang ZW (2008) Regulation of synaptic transmission by presynaptic CaMKII and BK channels. *Mol Neurobiol* 38:153-166.

Wei A, Jegla T, Salkoff L (1996) Eight potassium channel families revealed by the C. elegans genome project. *Neuropharmacology* 35:805-829.

Wei A, Solaro C, Lingle C, Salkoff L (1994) Calcium sensitivity of BK-type K_{Ca} channels determined by a separable domain. *Neuron* 13:671-681.

Williams SE, Wootton P, Mason HS, Bould J, Iles DE, Riccardi D, Peers C, Kemp PJ (2004) Hemoxygenase-2 is an oxygen sensor for a calcium-sensitive potassium channel. *Science* 306:2093-2097.

Woodfield KY, Price NT, Halestrap AP (1997) cDNA cloning of rat mitochondrial cyclophilin. *Biochim Biophys Acta* 1351:27-30.

Xu W, Liu Y, Wang S, McDonald T, Van Eyk JE, Sidor A, O'Rourke B (2002) Cytoprotective role of Ca^{2+}- activated K^+ channels in the cardiac inner mitochondrial membrane. *Science* 298:1029-1033.

Yang J, Liu X, Bhalla K, Kim CN, Ibrado AM, Cai J, Peng TI, Jones DP, Wang X (1997) Prevention of apoptosis by Bcl-2: release of cytochrome c from mitochondria blocked. *Sience* 275:1129-1132.

Ye D, Pospisilik JA, Mathers DA (1996) Nitroblue tetrazolium blocks BK channels in cerebrovascular smooth muscle cell membranes. *Br J Pharmacol* 129:1035-1041.

Yoshida A, Oda M, Ikemoto Y (1991) Kinetics of the Ca^{2+}-activated K^+ channel in rat hippocampal neurons. *Jpn J Physiol* 41:297-315.

Zhang H, Heim J, Meyhack B (1998) Redistribution of Bax from cytosol to membranes is induced by apoptotic stimuli and is an early step in the apoptotic pathway. *Biochem Biophys Res Commun* 251:454-459.

Zhou M, Demo SD, McClure TN, Crea R, Bitler CM (1998) A novel splice variant of the cell death-promoting protein BAX. *J Biol Chem* 273:11930-11936.

8 Abbreviations

ADP	adenosine diphosphate
AIF	apoptosis-inducing factor
ANT	Adenine nucleotide translocator
ATP	adenosine-5'-triphosphate
Bax	Bcl-2 associated protein X
Bcl-2	B cell lymphoma 2
Bcl-$_W$	Bcl-2 like 2
Bcl-$_{XL}$	B-cell lymphoma-extra large
Bcl-$_{XS}$	B-cell lymphoma-extra short
BH	B cell homology
Bid	BH 3 interacting domain death agonist
Bik	Bcl-2 interacting killer
BK	Ca^{2+} activated large-conductance potassium channel
BSA	bovine serum albumin
cAMP	cyclic adenosine monophosphate
Caspase	cysteine-aspartic acid proteases
Chtx	charybdotoxin
CLC	chloride channel
CLIC	chloride intracellular channel
CsA	cyclosporine A
dATP	2'-deoxyadenosine 5'-triphosphate
DMEM	Dulbecco's modified Eagle medium
DNA	desoxyribonucleic acid
dSlo	drosophila slowpoke locus
DTN	dithionite
EDTA	ethylenediaminetetraacetic acid
EGTA	ethylene glycol tetraacetic acid
FADD	Fas-associated death domain
GST	glutathionyl-s-transferase
Hepes	4-(2-hydroxyethyl)-1-piperazineethanesulfonic acid
HIF	hypoxia-inducible factor
hslo	human homologue of dSlo
Ibtx	iberiotoxin

IK	Ca^{2+} activated intermediate-conductance potassium channel
IMAC	inner membrane anion channel
IMM	inner mitochondrial membrane
K_{ATP}	ATP sensitive potassium channel
$K_{V1.3}$	voltage-gated potassium channel, shaker-related subfamily, member 3
MPT	mitochondrial permeability transition
MSE	mannitol-sucrose-EGTA
N_2	nitrogen
mslo	mouse homologue of dSlo
mV	millivolt
nS	nanosiemens
OMM	outer mitochondrial membrane
PKA	protein kinase A
P_o	open probability
pS	picosiemens
PTP	permeability transition pore
QA	quaternary ammonium
RBM	rat brain mitochondria
RCK	regulator of conductance for potassium domain
RLM	rat liver mitochondria
ROS	reactive oxygen species
SK	Ca^{2+} activated small-conductance potassium channel
TBA	tetrabutylammonium hydroxide
TEA	tetraethylammonium chloride
TIM	mitochondrial translocase of the inner membrane
TM	transmembrane unit
TNF	tumor necrosis factor
TOM	mitochondrial translocase of the outer membrane
TRADD	TNF receptor-associated death domain
VDAC	voltage-dependent anion channel
$\Delta\Psi$	mitochondrial membrane potential

9 Appendix

I. Publications during Ph. D studies

1. Gu XG, Siemen D, Parvez S, **Cheng Y**, Xue J, Sun X, Jonas EA, Haddad GG (2007) Hypoxia increases BK channel activity in the inner mitochondrial membrane. *Biochem Biophys Res Commun* 358:311-316.

2. **Cheng Y**, Gu XQ, Bednarczyk P, Wiedemann FR, Haddad GG, Siemen D (2008) Hypoxia increases activity of the BK-channel in the inner mitochondrial membrane and reduces activity of the permeability transition pore. *Cell Physiol Biochem* 22:127-136.

3. **Cheng Y**, Debska-Vielhaber G, Siemen D (2009) Interaction of mitochondrial potassium channels with the permeability transition pore. *FEBS Lett.* 2009 Dez 27 (Epub ahead of print).

4. *Cheng Y, Gulbins E, Siemen D etc. The mtBK-channel is modified by apoptotic factors: Bax and Bcl-$_{XL}$ (in preparation).*

5. *Bednarczyk P, **Cheng Y**, Szewczyk A, Siemen D etc. The influence of the mitochondrial respiratory chains on the activity of the mtBK-channel (in preparation).*

II. Oral Presentations

1. **Cheng Y**. (2009) Hypoxia increases activity of the BK-channel in the inner mitochondrial membrane and reduces activity of the permeability transition pore. "Redox-Regulation in Acute and Chronic Inflammation", German-Italian conference in Loveno di Menaggio, Italy, Mar 11-13, 2009.

III. Poster Presentations

1. Siemen D, **Cheng Y**, Trieu I, Parvez S, Hertel S, Schultze A, Wiedemann FR. (2007) Block of the mitochondrial permeability transition pore may cause neuroprotection. The 86th Annual Meeting of the German Physiological Society, Hannover, Germany, Mar. 25-28, 2007. *Acta Physiol.* 189, p90.

2. **Cheng Y**, Gu XQ, Bednarczyk P, Zhao H, Haddad GG, Siemen D (2007) Hypoxia modifies mtBK-channels of astrocyte-cell line. The 37th Annual Meeting of the American Society for Neuroscience, San Diego, USA, Nov. 3-7, 2007. *Abstracts Sunday* p98.

3. **Cheng Y**, Gu XQ, Bednarczyk P, Siemen D (2008) Hypoxia modulates activity of mitochondrial ion channels. The 87th Annual Meeting of the German Physiological Society of Physiology, Cologne, Germany, Mar. 2-5, 2008. *Acta Physiol.* 192, p181.

4. **Cheng Y**, Gu XQ, Bednarczyk P, Siemen D. (2008) Modulation of the activity of the mtBK-channel and of the permeability transition pore by hypoxia. Neuroprotection and Neurorepair - Cerebral Ischemia and Stroke, 5th International Symposium in Magdeburg, Germany, May 17 – 20, 2008.

5. Siemen D, Kupsch K, Schultz A, Hertel S, **Cheng Y**, Kreutzmann P, Schönfeld P (2009) Possible explanation of the contrasting effects of minocycline in experiments on mitochondria and in a clinical study. The 88th Annual Meeting of the German Physiological Society, Giessen, Germany, Mar. 22-25, 2009. *Acta Physiol.* 195, pp. 67-68.

Curriculum Vitae

Name:	Yu Cheng
Birthday:	November 28, 1976
Place of Birth:	Liaoning, P.R. China
Marital status:	Single
Nationality:	Chinese

Educations:

Sep. 1995 – Jun. 2000	Bachelor in medicine at China Medical University in Shenyang/ Liaoning, P.R. China
Mar. 2001 – Jun. 2002	German Course at the Martin-Luther-University, Halle-Wittenberg, Germany.
Sep. 2002 – Aug. 2003	Computer Science at the Martin-Luther-University of Halle-Wittenberg, Germany.
Sep. 2003 – Oct. 2005	M. E. in Biomedical Engineering at the Martin-Luther-University, Halle-Wittenberg, Germany. Thesis: Analysis of the gene expression of the rats' brain after focal trauma.
Jul. 2006 -	Ph.D student at the Otto-von-Guericke-University, Magdeburg, Germany.